

AD-A094 554

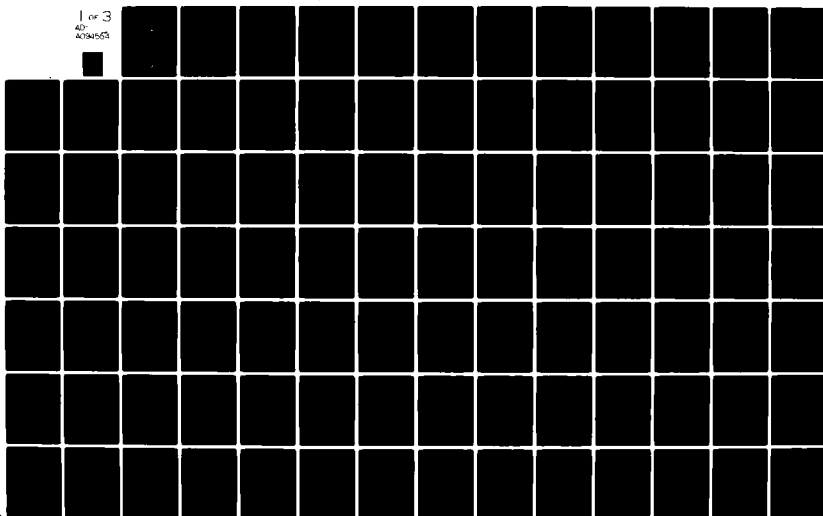
NAVAL POSTGRADUATE SCHOOL MONTEREY CA  
ADAPTIVE NOTCH FILTER SUPPRESSION OF BENDING MODES.(U)  
DEC 80 W L MARKS

F/G 9/2

UNCLASSIFIED

NL

1 of 3  
AD-  
A094562



NAVAL POSTGRADUATE SCHOOL  
Monterey, California

(2)  
LEVEL 17

AD A094554



# THESIS

ADAPTIVE NOTCH FILTER  
SUPPRESSION OF BENDING MODES

by

William L. Marks

December 1980

Thesis Advisor:

R. D. Strum

Approved for public release; distribution unlimited

DBC FILE COPY

DTIC  
ELECTE  
FEB 5 1981  
S F D

81 2 04 014

REPORT DOCUMENTATION PAGE		READ INSTRUCTIONS BEFORE COMPLETING FORM	
1. REPORT NUMBER	2. GOVT ACCESSION NO.	3. RECIPIENT'S CATALOG NUMBER	
	AD-A094	554	
4. TITLE (and Subtitle)		5. TYPE OF REPORT & PERIOD COVERED	
Adaptive Notch Filter Suppression of Bending Modes.		Master's Thesis December 1980	
7. AUTHOR(s)		6. PERFORMING ORG. REPORT NUMBER	
William L. Marks			
9. PERFORMING ORGANIZATION NAME AND ADDRESS		8. CONTRACT OR GRANT NUMBER(s)	
Naval Postgraduate School Monterey, California 93940			
11. CONTROLLING OFFICE NAME AND ADDRESS		10. PROGRAM ELEMENT, PROJECT, TASK AREA & WORK UNIT NUMBERS	
Naval Postgraduate School Monterey, California 93940			
14. MONITORING AGENCY NAME & ADDRESS (if different from Controlling Office)		12. REPORT DATE	
		December 1980	
		13. NUMBER OF PAGES	
		222	
		15. SECURITY CLASS. (of this report)	
		UNCLASSIFIED	
		16a. DECLASSIFICATION/DOWNGRADING SCHEDULE	
16. DISTRIBUTION STATEMENT (of this Report)		Accession For	
Approved for public release; distribution unlimited		NTIS GRA&I	
		DTIC TAB	
		Unannounced	
		Justification	
17. DISTRIBUTION STATEMENT (of the abstract entered in Block 20, if different from Report)		By	
		Distribution/	
		Availability Codes	
18. SUPPLEMENTARY NOTES		Dist	
		Special	
		A	
19. KEY WORDS (Continue on reverse side if necessary and identify by block number)			
Adaptive Digital Notch Filter; Bending Mode Suppression; Trident Missile; Adaptive Control System; Nonlinear Control System			
20. ABSTRACT (Continue on reverse side if necessary and identify by block number)			
A simple, microprocessor oriented algorithm is developed to identify, track and suppress bending mode signals from a control system's rate and position feedback signals using adaptive digital notch filters. The algorithm can be used to suppress bending modes having center frequencies as close as one octave above the control system gain cross-over frequency without introduction of the exces- sive phase loss associated with conventional lowpass filtering techniques. A third order model of the trident missile autopilot			

pitch attitude control loop is contaminated with two dynamic, destabilizing bending modes and used as a concept demonstration model. The algorithm is demonstrated by stabilizing the pitch attitude loop in the presence of two bending modes with unknown gains, damping, center frequencies and rates of change of center frequencies.

Approved for public release; distribution unlimited

ADAPTIVE NOTCH FILTER  
SUPPRESSION OF BENDING MODES

by

William L. Marks  
Commander, U. S. Navy  
B.S.M.E., Iowa State University, 1966

Submitted in partial fulfillment of the  
requirements for the degree of

MASTER OF SCIENCE IN ELECTRICAL ENGINEERING

from the

NAVAL POSTGRADUATE SCHOOL  
December 1980

Author

William L. Marks

Approved by:

Robert T. Strum

Thesis Advisor

D. E. Kirk

Second Reader

D. E. Kirk

Chairman, Department of Electrical Engineering

William M. Toller

Dean of Science and Engineering

## ABSTRACT

A simple, microprocessor oriented algorithm is developed to identify, track and suppress bending mode signals from a control system's rate and position feedback signals using adaptive digital notch filters. The algorithm can be used to suppress bending modes having center frequencies as close as one octave above the control system gain cross-over frequency without introduction of the excessive phase loss associated with conventional lowpass filtering techniques. A third order model of the trident missile autopilot pitch attitude control loop is contaminated with two dynamic, destabilizing bending modes and used as a concept demonstration model. The algorithm is demonstrated by stabilizing the pitch attitude loop in the presence of two bending modes with unknown gains, damping, center frequencies and rates of change of center frequencies.

## TABLE OF CONTENTS

I.	INTRODUCTION- - - - -	9
A.	THE BODY BENDING PROBLEM- - - - -	9
B.	THE PROPOSED SOLUTION - - - - -	12
II.	MODEL DEVELOPMENT - - - - -	18
A.	THE MODEL OF THE PLANT- - - - -	18
B.	THE CHARACTERISTICS OF THE PLANT- - - - -	22
C.	THE MODEL OF THE BENDING MODES- - - - -	33
D.	CHARACTERISTICS OF THE PLANT WITH TWO BENDING MODES - - - - -	39
III.	ADAPTIVE DIGITAL FILTER DESIGN- - - - -	63
A.	FACTORS AFFECTING THE DESIGN- - - - -	63
B.	DESIGN OF THE ALGORITHM MODULES - - - - -	64
1.	The Bandpass Filter Module- - - - -	64
2.	The Zero Crossing Detector Module - - - - -	71
3.	The Frequency Averaging Module- - - - -	79
4.	Design of the Notch Filter Module - - - - -	80
5.	Flow Chart of the Algorithm - - - - -	87
C.	TEST OF THE ALGORITHM - - - - -	92
IV.	SIMULATION STUDIES- - - - -	99
A.	DIGITAL SIMULATION LANGUAGE (DSL/360) - - - - -	99
B.	BLOCK DIAGRAM OF THE SIMULATION MODEL - - - - -	99
C.	SIMULATION CONDITIONS - - - - -	99
D.	SIMULATION RESULTS- - - - -	102

V. CONCLUSIONS AND RECOMMENDATIONS - - - - -	120
A. CONCLUSIONS - - - - -	120
B. RECOMMENDATIONS FOR FURTHER STUDIES - - - - -	121
COMPUTER PROGRAMS - - - - -	123
LIST OF REFERENCES- - - - -	221
INITIAL DISTRIBUTION LIST - - - - -	222



# TABLE OF SYMBOLS

$\theta_c$	Missile pitch attitude angle command in radians
$\theta$	Missile pitch attitude angle in radians = $x_1$
$\dot{\theta}$	Missile pitch rate in radians/seconds = $x_2$
$\alpha$	Angle of attack in pitch plane in radians = $x_3$
$x_4, x_5, x_6, x_7$	Bending mode dynamic state variables
$M_\alpha$	Aerodynamic stability derivative (pitch plane) in second <sup>-2</sup> $= \frac{\bar{q} S_o C_{n\alpha}}{I_{yy}}$
$M_\delta$	Aerodynamic stability derivative (pitch plane) in second <sup>-2</sup> $= \frac{T l_D}{I_{yy}}$
$Z_\alpha$	Aerodynamic force stability derivative (pitch) coefficient in ft/sec <sup>2</sup> /RAD $= \frac{\bar{q} S_o C_{n\alpha}}{M}$
$Z_\delta$	Pitch force rigid body coefficient forcing from thrust in ft/sec <sup>2</sup> /RAD $= \frac{T}{M}$
$\bar{q}$	Aerodynamic Pressure in lb/ft <sup>2</sup>
$S_o$	Missile aerodynamic reference area in ft <sup>2</sup>
$C_{n\alpha}$	Aerodynamic normal coefficient (pitch plane) in radian <sup>-1</sup>
$l_\alpha$	Distance from vehicle C.G. to guidance accelerometer in ft.
$I_{yy}$	Vehicle pitch moment of inertia in slug-ft <sup>2</sup>
$T$	Vehicle axial thrust in lb.

$l_D$	Distance from nozzle pivot point to vehicle C.G. in ft.
$M$	Vehicle mass in slug
$K_\theta$	Pitch autopilot attitude gain
$K_{r\theta}$	Pitch autopilot rate gain
$V$	Vehicle velocity in ft/second
$\zeta$	Damping ratio
$\omega_n, W$	Undamped natural frequency in radians
$P_{rg}$	Rate gyro gain volts/rad/sec
$\theta_{GA}$	Attitude gyro gain volts/rad
$G_L$	Low frequency bending mode gain
$G_h$	High frequency bending mode gain
$B_L$	Low frequency bending mode bandwidth in radians/sec
$B_h$	High frequency bending mode bandwidth in radians/sec
$\omega_d$	Digital frequency, radians

## I. INTRODUCTION

The purpose of this thesis is to develop a simple, micro-processor-oriented scheme that eliminates body bending mode signals in a missile control system by adaptive digital notch filtering of the bending mode resonant frequencies from the rate and attitude gyro feedback signals. Although this thesis uses the Trident Fleet Ballistic Missile as a conceptual demonstration model, the process is applicable to many control systems having unknown and/or time varying mechanical resonances.

### A. THE BODY BENDING PROBLEM

Body bending is a composite term which encompasses the coupling of all structure-borne vibrations from various sources into the missile control system through the mechanical sensors such as rate gyros and accelerometers. The effect of the body bending mode signals in the rate and attitude gyro feedback signals is destabilizing since if left unattenuated, the missile control system tries to compensate for the sensed body bending rate through the thrust vector control (TVC) system thus further exciting the bending mode and the inertial or rigid body rates soon become insignificant and go uncorrected.

Some of the sources of body bending are:

1. The missile acting as a cantilevered beam.

2. Hydraulic servo resonance.

3. Structural bending at the attachment points for hydraulic actuators.

4. Beam-like resonance of sub-assemblies such as upper stage motors and payload.

The body bending problem in missiles is traditionally approached in one of three ways:

1. The mechanical sensors are physically located at nulls in the lower frequency bending modes and the natural bandwidth of the control system and lowpass filters are used to attenuate the higher frequency bending modes. Reference [1] contains a detailed description of the analysis and testing required to implement this approach in the control system of the XSM-65 missile. The popular name, if any, of the XSM-65 missile is unknown.

2. The mechanical sensors are physically located at a position in the missile where the deflections due to the lower frequency body bending modes are in phase with each other. Phase shifting networks are used to ensure that the bending mode signals are fed back in such a manner that the bending modes are attenuated. Lowpass filters are still used to attenuate the higher frequency bending modes. Reference [2] contains a general description of how this method is implemented in the control system for the Saturn Missile.

3. Lowpass or bandstop filters are used in the feedback control loops to attenuate the body bending mode frequencies from the rate and attitude gyro feedback signals. A general description of how this method is used in the Trident Missile Control System is contained in Ref. [3].

In the Trident Missile the above three approaches have many undesirable features. Location of the sensors at nulls or where the body bending modes are in phase requires a very precise knowledge of the bending mode characteristics and the freedom in the initial design to locate the sensors at the anticipated optimum locations. In a solid fuel missile such as the Trident, the location of the sensors is predetermined to be located with the other flight control electronics with very little latitude to select a null or position where the bending modes are in phase. The second major limitation is the lack of precise knowledge of the bending mode characteristics. The bending mode resonant frequencies, gains, damping and phase are a function of many factors including time into the flight, attitude, payload configuration, skin temperature, and thrust level. For example, the Trident Missile is designed to compensate for as much as a twenty-five percent variation in thrust level due to slight variations in the solid propellant mixture and casting while only a three percent thrust variation is acceptable on the liquid fueled Saturn Missile [2]. Without a precise knowledge of the parameters controlling the bending

mode resonant frequencies, gains, damping and phase, the lowpass and bandstop filters must be designed on a worst case basis and as a result reduce the control system bandwidth and phase margins much more than if a narrow notch filter had been used at each specific bending mode frequency to remove the bending mode component from the rate and position gyro output signals.

As the Trident Missile evolves into the next generation, the anticipated bending mode frequencies will become much lower and approach the natural frequencies of the flight control system. The use of conventional lowpass filters under these conditions would produce so much phase loss that the missile would become unstable.

#### B. THE PROPOSED SOLUTION

The proposed solution to the bending mode problem is an extension of preliminary work done by Lockheed Missiles and Space Company [3].

If the bending mode resonant frequencies can be determined in near real time during the flight and tracked as their controlling parameters change, then adaptive notch digital filters in the rate and position gyro signal feedback paths can be implemented to attenuate a selected number of bending mode signals that are contaminating the desired rigid body rate and attitude signals.

The difficulty in the implementation of such a solution lies in the in-flight determination of the bending mode frequencies rapidly and with sufficient accuracy. The rapid determination of the bending mode frequencies is essential in order to place the notch filter at the proper bending mode frequency before the bending mode signals can degrade the missile attitude and rates to a point from which it cannot recover within the allowable flight trajectory envelope. The allowable time for the initial determination of the bending mode frequencies is a function of the initial frequency and bandwidth of the individual notch filters. In general the time available to eliminate the effects of the bending modes before the Trident Missile deviates from an acceptable flight trajectory is one-half second. The requirement for accuracy is essential to allow the minimum bandwidth notch filters to be used. As successive notch filters are added to the control system to attenuate the bending mode signals, an increasing amount of phase loss will be experienced at the frequencies used by the control system resulting in a decrease in the already minimal phase margin for overall missile stability. If very narrow notch filters are used to minimize the phase loss at the control system frequencies, then the center frequency of the notch must be placed much more accurately to be effective.

Four methods were investigated as to their potential to be used for inflight bending mode frequency identification and tracking:

1. Reference [3] summarizes the use of Fourier integral filters to measure the power spectral density at integer frequencies. Second order curve fitting techniques were then used to estimate the bending mode frequencies from the output of the filters. The major drawback of this technique is that it required at least one-half second of integration time for each repeated frequency determination. Reference [3] did not address the ability of this technique to accurately track a dynamic bending mode, although the data indicated that a bending mode that was changing as little as 0.2 hertz per second would cause sufficient distortion of the frequency determination as to render the technique ineffective.

2. The author conducted a feasibility study of using a Fast Fourier Transform (FFT) algorithm to determine the spectrum of the rate gyro output signal in order to determine the bending mode frequencies. The method was disregarded for two reasons. The rate gyro signal would have to be sampled for ten seconds to obtain a minimum frequency resolution of 0.1 hertz and, the computational capability required to execute the FFT algorithm was felt to be excessive.



3. The feasibility of using a phaselock loop to lock-on and track a bending mode frequency was investigated by the author. Simulation of a phaselock loop with an eight-hertz center frequency and a three-hertz acquisition range revealed that while the tracking characteristics of the phaselock loop were very good, the ability to achieve lock with a random phase signal at the extremes of its acquisition range was unreliable if the signal was contaminated with frequency components from the plant and a second bending mode at anticipated signal levels. The technique was not pursued further but with the addition of prefilters on the phaselock loop input this technique has the potential to be more effective than the technique used in this thesis. Considerable refinement in the simulation of the phaselock loop nonlinearities would be required.

4. The technique used in this thesis to identify and track the bending mode frequencies uses a microprocessor to compute the frequency of each bending mode by use of digital bandpass filters and linear estimation of the zero crossing times. The use of discrete signal processing by the microprocessor will not require additional sampling circuitry since the missile attitude and rate gyro signals are currently sampled and put in digital form in the Trident Missile for use in the digital autopilot. As shown in Figure 1-1, the microprocessor uses the sampled rate gyro data by passing it through a set of parallel digital

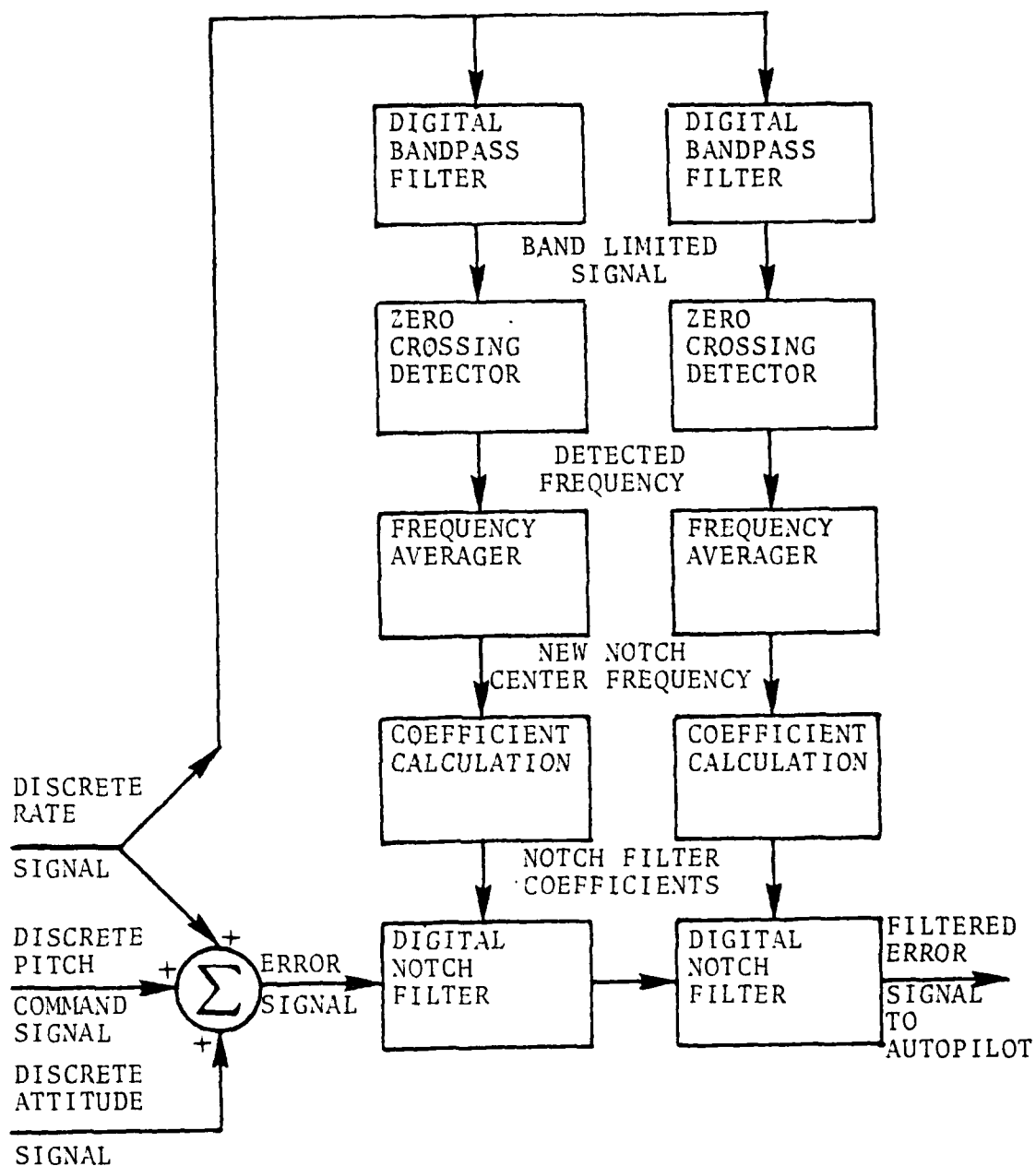


Figure 1-1 Microprocessor Algorithm Modules

bandpass filters in order to decompose the signal into frequency bands that are only wide enough to contain one bending mode frequency. The output of each of the bandpass digital filters is examined after each sample to see if the amplitude of the signal in that band has changed signs. If the amplitude has changed signs then the time of the zero crossing is linearly estimated based on the amplitude of the signal before and after the zero crossing and the sampling period. The half period detected is converted to a frequency and averaged with the frequency that the digital notch filter devoted to that band is currently tracking. The average of the current and computed frequency is then used to compute new coefficients such that the digital notch filter will be centered at the new average frequency. The details of the algorithm and design are discussed in Chapter Three and the concept is demonstrated by simulation in Chapter Four.

## II. MODEL DEVELOPMENT

In order to verify the ability of the tracking notch filter concept to stabilize the missile in the presence of bending mode feedback, a model of the system was developed to be used as the basis for simulation.

### A. THE MODEL OF THE PLANT

Figure 2-1 is a block diagram representation of the reduced order pitch plane attitude control loop of the Trident I Missile autopilot. The model was provided by Lockheed Missile and Space Company by reference [3], and was modified only to the extent that the signs at the summers for  $\dot{x}_1$  and  $\dot{x}_3$  were changed to allow all the model coefficients to be considered positive quantities. Table 2-1 shows the time varying values for the parameters used in this model. The model shown in Figure 2-1 represents the rigid body dynamics of the missile and is referred to as the plant. When bending modes are added to the rigid body model the resulting composite model is referred to as the system.

The state space representation of the plant for any time is:

$$\dot{x}_1 = x_2$$

$$\dot{x}_2 = -K_\theta M_s x_1 - K_{r\theta} K_\theta M_\delta x_2 - M_\alpha x_3 - K_\theta M_\delta \theta_c$$

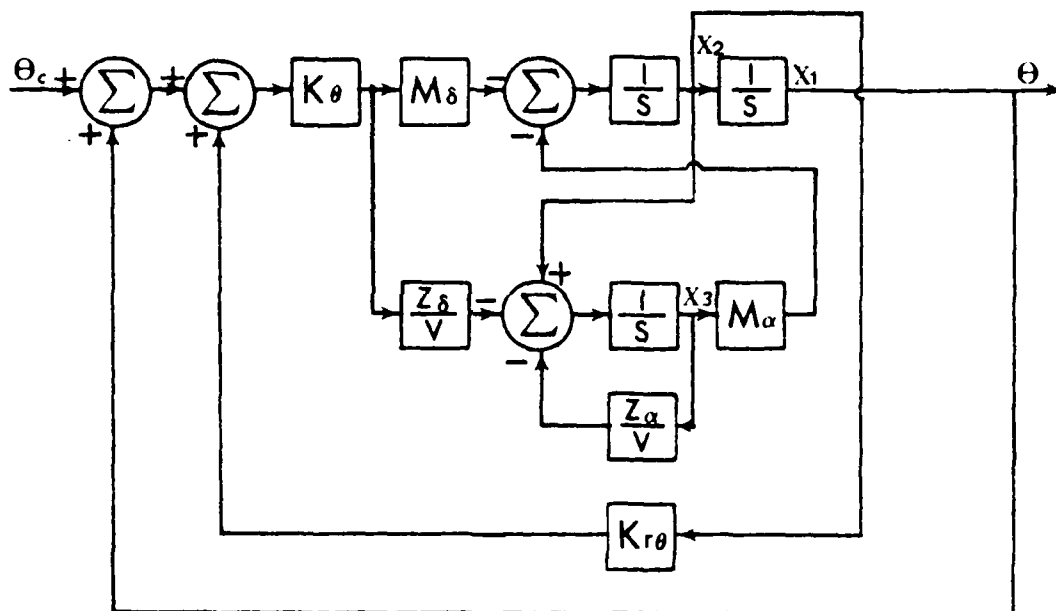


Figure 2-1 Pitch Plane Attitude Control Loop  
(Plant)

TABLE 2-1

MISSILE PARAMETER VALUES AT VARIOUS TIMES INTO THE FLIGHT

PARAMETER	T=25 SEC.	T=40 SEC.	T=50 SEC.
$M_{\alpha}$	18.625	28.625	17.5
$M_{\delta}$	22.51	24.17	32.0
$z_{\alpha}$	88.87	180.0	140.0
$z_{\delta}$	119.19	113.75	137.5
V	1750	2500	3400
$\psi_{rg}$	0.06	0.06	0.06
$\psi_{GA}$	0.06	0.06	0.06
$K_{\theta}$	1.5	1.48	0.946
$K_{r\theta}$	0.2	0.2	0.2

NOTE: The units of each parameter are listed on the list of symbols. The signs of the parameters are all positive to be consistent with the structure of the model used.

$$\dot{x}_3 = -K_{\theta} \frac{Z}{V} x_1 + (1 - K_{r\theta} K_{\theta} \frac{Z}{V}) x_2 - \frac{Z}{V} x_3 - K_{\theta} \frac{Z}{V} \Theta_c$$

where:

$x_1$  is the missile pitch angle.

$x_2$  is the missile pitch angle rate.

$x_3$  is the angle of attack.

Using matrix notation the plant is then described by:

$$\dot{\underline{x}} = \underline{A} \underline{x} + \underline{B} \Theta_c$$

$$\Theta = \underline{C} \underline{x}$$

where

$$\underline{A} = \begin{bmatrix} 0 & 1 & 0 \\ -K_{\theta} M_{\delta} & -K_{r\theta} K_{\theta} M_{\delta} & -M_{\alpha} \\ -K_{\theta} \frac{Z}{V} & (1 - K_{r\theta} K_{\theta} \frac{Z}{V}) & -\frac{Z}{V} \end{bmatrix}$$

$$\underline{B} = \begin{bmatrix} 0 & -K_{\theta} M_{\delta} & K_{\theta} \frac{Z}{V} \end{bmatrix}^T$$

$$\underline{C} = \begin{bmatrix} 1 & 0 & 0 \end{bmatrix}$$

The transfer function relating the missile pitch angle  $\theta$  to the commanded pitch angle  $\theta_c$  is:

$$\frac{\theta(s)}{\theta_c(s)} = H(s)$$

$$H(s) = \frac{-K_\theta [M_\delta s + (M_\delta \frac{Z_\alpha}{V} - M_\alpha \frac{Z_\delta}{V})]}{s^3 + (\frac{Z_\alpha}{V} + K_\theta K_{r\theta} M_\delta) s^2 + [M_\alpha + K_{r\theta} K_\theta (M_\delta \frac{Z_\alpha}{V} - M_\alpha \frac{Z_\delta}{V}) + K_\theta M_\delta] s + K_\theta (M_\delta \frac{Z_\alpha}{V} - M_\alpha \frac{Z_\delta}{V})}$$

(1)

The transfer function can be factored with a root finder and used to plot the poles and zeros of the transfer function in order to provide an intuitive feeling as to the response of the system not otherwise apparent with the state-space representation. The state-space representation of the system is used primarily in the simulation programs to obtain the time-domain solution to the differential equations of motion.

#### B. THE CHARACTERISTICS OF THE PLANT

The model of the plant given in Figure 2-1 is a model of the rigid body dynamics including two Newtonian integrators and the positive feedback of the angle of attack,  $x_3$ . The



output pitch angle  $\theta$  is opposite in sign to the commanded pitch  $\theta_c$ . This reversal is compensated for in the outer guidance loop not included in this model. The sign of the forward gains  $M_\delta$  and  $Z_\delta$  are normally specified as negative quantities which results in a net negative feedback. For computational convenience the gains are treated as positive quantities and the signs at the summers have been changed. The sign of the rate and position feedback summers remains positive to clearly indicate the nature of the positive feedback of the bending modes from the pitch rate and pitch angle gyros.

The model of the plant was designed to simulate the transient behavior of the system and not the steady state behavior. As a result the simulation studies are only valid for about two seconds of transient behavior.

To establish a baseline or nominal performance the plant was simulated for a ramp and a step input with system parameter values fixed at the time = 40 second values. The reasoning behind the selection of inputs and parameter values is discussed in Chapter Four.

Selecting the appropriate values for the system parameters from Table 2-1 for time = 40 seconds, the transfer function, given by equation (1) becomes:

$$H(s) = \frac{-35.77(s+0.01779)}{(s+0.0098)(s+3.608 \pm j 7.17)} \quad (2)$$

The poles and zeros of the transfer function are plotted in Figure 2-2.

An examination of the poles and zeros of the transfer function indicates the system is stable with a pair of complex poles having a natural frequency  $\omega_n = 8.02$  RAD/SEC and a coefficient of damping  $\xi = 0.449$ . There is also a very slow pole at  $s = -0.0098$  and a zero at  $s = -0.01779$ .

To establish the baseline or nominal performance of the plant without bending modes, the plant was simulated using the IBM DSL/360 language. The values of the plant parameters from Table 2-1 for time = 40 seconds are used throughout this thesis. A detailed discussion of the simulation programs and the selection of the plant parameter values is contained in Chapter Four. Figure 2-3 illustrates the plant response to a step input pitch command of 0.1 radians. Figure 2-4 illustrates the response of the plant to a ramp input of 0.05 radians/sec.

Note: It will be the convention in this thesis when presenting computer generated output in the form of a figure to include the computer program that was used to generate that figure in the computer program appendix properly labelled to indicate the figure number. If reference is made to the program it will be referred to as program (figure number).

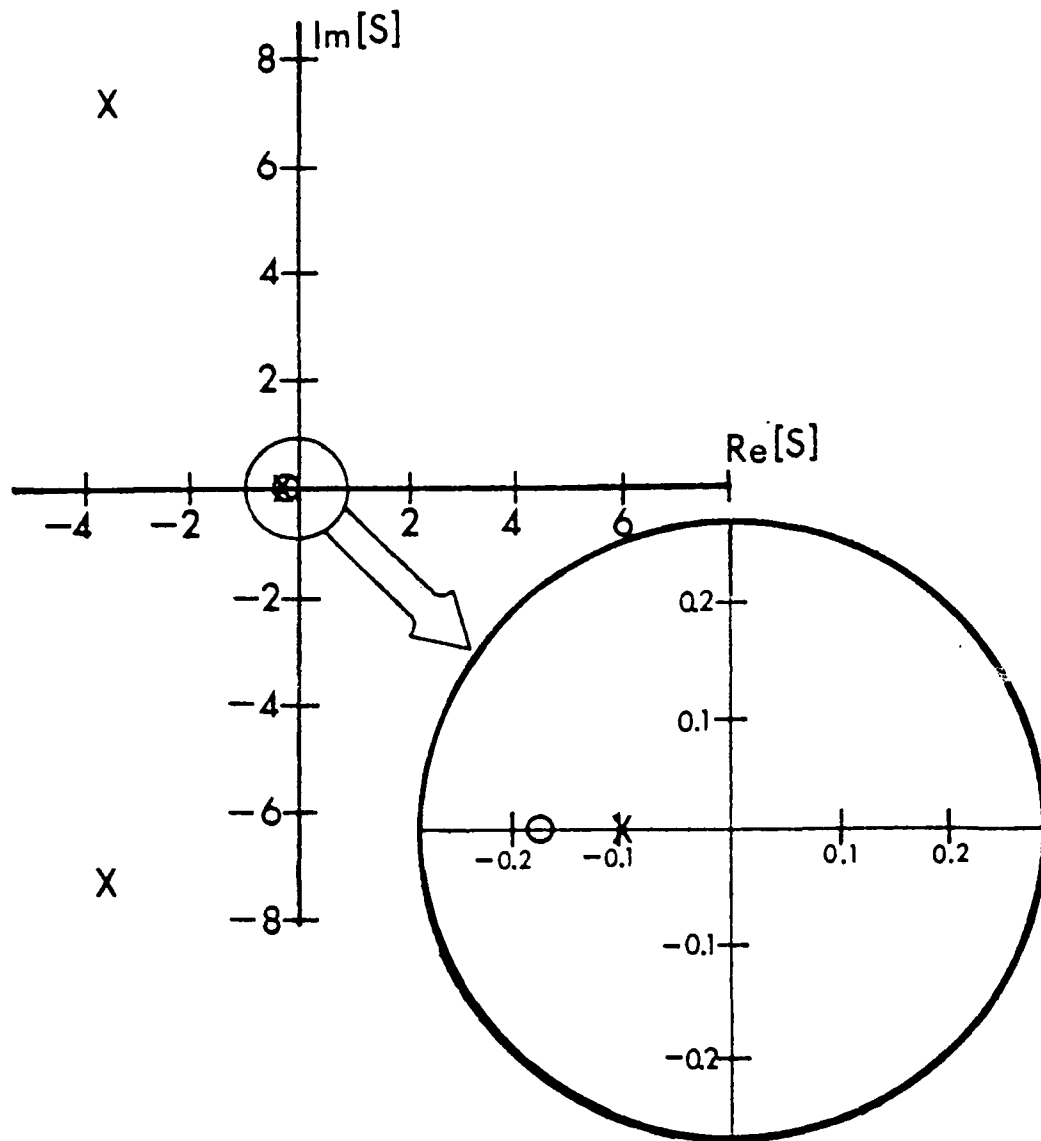
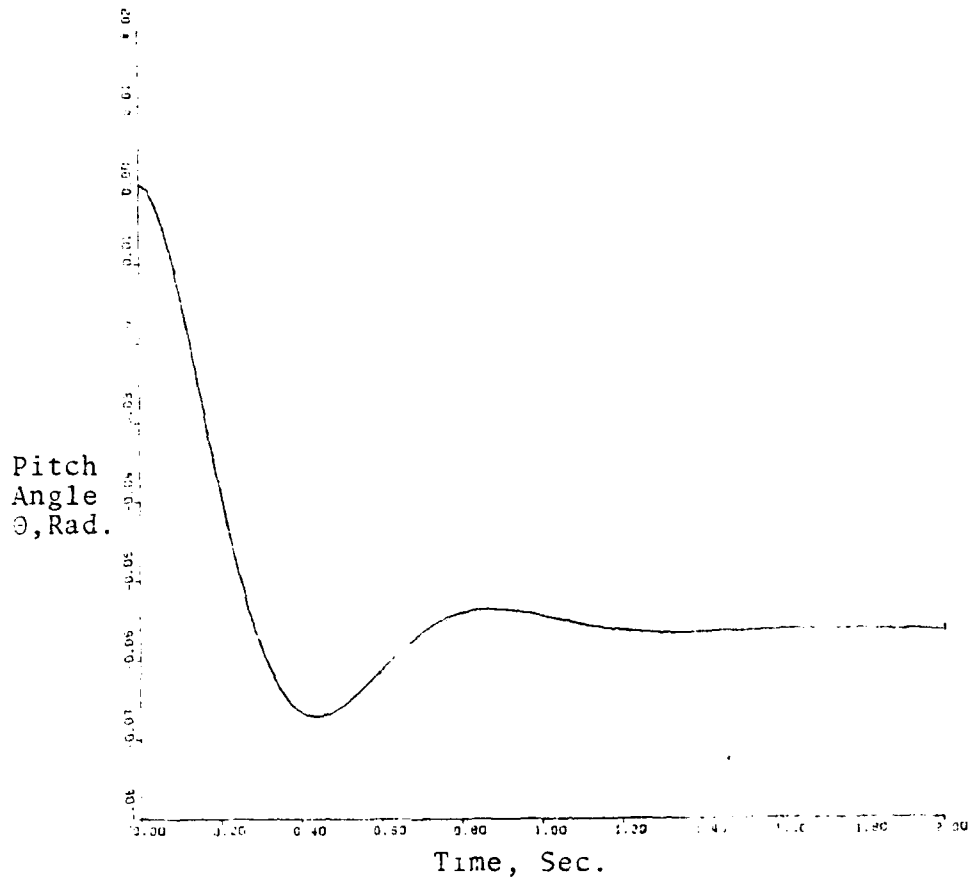


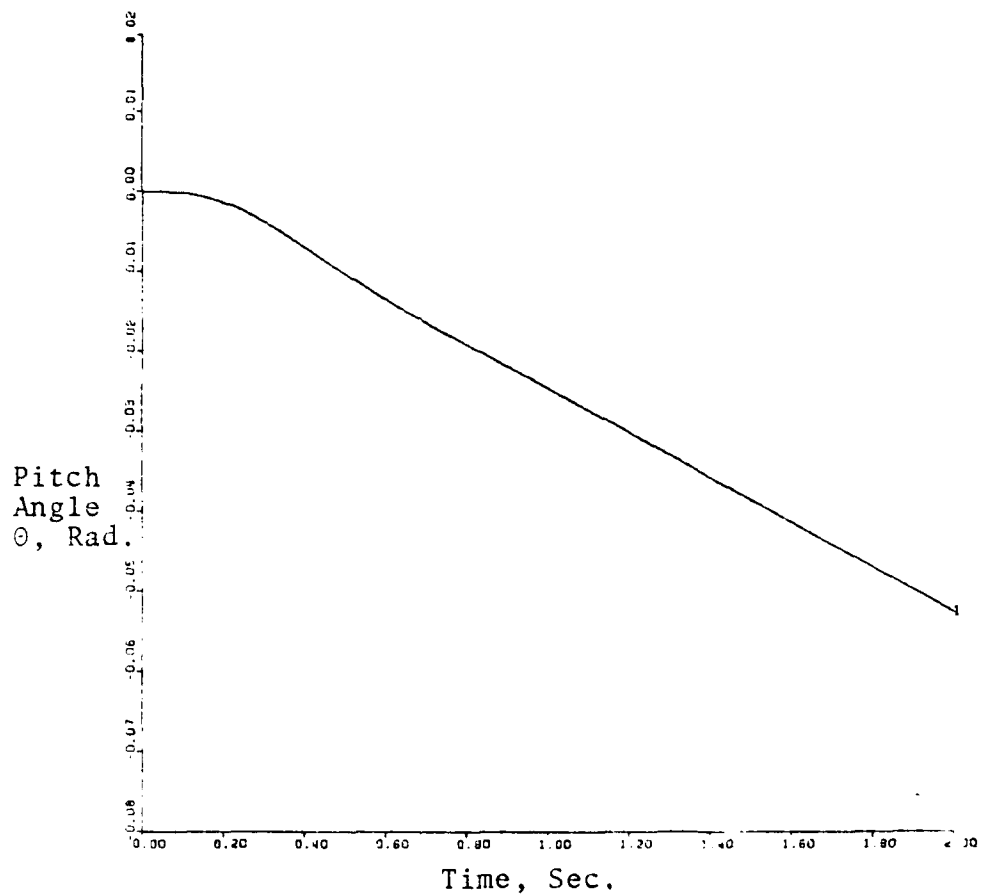
Figure 2-2 Locations of the Poles and Zeros of the Plant



System: Third order missile model without bending modes

Input: 0.1 Radian step pitch command

Figure 2-3 Missile response for a step command



System: Third order missile model without bending modes

Input:  $0.05t$  radian/sec ramp pitch command

Figure 2-4 Missile response for a ramp command

Although all simulations in this thesis are performed using the third-order model of the plant, it is possible to reduce the model to a second-order model without introducing significant error. The second-order model provides a convenient preliminary design model since the characteristics of second-order systems are well established. The second-order model is derived by analysis of the time domain response of the third-order system and eliminating the effects of the slow pole and zero. The validity of the second-order model is established by comparison with the third-order model simulation results.

To obtain the time domain response to a 0.1 radian step input the transfer function of equation (2) will be multiplied by  $0.1/s$  and the resulting function expanded in a partial fraction expansion.

$$\theta(s) = \frac{0.1}{s} H(s) = \frac{-3.577(s+0.01779)}{s(s+0.0098)(s+3.608 \pm j 7.17)}$$

which yields:

$$\theta(t) = -0.1 + 0.0453 e^{-0.0098t} + 0.06218 e^{-3.608t} \cos(7.17t - 0.453)$$

at  $t = 2.0$  sec.

$$\begin{aligned} \theta(2) &= -0.1 + 0.0453(0.98) + 0.06218(0.00072) \cos(14.34 - 0.453) \\ &= -0.552 \end{aligned}$$

Examining the time domain response one finds that the influence of the slow pole is so slow that one may consider the response of the system due to that pole to be essentially a constant for the two second duration of the simulation with less than two percent error. Treating the term due to the slow pose as a constant reduces the time-domain solution to:

$$\theta(t) = -0.0547 + 0.06218e^{-3.608t} \cos(7.17t - 0.453) \quad (3)$$

The system now can be considered as second-order and the response can be very closely approximated from tabulations of the characteristics of second order systems [4].

The transform of equation (3) is

$$L[\theta(t)] = \theta(s) = \frac{-0.0547}{s} + \frac{(0.05589)(s+7.098)}{s^2 + 7.226s + 64.4265}$$

Placing all terms over a common denominator:

$$\theta(s) = \frac{-0.0547 s^2 - 0.3952 s - 3.524 + 0.05589 s^2 + 0.3967 s}{s(s^2 + 7.226 s + 64.4265)}$$

Cancelling the essentially equal  $s^2$  and  $s$  terms in the numerator and factoring out the transform of the 0.1 radian step input ( $0.1/s$ ) yields the following reduced order transfer function relating the missile pitch angle  $\theta$  to the commanded pitch angle  $\theta_c$ .

$$\frac{\theta(s)}{\theta_c(s)} = H_r(s) = \frac{-35.24}{s^2 + 7.226 s + 64.4265} \quad (3a)$$

The steady state gain of the system is:

$$\lim_{s \rightarrow 0} \frac{s H_r(s)}{s} = -0.547$$

The peak overshoot will be:

$$M_{pt} = 1 + e^{-\frac{\pi \zeta}{\sqrt{1 - \zeta^2}}} = 1.21$$

The time of peak overshoot will be

$$t_p = \frac{\pi}{\omega_n \sqrt{1 - \zeta^2}} = 0.438 \text{ sec}$$

Using the approximation for the settling time

$$t_s = \frac{4.0}{\zeta \omega_n} = 1.11 \text{ sec}$$

The validity of the second-order model for a ramp input is established by comparison of the value of the missile pitch angle determined analytically from the second-order transfer function at time = 2 seconds with the value resulting from the simulation of the third-order plant.

Given a transfer function in the form:

$$G(s) = \frac{B_0 + B_1 s + B_2 s^2 + \dots + B_m s^m}{A_0 + A_1 s + A_2 s^2 + \dots + A_n s^n}$$



The steady state time domain response of the output to a ramp input,  $u(t) = at$ , can be determined from the following formula [5]:

$$y_s(t) = \frac{B_0}{A_0} at + \frac{(A_0 B_1 - B_0 A_1)}{A_0^2}$$

Using the second-order transfer function determined in equation (3a) one finds that the output at time=2 for a ramp input,  $u(t) = 0.05t$  is:

$$\theta_s(t) = \frac{-35.24(0.05)t}{64.4265} + \frac{0.05(35.24)(7.226)}{(64.4265)^2} = -0.05242$$

Table 2-2 summarizes the results obtained from the second-order model with those resulting from simulation of the third-order model. Again, it must be noted that the simulation studies contained in this thesis were performed using the third-order model of the plant. The second-order model was derived only as a convenient preliminary design tool for any subsequent studies.

TABLE 2-2

## COMPARISON OF THIRD-ORDER AND SECOND-ORDER MODEL RESPONSES

CHARACTERISTIC	SECOND- ORDER MODEL	THIRD- ORDER SIMULATION
MAXIMUM OVERSHOOT	1.21	1.21
TIME AT MAX. OVERSHOOT	0.44 SEC	0.44 SEC
STEADY STATE GAIN	-0.5625	-0.547
SETTLING TIME (2%)	1.11 SEC	1.11 SEC
RAMP OUTPUT AT T=2 SEC	-0.0524	-0.0526

### C. THE MODEL OF THE BENDING MODES

Reference [3] provided the model of the plant with one bending mode shown in Figure 2-5. The bending mode attitude signal  $x_4$  and bending mode rate signal  $x_5$  are added to the rigid body attitude signal  $x_1$  and rigid body rate signal  $x_2$  respectively. The composite attitude and rate signals are each fed back to the system input in a positive sense and the overall system becomes highly unstable.

Reference [2] states that the bending mode contamination of the rigid body rate signal has a much greater destabilizing effect than does the bending mode contamination of the rigid body attitude signal. The bending mode model is therefore based on modeling the bending mode rate and the bending mode attitude signal is formed by integrating the rate signal.

Reference [6] contains the bending mode frequency response for a Poseidon Missile when the bending modes were excited by slewing the first stage TVC nozzles. Although the data was measured on the Poseidon Missile with various flight configurations, the results are consistent with the general distribution of bending modes shown in Figure 3.3-1 of Ref. [2]. The distribution of the bending modes indicates that the bandwidth of the bending modes increases as the center frequency of the bending mode increases. The distribution of the bending modes used in this thesis is shown in Figure 2-6. The low frequency bending mode may be centered anywhere in a band from 5 to 8 hertz and the high frequency



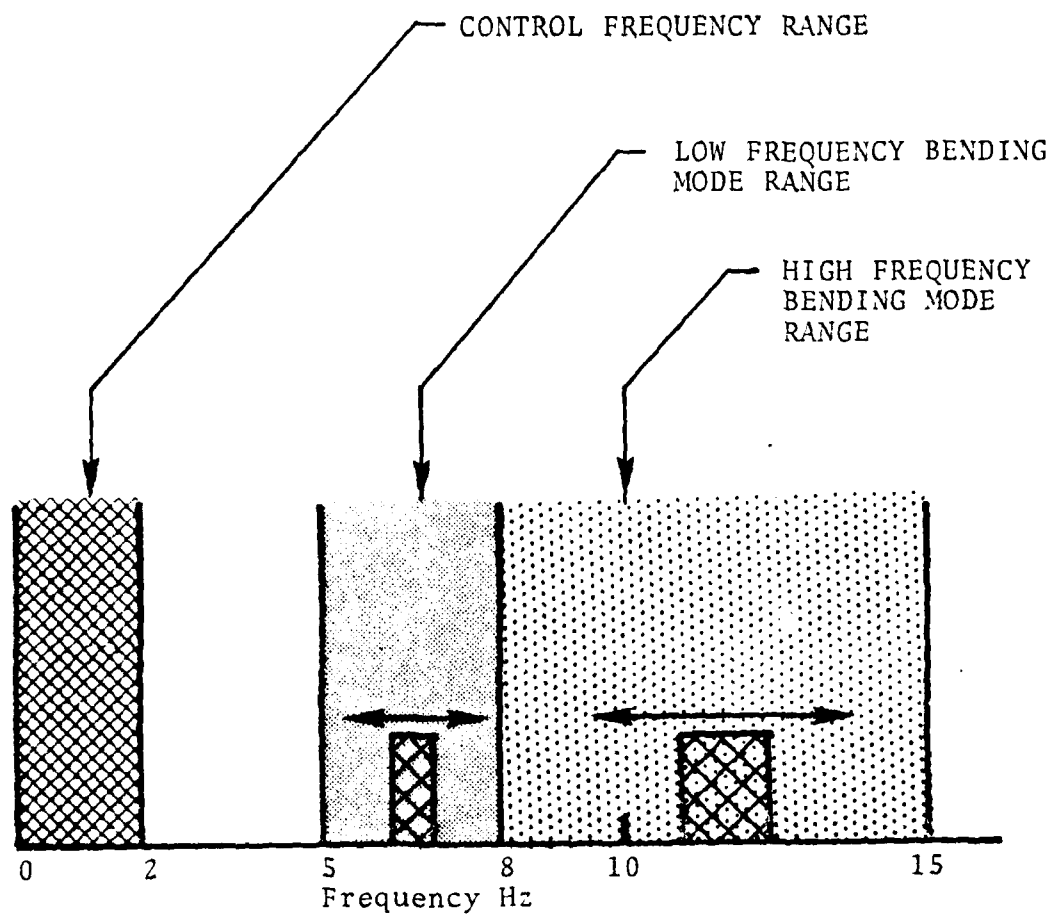


Figure 2-6 Dynamic Bending Mode Distribution

bending mode may be centered anywhere in the band from 8 to 15 hertz. The high frequency bending mode has approximately twice the bandwidth of the low frequency bending mode. The simulation studies contained in Chapter Four demonstrate the ability of the adaptive notch filtering scheme to identify, track and filter bending modes that have time varying gains, bandwidths and center frequencies.

The bending mode rates were modeled as the outputs of bandpass filters with a very high Q. The transfer function relating the output  $Y(s)$  to the input  $U(s)$  for a general second-order bandpass filter is:

$$G(s) = \frac{Bs}{s^2 + Bs + W_c^2}$$

where:

$W_c$  = the center frequency of the filter

$B$  = the 3 dB bandwidth of the filter

The block diagram of  $G(s)$  is shown in Figure 2-7.  $Y(s)$  represents the bending mode rate output and since the bending mode attitude output is the integral of the bending mode rate, an output of the bending mode attitude is also available from the rate model as indicated in Figure 2-8 where  $Y_1(s)$  is the bending mode rate output and  $Y_2(s)$  is the bending mode attitude output.

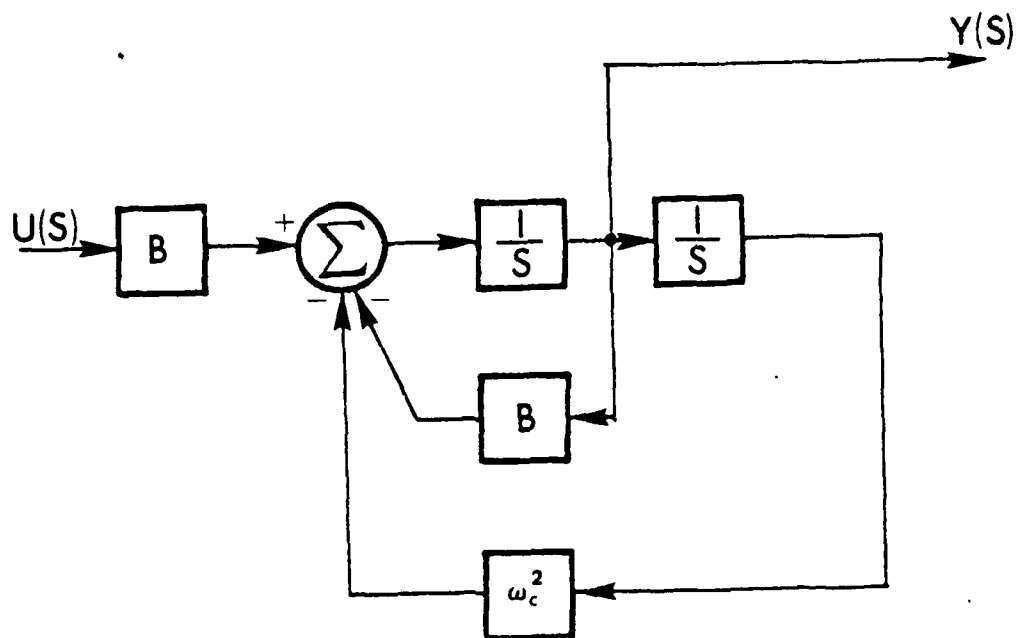


Figure 2-7 Bending Mode Rate Model

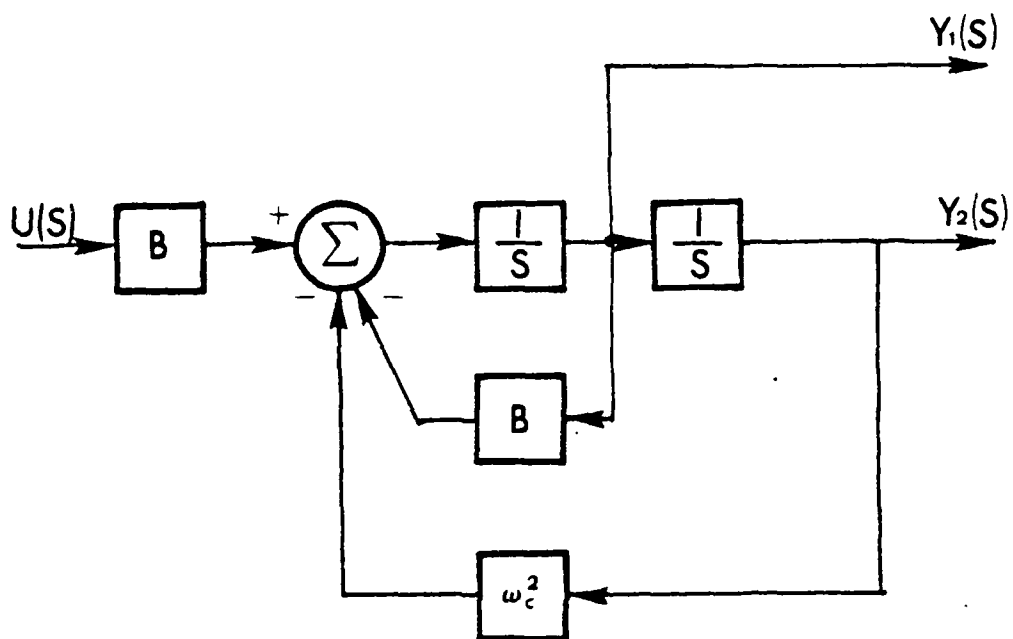


Figure 2-8 Bending Mode Rate and Attitude Model



Inspection of Figure 2-8 reveals that modeling the bending mode rate as a bandpass filter is equivalent to the bending mode model shown in Figure 2-5.

Figure 2-9 shows the system model consisting of the plant and two bending modes that are used for the simulation studies in this thesis.

#### D. CHARACTERISTICS OF THE PLANT WITH TWO BENDING MODES

Preliminary values for the bending mode parameters of gain, center frequency and bandwidth were selected for the purposes of analysis and to develop some insight as to the elements controlling the behavior of the system. The bending mode parameters are varied during the simulation studies presented in Chapter Four but the detailed analysis is not repeated for each parameter study.

The bending mode parameters selected for analysis of the system are:

$$G_h = 20.0$$

$$B_h = 1.10 \text{ RAD/SEC}$$

$$W_h = 62.83 \text{ RAD/SEC (10 Hz center frequency)}$$

$$G_L = 240.0$$

$$B_L = 0.1 \text{ RAD/SEC}$$

$$W_L = 37.7 \text{ RAD/SEC (6 Hz center frequency)}$$

The frequency response of the transfer function relating the missile pitch angle  $\theta(s)$  to the input pitch command  $\theta_c(s)$  with the rate and attitude feedback loops open was determined

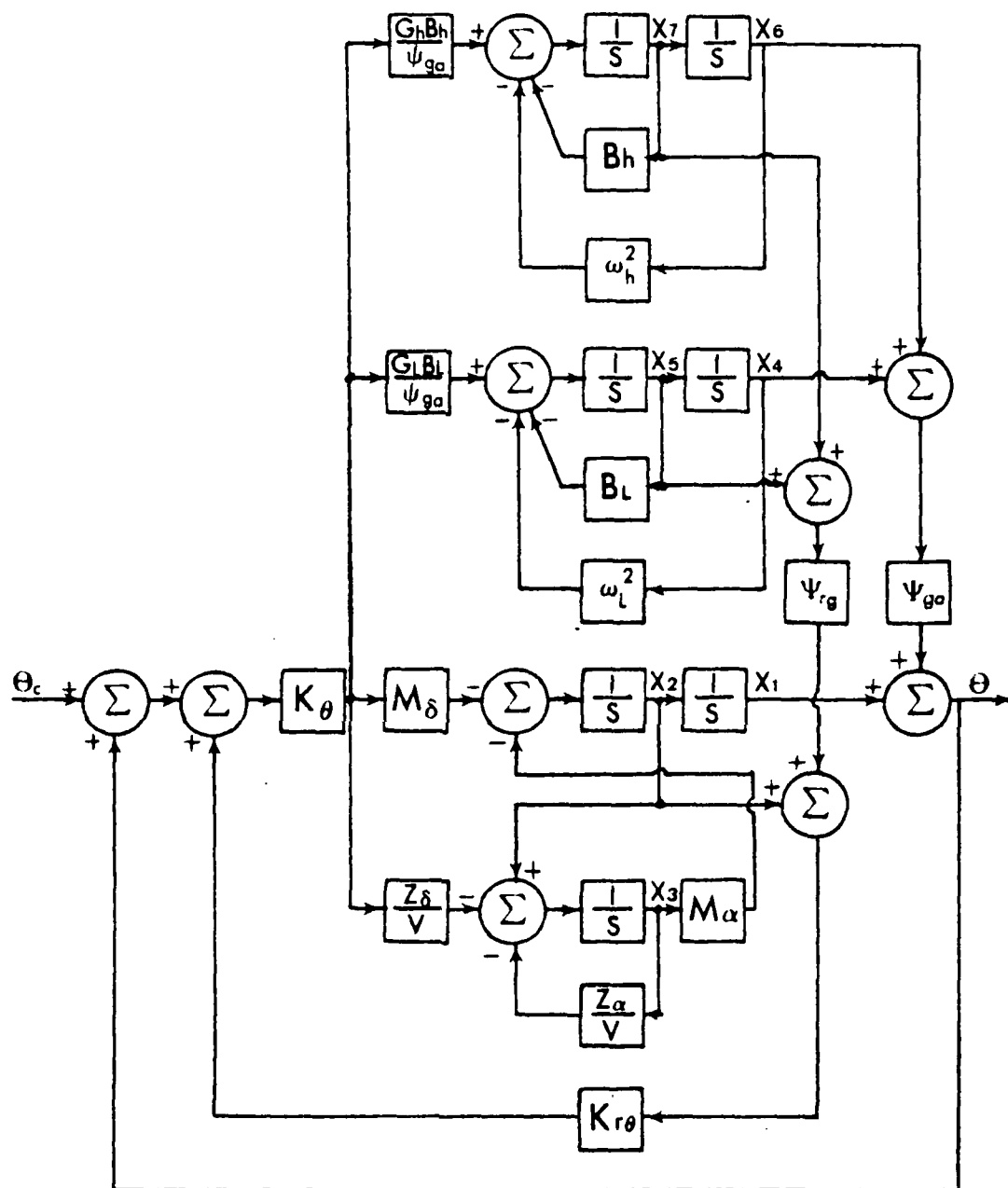


Figure 2-9 Model of Plant with Two Bending Modes

for various configurations of the plant and bending modes shown in Figure 2-9. The plant parameters from Table 2-1 for time = 40 seconds were used.

Figure 2-10 shows the open loop frequency response of the plant with no bending modes.

Figure 2-11 shows the open loop frequency response of the 6.0 Hz bending mode alone.

Figure 2-12 shows the open loop frequency response of the plant and the 6.0 Hz bending mode.

Figure 2-13 shows the open loop frequency response of the 10.0 Hz bending mode alone.

Figure 2-14 shows the open loop frequency response of the plant and the 10.0 Hz bending mode.

Figure 2-15 shows the open loop frequency response of the plant with both the 6.0 Hz and the 10.0 Hz bending modes.

The matrix representation of the state equations derived from the closed loop system shown in Figure 2-9 is:

$$\dot{\underline{x}} = \underline{A}\underline{x} + \underline{B}\theta_c$$

$$\theta = \underline{C}\underline{x}$$

where:

$x_1$  is the rigid body pitch angle of the missile

$x_2$  is the rigid body pitch rate of the missile

$x_3$  is the missile angle of attack

$x_4$  is the pitch angle resulting from the lower frequency bending mode

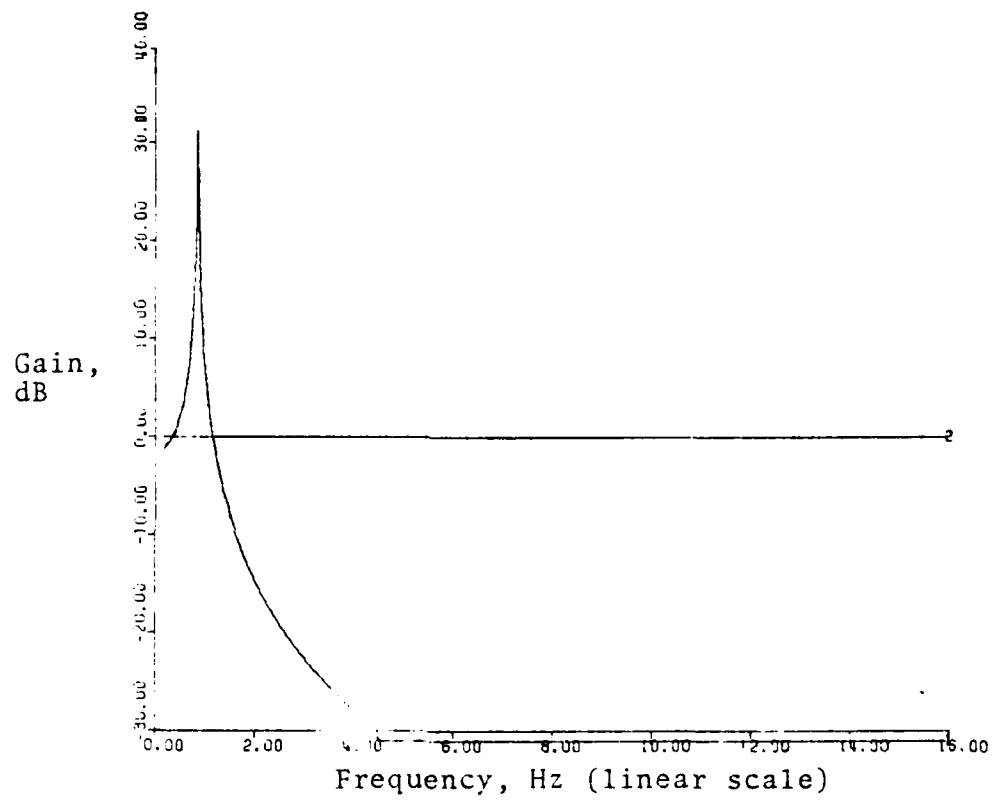


Figure 2-10 Open Loop Frequency Response of the Plant

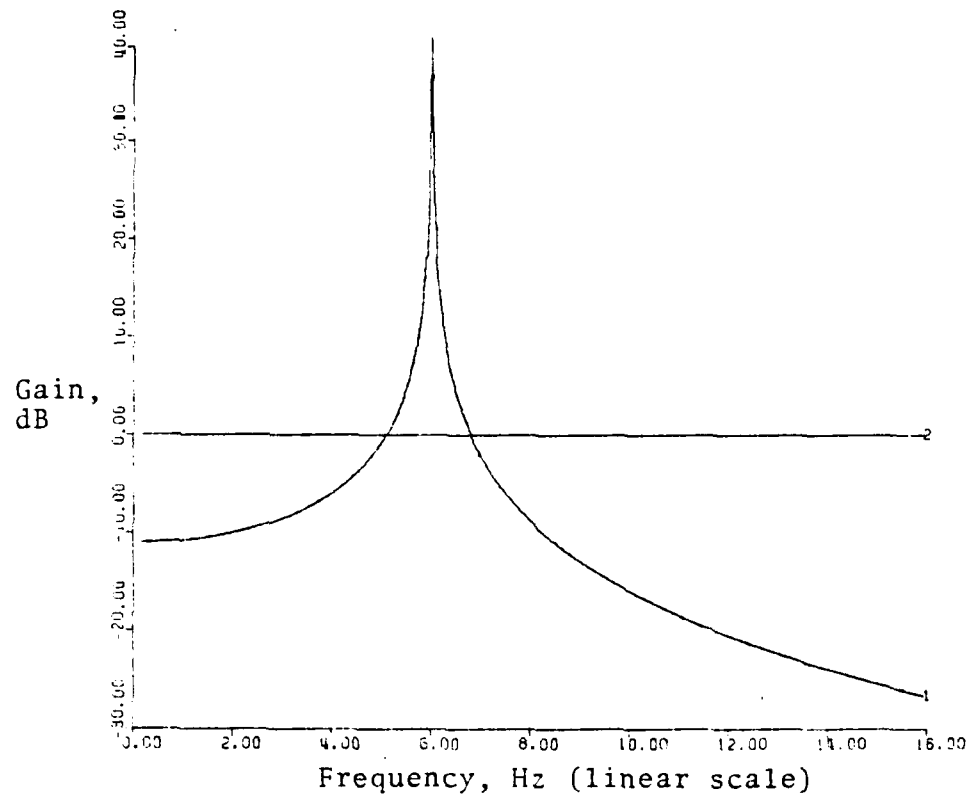


Figure 2-11 Open Loop Frequency Response Of Low Frequency Bending Mode

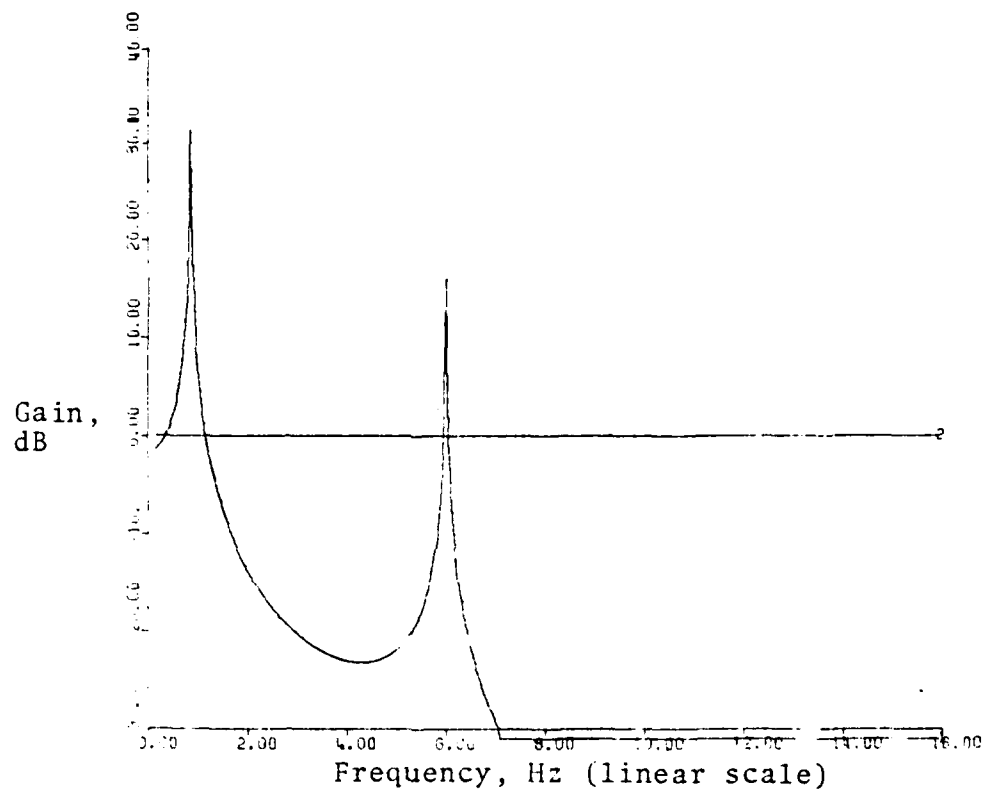


Figure 2-12 Open Loop Frequency Response of the Plant and Low Frequency Bending Mode

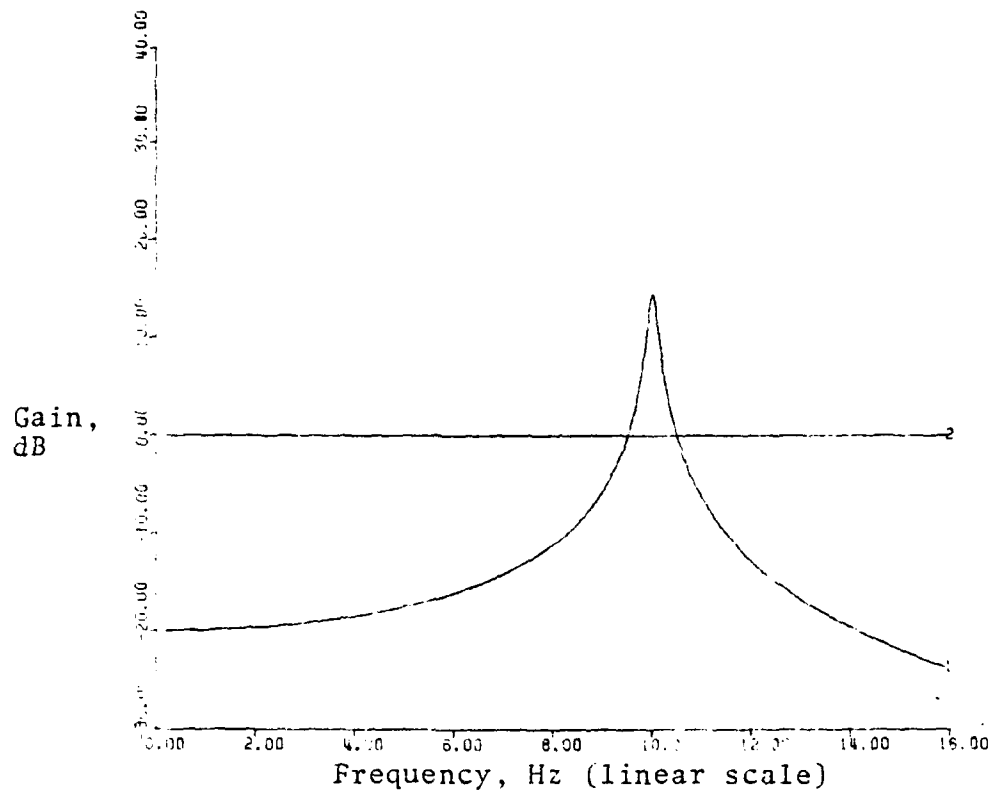


Figure 2-13 Open Loop Frequency Response of the High Frequency Bending Mode

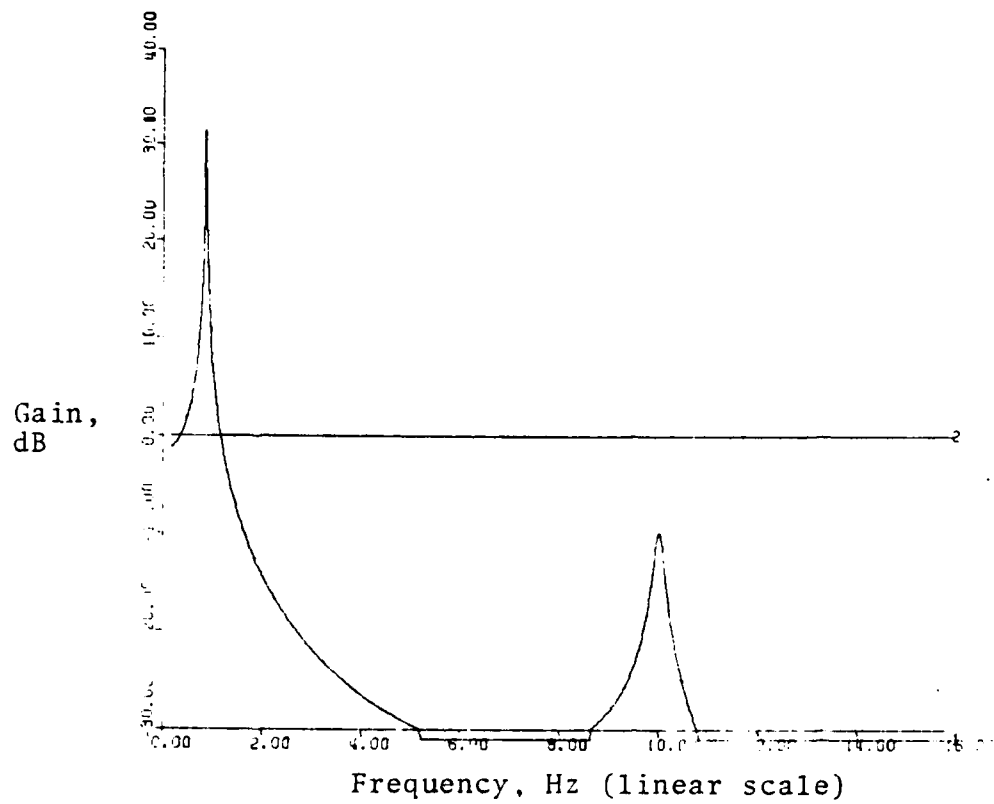


Figure 2-14 Open Loop Frequency Response of the Plant and High Frequency Bending Mode



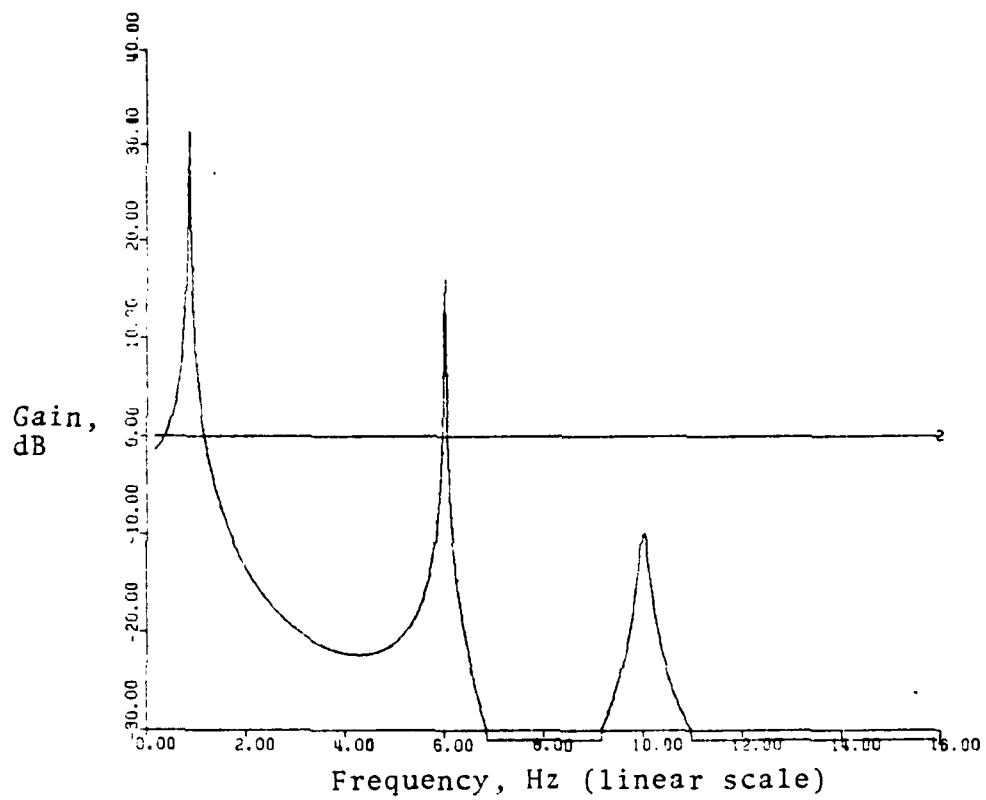


Figure 2-15 Open Loop Frequency Response of Plant with two Bending Modes

$x_5$  is the pitch rate resulting from the lower frequency bending mode

$x_6$  is the pitch angle resulting from the higher frequency bending mode

$x_7$  is the pitch rate resulting from the higher frequency bending mode

$\theta_c$  is the commanded pitch angle

$\theta$  is the missile pitch angle

The A matrix is:

A11	A12	A13	A14	A15	A16	A17
A21	A22	A23	A24	A25	A26	A27
A31	A32	A33	A34	A35	A36	A37
A41	A42	A43	A44	A45	A46	A47
A51	A52	A53	A54	A55	A56	A57
A61	A62	A63	A64	A65	A66	A67
A71	A72	A73	A74	A75	A76	A77

The B matrix is:

$[B1 \ B2 \ B3 \ B4 \ B5 \ B6 \ B7]^T$

The C matrix is:

$[C1 \ C2 \ C3 \ C4 \ C5 \ C6 \ C7]$

where:

$$A11 = 0.0$$

$$A12 = 1.0$$

$$A13 = 0.0$$

$$A14 = 0.0$$

$$A15 = 0.0$$

$$A16 = 0.0$$

$$A17 = 0.0$$

$$A41 = 0.0$$

$$A42 = 0.0$$

$$A43 = 0.0$$

$$A44 = 0.0$$

$$A45 = 1.0$$

$$A46 = 0.0$$

$$A47 = 0.0$$

$$A71 = G_H B_H \frac{K_\theta}{\psi_{GA}}$$

$$A72 = G_H B_H K_{r\theta} \frac{K_\theta}{\psi_{GA}}$$

$$A73 = 0.0$$

$$A21 = -K_\theta M_\delta$$

$$A22 = -K_{r\theta} K_\theta M_\delta$$

$$A23 = M_\alpha$$

$$A24 = -\psi_{GA} z_\theta M_\delta$$

$$A25 = -\psi_{rG} z_{r\theta} z_\theta M_\delta$$

$$A26 = -\psi_{GA} z_\theta M_\delta$$

$$A27 = -\psi_{rG} z_{r\theta} z_\theta M_\delta$$

$$A51 = \frac{G_L B_L}{\psi_{GA}}$$

$$A52 = G_L B_L K_{r\theta} \frac{K_\theta}{\psi_{GA}}$$

$$A53 = 0.0$$

$$A54 = G_L B_L K_\theta - W_L^2$$

$$A55 = G_L B_L \psi_{rG} K_{r\theta} \frac{K_\theta}{\psi_{GA}} - B_L$$

$$A56 = G_L B_L K_\theta$$

$$A57 = G_L B_L K_{r\theta} K_\theta \frac{\psi_{rG}}{\psi_{GA}}$$

$$B1 = 0.0$$

$$B2 = K_\theta M_\delta$$

$$B3 = -K_\theta \frac{z_\delta}{V}$$

$$A31 = K_\theta \frac{z_\delta}{V}$$

$$A32 = 1 - K_{r\theta} K_\theta \frac{z_\delta}{V}$$

$$A33 = -\frac{z_\alpha}{V}$$

$$A34 = -\psi_{GA} z_\theta \frac{z_\delta}{V}$$

$$A35 = -\psi_{rG} z_{r\theta} z_\theta \frac{z_\delta}{V}$$

$$A36 = -\psi_{GA} z_\theta \frac{z_\delta}{V}$$

$$A37 = -\psi_{rG} z_{r\theta} z_\theta \frac{z_\delta}{V}$$

$$A61 = 0.0$$

$$A62 = 0.0$$

$$A64 = 0.0$$

$$A65 = 0.0$$

$$A66 = 0.0$$

$$A66 = 0.0$$

$$A67 = 1.0$$

$$C1 = 1.0$$

$$C2 = 0.0$$

$$C3 = 0.0$$

$$\begin{aligned}
A74 &= G_H B_H K_\theta & B4 &= 0.0 & C4 &= \psi_{rg} \\
A75 &= G_H B_H K_{r\theta} K_{\theta \psi_{GA}} \frac{\psi_{rg}}{\psi_{GA}} & B5 &= G_L B_L \frac{K_\theta}{\psi_{GA}} & C5 &= 0.0 \\
A76 &= G_H B_H K_{\theta} - W_H^2 & B6 &= 0.0 & C6 &= \psi_{GA} \\
A77 &= G_H B_H K_{r\theta} K_{\theta \psi_{GA}} \frac{\psi_{rg}}{\psi_{GA}} - B_H & B7 &= G_H B_H \frac{K_\theta}{\psi_{GA}} & C7 &= 0.0
\end{aligned}$$

The closed loop transfer function  $H(s)$  relating the missile pitch angle  $\theta$  to the commanded pitch angle  $\theta_c$  is:

$$H(s) = \frac{N_5 s^5 + N_4 s^4 + N_3 s^3 + N_2 s^2 + N_1 s + N_0}{s^7 + D_6 s^6 + D_5 s^5 + D_4 s^4 + D_3 s^3 + D_2 s^2 + D_1 s + D_0}$$

where:

$$N_5 = -M_\delta + G_H B_H + G_H B_H$$

$$N_4 = -B_H M_\delta - M_\delta B_L + (M_\alpha \frac{Z_\delta}{V} - M_\delta \frac{Z_\alpha}{V}) + G_L B_L B_H + \frac{Z_\alpha}{V} B_L B_H + \frac{Z_\alpha}{V} B_L B_H + G_H B_H \frac{Z_\alpha}{V} + G_H B_L B_H$$

$$N_3 = -M_\delta W_H^2 - M_\delta B_L B_H + B_H (M_\alpha \frac{Z_\delta}{V} - M_\delta \frac{Z_\alpha}{V}) + B_L (M_\alpha \frac{Z_\delta}{V} - M_\delta \frac{Z_\alpha}{V}) - M_\delta W_L^2 + G_L W_H^2 B_L$$

$$+ G_L B_L B_H \frac{Z_\alpha}{V} + M_\alpha G_L B_L + M_\alpha G_H B_H + G_H B_L B_H \frac{Z_\alpha}{V} + G_H W_L^2 B_H$$

$$N_2 = -M_\delta W_H^2 B_L + W_H^2 (M_\alpha \frac{Z_\delta}{V} - M_\delta \frac{Z_\alpha}{V}) - M_\delta W_L^2 B_H + B_L B_H (M_\alpha \frac{Z_\delta}{V} - M_\delta \frac{Z_\alpha}{V})$$

$$+ W_L^2 (M_\alpha \frac{Z_\delta}{V} - M_\delta \frac{Z_\alpha}{V}) + W_H^2 G_L B_L \frac{Z_\alpha}{V} + B_H G_L B_L M_\alpha + B_L G_H B_H M_\alpha + W_L^2 G_H B_H \frac{Z_\alpha}{V}$$

$$N_1 = -M_S W_H^2 W_L^2 + W_H^2 B_L (M_\alpha \frac{Z_\delta}{V} - M_\delta \frac{Z_\alpha}{V}) + B_H W_L^2 (M_\alpha \frac{Z_\delta}{V} - M_\delta \frac{Z_\alpha}{V}) + W_H^2 G_L B_L M_\alpha \\ + W_L^2 G_H B_H M_\alpha$$

$$N_0 = W_H^2 W_L^2 (M_\alpha \frac{Z_\delta}{V} - M_\delta \frac{Z_\alpha}{V})$$

$$D_6 = B_L + B_H + \frac{Z_\alpha}{V} - K_\theta K_{r\theta} N_5$$

$$D_5 = W_L^2 + B_L \frac{Z_\alpha}{V} + M_\alpha + B_L B_H + B_H \frac{Z_\alpha}{V} + W_H^2 - K_\theta K_{r\theta} N_4 - K_\theta N_5$$

$$D_4 = B_L M_\alpha + W_L^2 \frac{Z_\alpha}{V} + B_H W_L^2 + B_H B_L \frac{Z_\alpha}{V} + B_H M_\alpha + W_H^2 B_L + W_H^2 \frac{Z_\alpha}{V} - K_\theta K_{r\theta} N_3 - K_\theta N_4$$

$$D_3 = W_L^2 M_\alpha + B_H B_L M_\alpha + B_H W_L^2 \frac{Z_\alpha}{V} + W_H^2 W_L^2 + W_H^2 B_L \frac{Z_\alpha}{V} + W_H^2 M_\alpha - K_\theta K_{r\theta} N_2 - K_\theta N_3$$

$$D_2 = B_H W_L^2 M_\alpha + B_L W_H^2 M_\alpha + W_L^2 W_H^2 \frac{Z_\alpha}{V} - K_\theta K_{r\theta} N_1 - K_\theta N_2$$

$$D_1 = W_L^2 W_H^2 M_\alpha - K_\theta K_{r\theta} N_0 - K_\theta N_1$$

$$D_0 = -K_\theta N_0$$

For the bending mode parameters selected and the plant parameters for time = 40 seconds the transfer function  $H(s)$  is:

$$H(s) = \frac{\theta(s)}{\theta_c(s)} = \frac{34.97(s+48.4)(s-48.7)(s+0.018)(s+0.215+/-j48.65)}{(s+0.01)(s+3.63+/-j6.997)(s-3.54+/-j38.15)(s-2.91+/-j62.25)}$$

The transfer function  $H(s)$  was factored using the "roots" program contained in Ref. [7]. The location of the poles was confirmed by finding the eigenvalues of the A matrix using the "BASMAT" program also contained in Ref. [7]. The poles and zeros of  $H(s)$  are plotted in Figure 2-16.

The system composed of the plant plus bending modes is clearly unstable with four poles of the closed loop transfer function in the right half of the S-plane.

Figure 2-17 shows the simulation the system shown in Figure 2-9 for a step input of 0.1 radians. Line 1 of Figure 2-17 is the response of the plant without bending modes and line 2 is the response of the system composed of the plant with bending modes. The vertical scaling in Figure 2-17 was restricted to keep the response of the plant in proper perspective. The restriction of the vertical scale causes saturation of the plot of the system response (line 2). Figure 2-18 shows the response of the system with the vertical scale extended to remove the effects of saturation of the plot. For clarity, the response of the plant without bending modes was not included in Figure 2-18.

To validate the simulation, the time response of the state equations with a 0.1 radian step input was determined by using the "RTRESP" program contained in Ref. [7]. The pitch angle of the missile,  $\theta$  was found to be described by the equation:

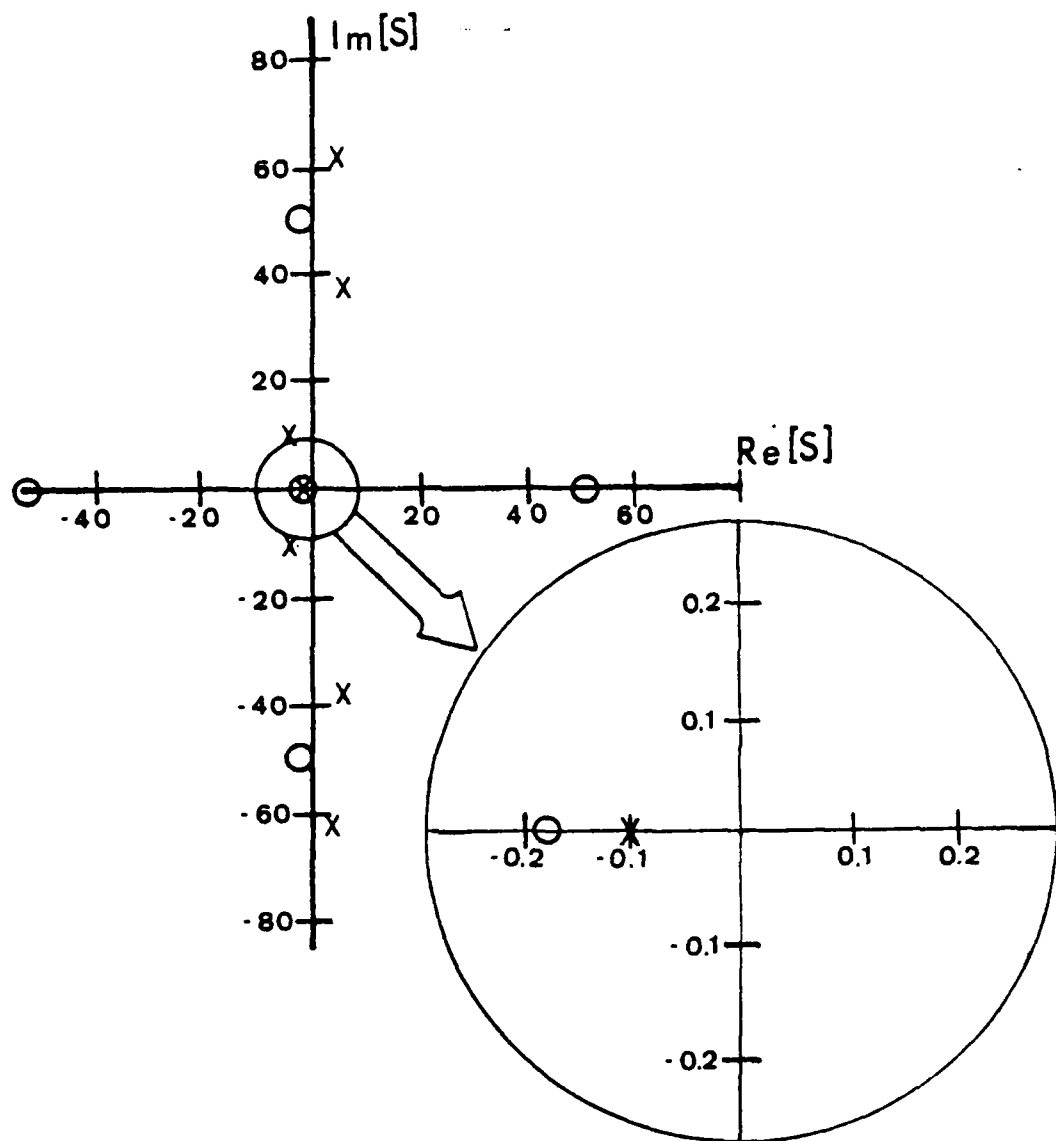
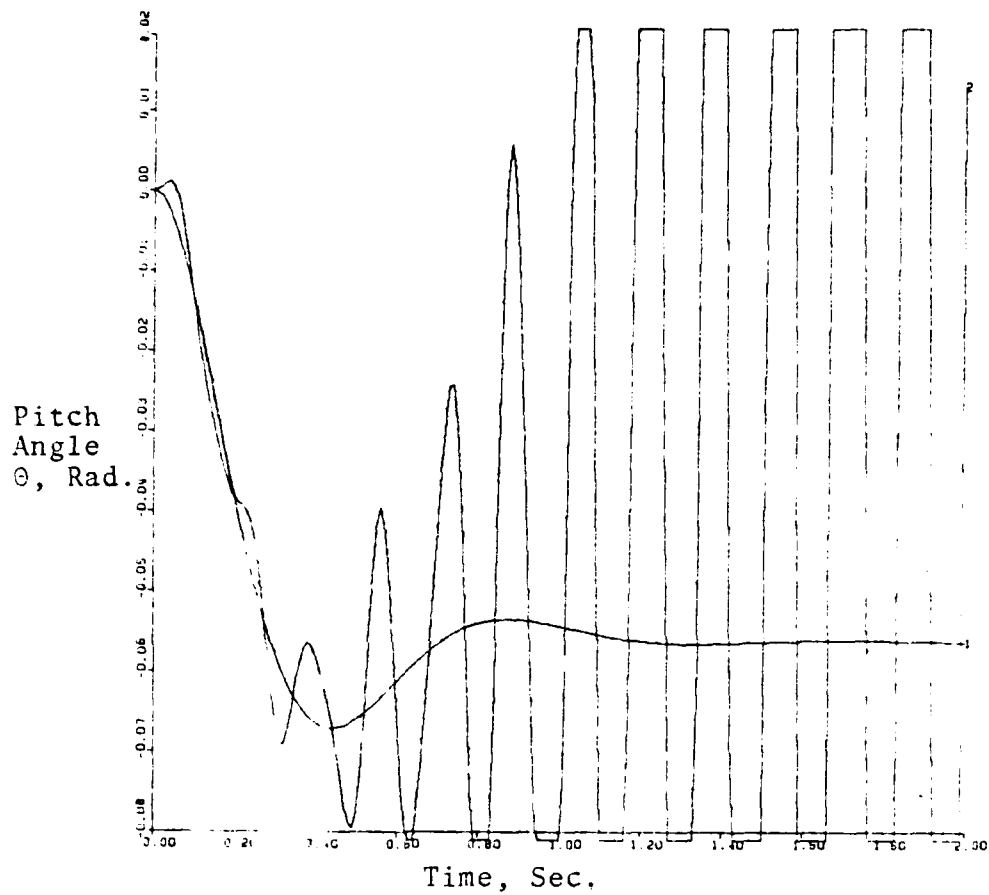


Figure 2-16 Location of Pole and Zeros of the Plant with Two Bending Modes



System; Third order missile model with two bending modes and no adaptive notch filters

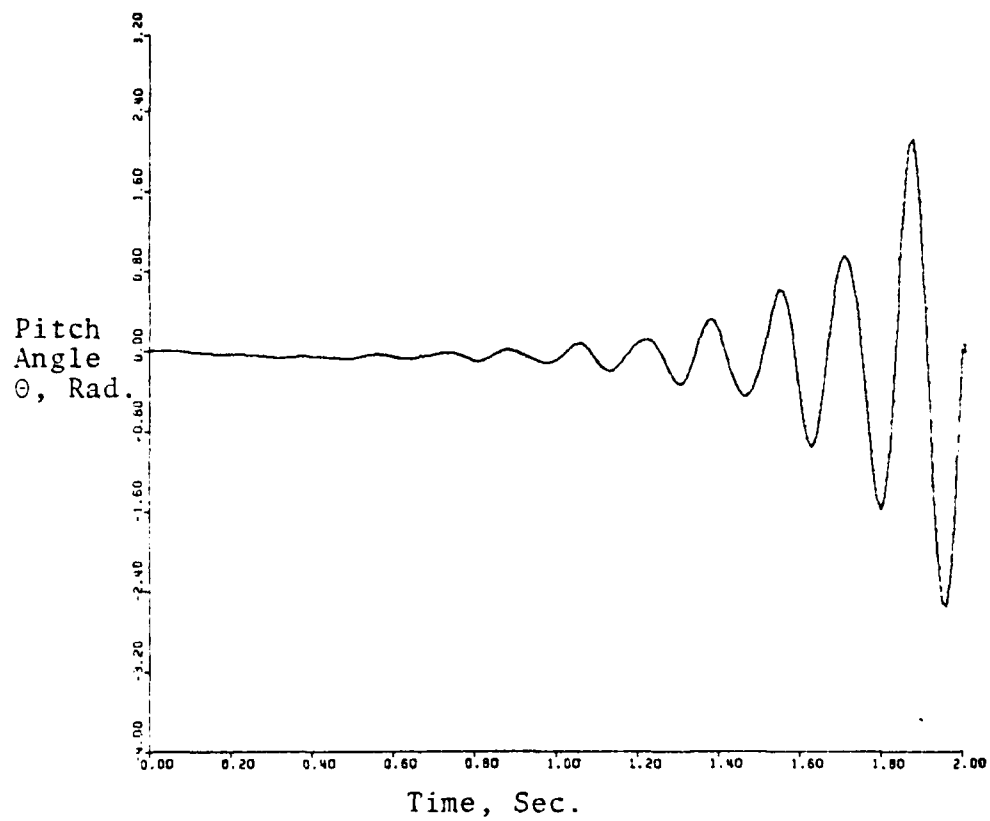
Input: 0.1 radian step command

Line 1 is the nominal missile response without bending modes

Line 2 is the missile response with two bending modes

Figure 2-17 Missile Response with Two Bending Modes





System: Third order missile model with two bending modes and no adaptive notch filters

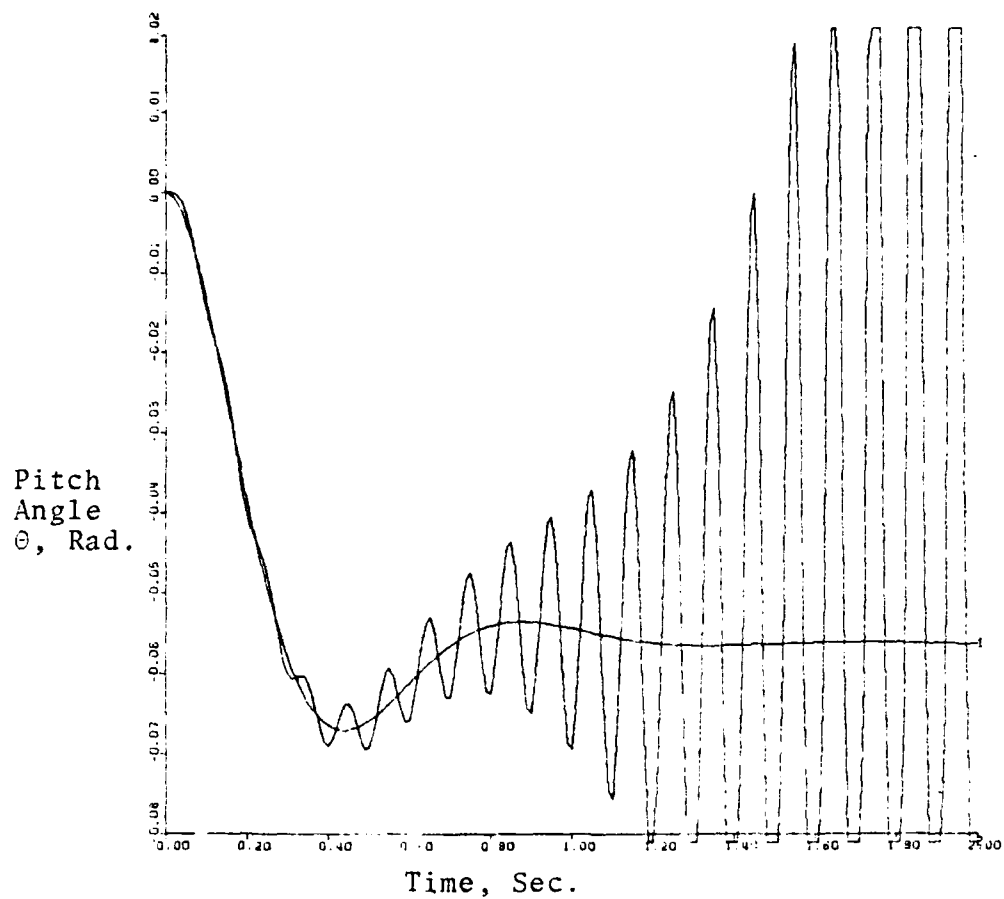
Input: 0.1 radian step command

Figure 2-18 Missile Response with Two Bending Modes (Expanded Scale)

$$\begin{aligned}\theta(t) = & -0.09952 + 0.0457 e^{-0.01t} \\ & + 0.0582 e^{-3.63t} \cos(6.997t-0.41) \\ & + 0.00246 e^{3.54t} \cos(38.15t-2.45) \\ & + 0.00093 e^{2.91t} \cos(62.25t+3.06)\end{aligned}$$

At time = 1.0 seconds, the above equation indicates the pitch angle will be  $\theta(1) = -0.10162$  radians. The numerical results of the simulation used to generate Figure 2-17 indicate the pitch angle to be  $\theta(1) = -0.1017$  radians. The preceeding results indicate the simulation program is valid.

The system was simulated with only the high frequency bending mode and with only the low frequency bending mode. The purpose of these simulations was to show that each bending mode would by itself destabilize the system and that the frequency of the oscillation of the resulting unstable system would reflect very nearly the center frequency of the bending mode that destabilized the system. Figure 2-19 illustrates the response of the system for a 0.1 radian step input when only the high frequency bending mode was present. Figure 2-20 shows the same simulation with an expanded vertical scale. Figure 2-21 shows the response of the system for a 0.1 radian step input with only the low frequency bending mode present. Figure 2-22 shows the same simulation with an expanded vertical scale. Figure 2-23 shows the system response with both bending modes for a ramp input  $\theta_c(t) = 0.05t$ .



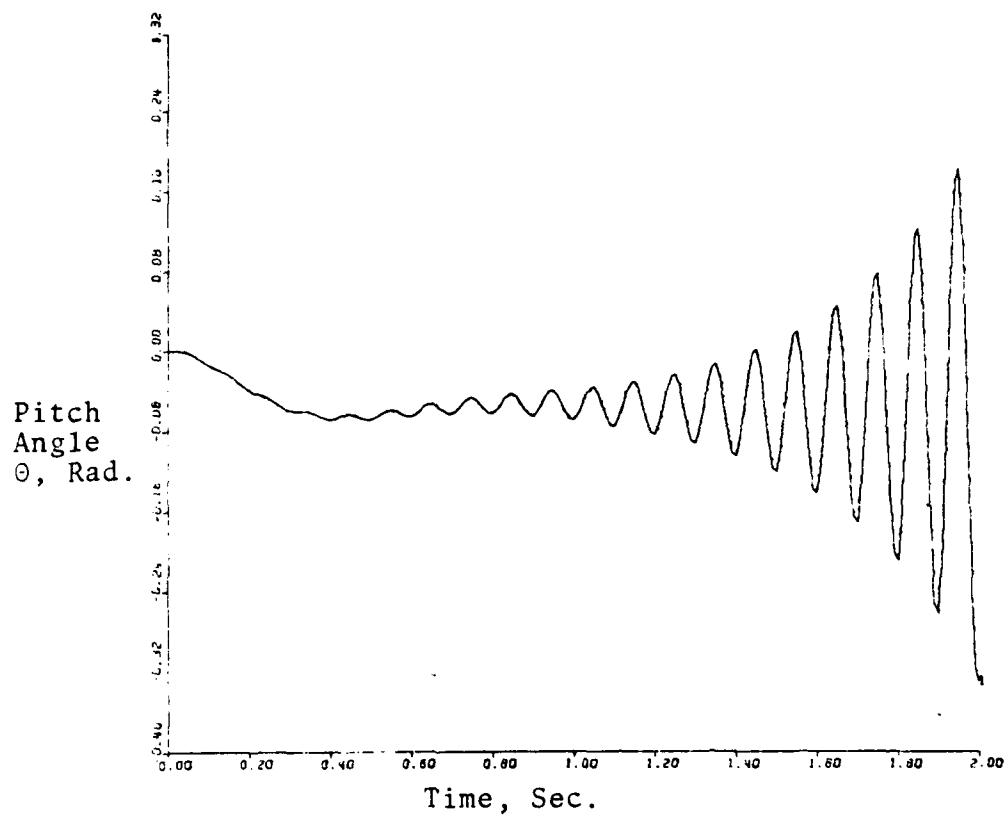
System; Third order missile model with 10 Hz bending mode and no adaptive notch filter

Input: 0.1 radian step command

Line 1 is the nominal missile response without bending modes

Line 2 is the missile response with 10 Hz bending modes

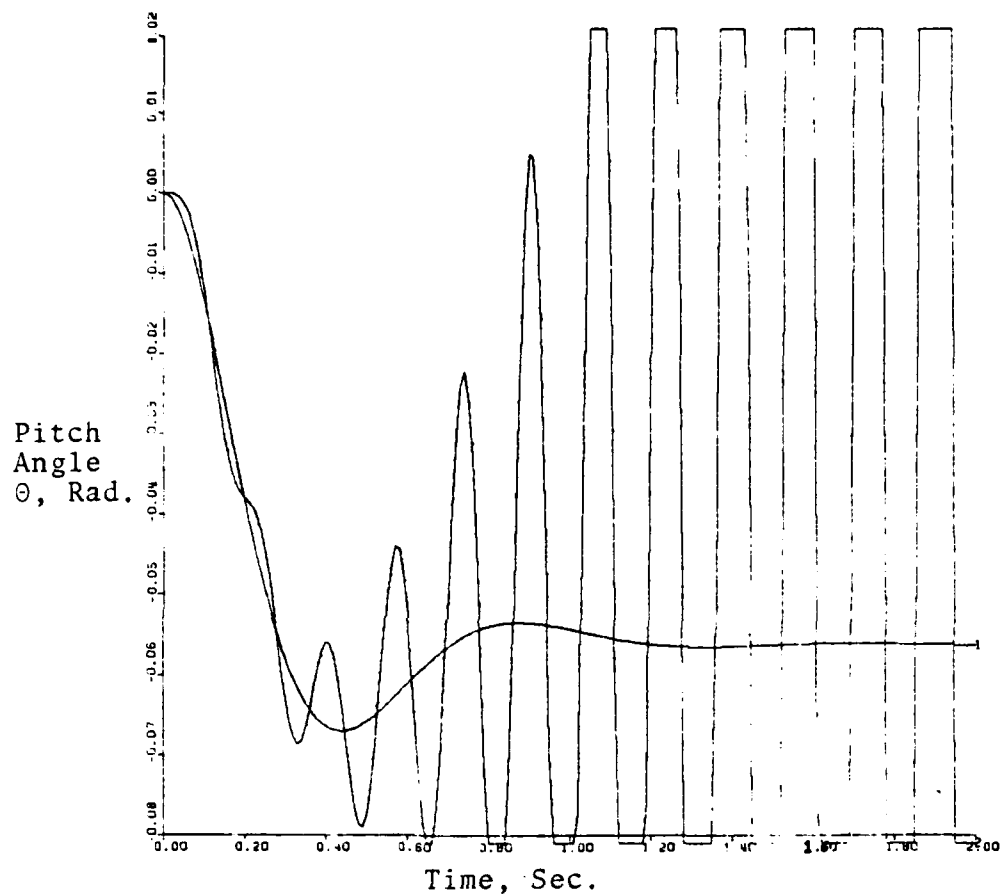
Figure 2-19 Missile Response with 10 Hz Bending Modes



System: Third order missile model with 10 Hz bending mode and no adaptive notch filter

Input: 0.1 radian step command

Figure 2-20 Missile Response with 10 Hz Bending Mode (expanded scale)



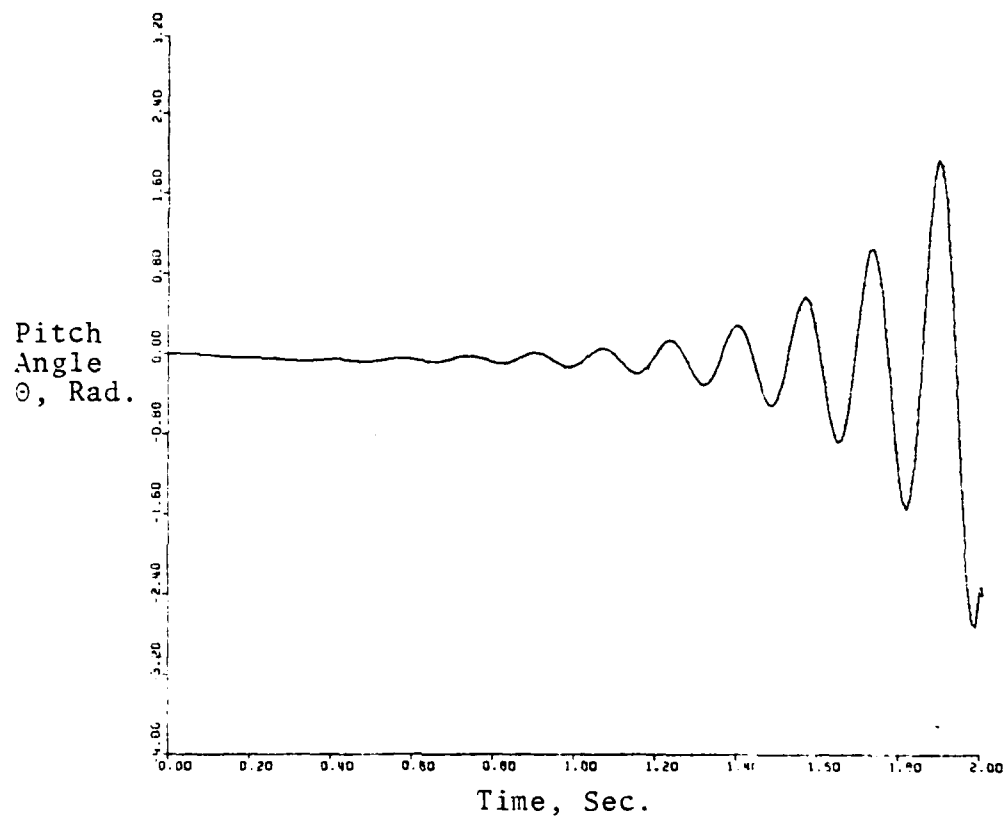
System: Third order missile model with 6 Hz bending mode and no adaptive notch filters

Input: 0.1 radian step command

Line 1 is the nominal missile response without bending modes

Line 2 is the missile response with 6 Hz bending modes

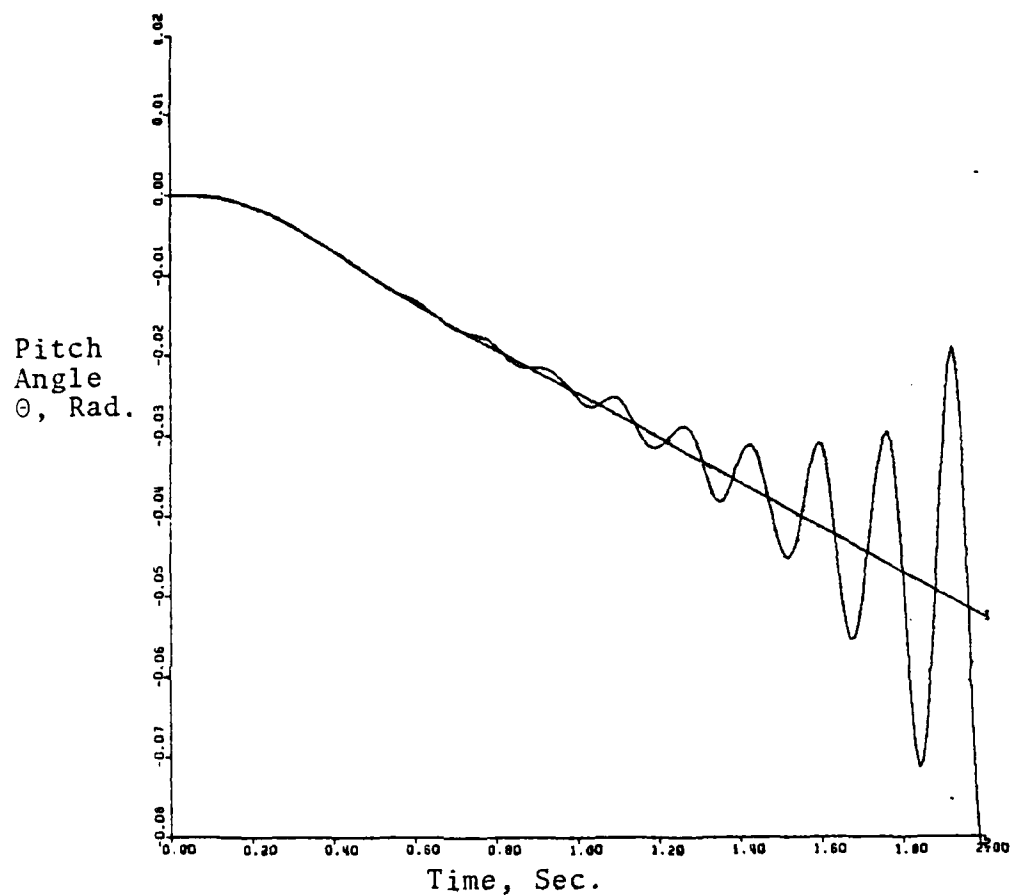
Figure 2-21 Missile Response with 6 Hz Bending Mode



System: Third order missile model with 6 Hz bending mode and no adaptive notch filters

Input: 0.1 radian step command

Figure 2-22 Missile Response with 6 Hz Bending Mode (expanded scale)



System: Third order missile model with 6 and 10 Hz bending modes and no adaptive notch filters

Input: 0.05 radian/sec ramp command

Line 1 is the nominal missile response without bending modes

Line 2 is the missile response with bending modes

Figure 2-23 Missile Response for a Ramp Input with Bending Modes

Figures 2-19 through 2-22 clearly indicate that each bending mode is in itself destabilizing. Analysis of the numerical data associated with Figures 2-19 through 2-22 confirms that the frequency of the oscillations is essentially at the frequency of the bending mode center frequency.



### III. ADAPTIVE DIGITAL FILTER DESIGN

#### A. FACTORS AFFECTING THE DESIGN

The emphasis of the design was simplicity. Significant improvement in the results could have been achieved by use of higher order filters and by using more sophisticated filters, but the improved performance would have been accomplished at the expense of obscuring the very simplicity which makes the proposed technique so appealing.

The sampling frequency used throughout this thesis is 100 hertz. This selection is dictated by the sampling frequency used by the autopilot in the Trident Missile. Higher sampling frequencies were found not to significantly improve the performance of the algorithm, however, sampling frequencies lower than 60 Hz degraded the algorithm to where it would not perform reliably.

The bending mode frequencies were selected such that one and only one bending mode would be in each of the bands of 5-8 hertz and 8-12 hertz as shown in Figure 2-6. A priori knowledge of the band or range of frequencies over which a given bending mode may vary during the flight of the missile is essential in this design. If specific events during the flight such as staging change the bands of the bending modes then the algorithm may also be modified to adapt to the new distribution with the only requirement being that the times

or events which change the band limitations be preprogrammed in the microprocessor algorithm.

## B. DESIGN OF THE ALGORITHM MODULES

Figure 3-1 shows the modular nature of the algorithm for the determination, tracking and notch filtering of the bending mode signals. The sequence of modules associated with the determination, tracking and notch filtering for each of the bending modes are collectively termed a channel. The channels are identical except for the numerical values of the coefficients; therefore, only the design of the 8-12 hertz (high) channel is presented in detail. The results of the design of each of the modules comprising the low channel are presented when different from the corresponding module in the high channel.

### 1. The Bandpass Filter Module

The overall bandpass filter was designed as two cascaded second-order bandpass sections. The first section is a first-order Butterworth lowpass Filter transformed into a bandpass filter and then transformed into the z-domain using the bilinear transformation. The second section is also a bandpass filter designed to adjust the overall shape of the gain curve to the desired form.

A first-order Butterworth lowpass Filter normalized to a cutoff frequency of 1 radian/second has a transfer function:

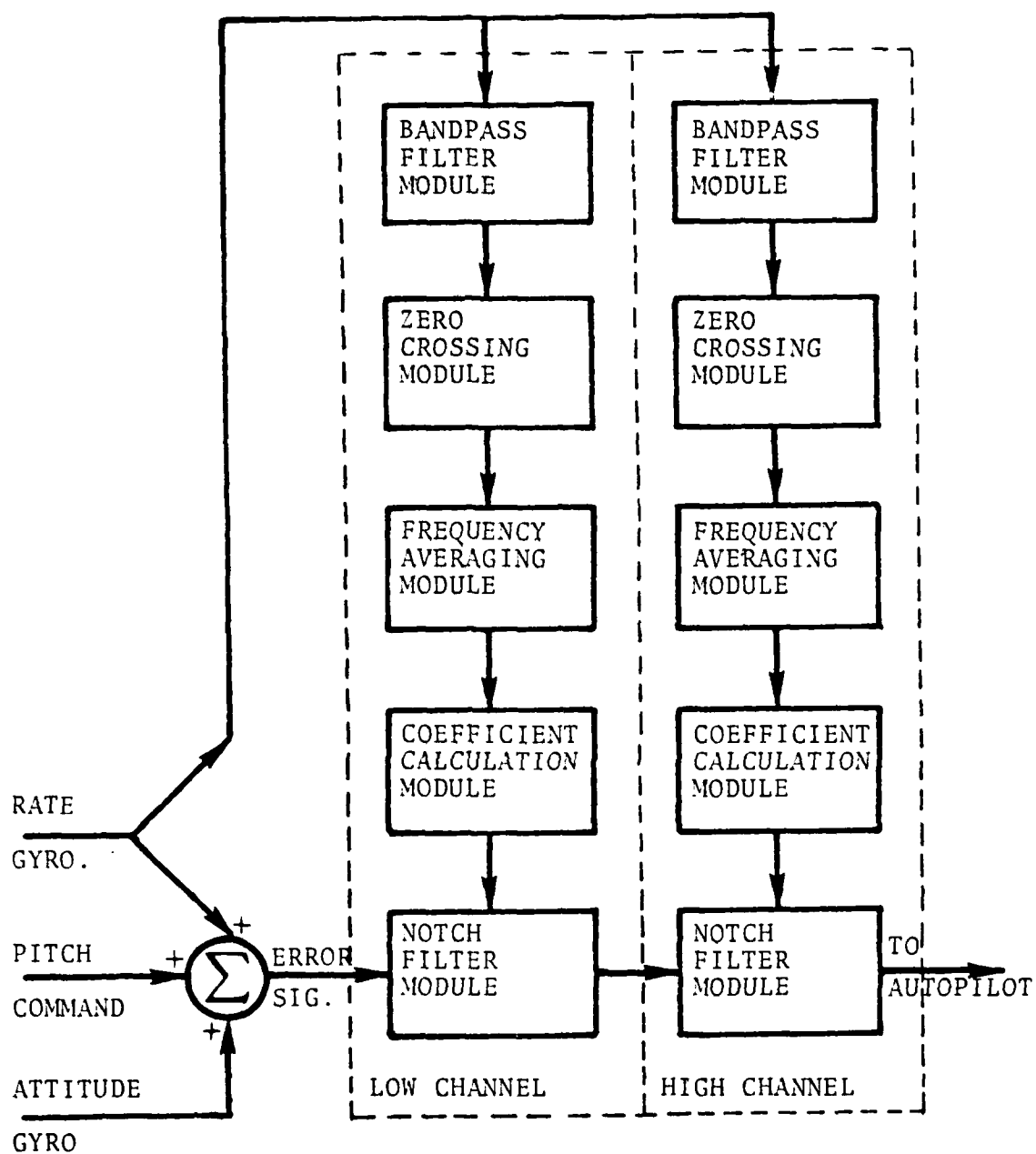


Figure 3-1 Adaptive Notch Filter Algorithm Modules

$$H_{LP}(s) = \frac{1}{s + 1}$$

The transformation from lowpass to bandpass is:

$$s \rightarrow \frac{s^2 + W_c^2}{Bs}$$

where:

B is the 3 dB bandwidth defined as  $W_c - W_L$

$W_c$  is the center frequency defined as  $\sqrt{W_c W_L}$

$W_c$  is the upper 3 dB frequency in rad/sec and  $W_L$  is the lower 3 dB frequency in rad/sec.

The resulting analog domain transfer function for the bandpass filter is:

$$H_{BP}(s) = \frac{Bs}{s^2 + Bs + W_c^2} \quad (4)$$

Before applying the bilinear transformation to transform the analog bandpass filter to the discrete domain it is necessary to prewarp the center frequency  $W_c$  [8]. The prewarping is done by using the following transformation:

$$W_A = \frac{2 \tan\left(\frac{\Omega_D}{2}\right)}{T} \quad (5)$$

where:

$\Omega_D$  is the desired discrete or digital frequency defined as:

$$\Omega_D = W_c T$$

T is the sampling frequency.

$W_c$  is the analog center frequency defined as  $W_c = (W_u W_L)^{1/2}$

Selecting 8.0 hertz as the lower cutoff frequency and 12.0 hertz as the upper cutoff frequency. The values to be used in equations (4) and (5) become:

$$W_L = 2\pi \cdot 8.0 = 50.265 \text{ rad/sec}$$

$$W_u = 2\pi \cdot 12.0 = 75.398 \text{ rad/sec}$$

$$W_c = (W_u W_L)^{1/2} = 61.652 \text{ rad/sec}$$

$$B = W_u - W_L = 25.133 \text{ rad/sec}$$

Applying equation (5) with the selected value of  $W_c$  yield the prewarped center frequency:

$$W_A = 63.582 \text{ rad/sec}$$

Substituting the above value, equation (4) becomes:

$$H(s) = \frac{25.133 s}{s^2 + 25.133 s + 4042.77} \quad (6)$$

The bilinear transformation for the s-domain to the z-domain is:

$$s = \frac{2(Z - 1)}{T(Z + 1)}$$

Applying the transformation to equation (6), the discrete transfer function for the bandpass filter becomes:

$$H_1(Z) = \frac{0.103(Z^2 - 1)}{Z^2 - 1.4677 Z + 0.79405}$$

After slight adjustments to obtain the desired gain and crossover frequency with the low frequency channel bandpass filter (see Figure 3-9), the transfer function  $H_1(Z)$  is:

$$H_1(Z) = \frac{0.1 (Z^2 - 1)}{Z^2 - 1.45625 Z + 0.81}$$

The pole and zero configuration of  $H_1(Z)$  is shown in Figure 3-2 and the frequency response of  $H_1(Z)$  is shown in Figure 3-3.

As expected, the frequency response of  $H_1(Z)$  is too flat to provide the needed stopband attenuation for the adjacent channels. The frequency response of the overall bandpass filter is greatly improved by adding a second section of filter with a sharp resonant peak at the center frequency. A bandpass filter with the desired resonant peak was designed directly in the z-domain using a digital filter frequency response program (program 3-5) to adjust the poles and zeros to obtain the desired characteristics. The transfer function of the second filter section is:

$$H_2(Z) = \frac{0.456(Z^2 - 0.809 Z + 0.25)}{Z^2 - 1.3753 Z + 0.7225}$$

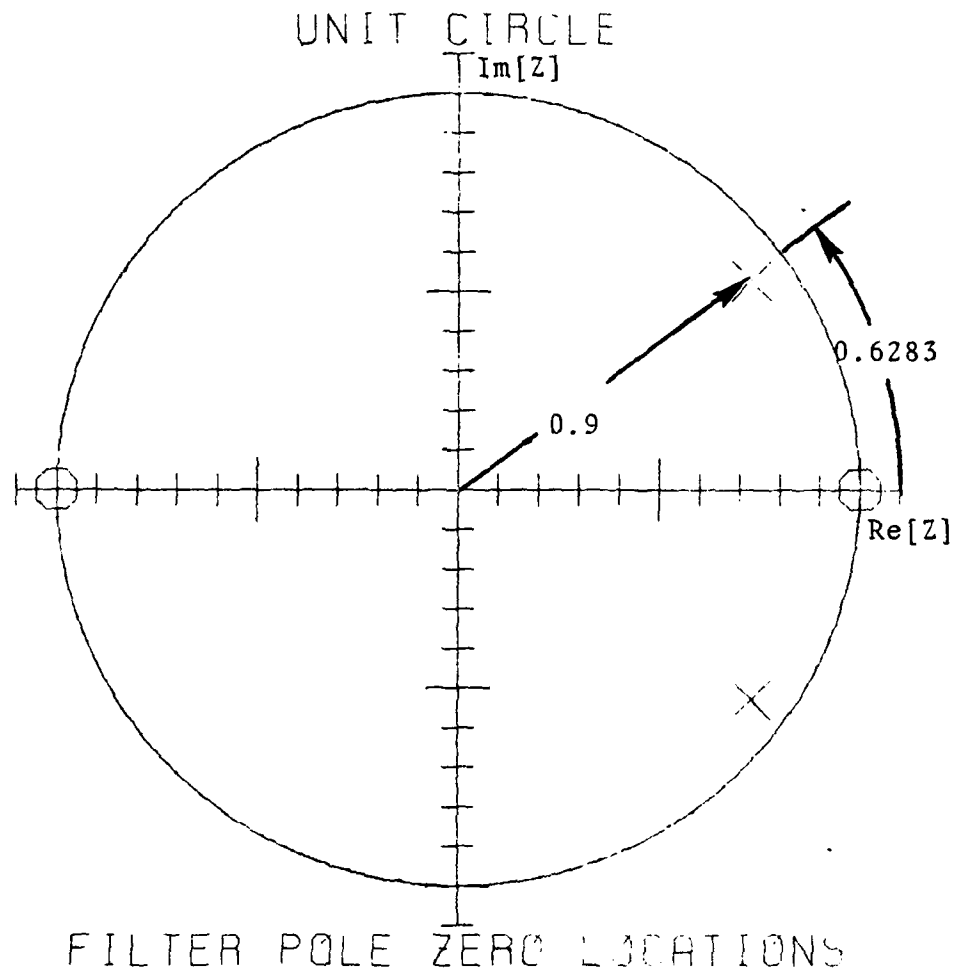


Figure 3-2 Discrete Bandpass Filter  
Pole/Zero Locations

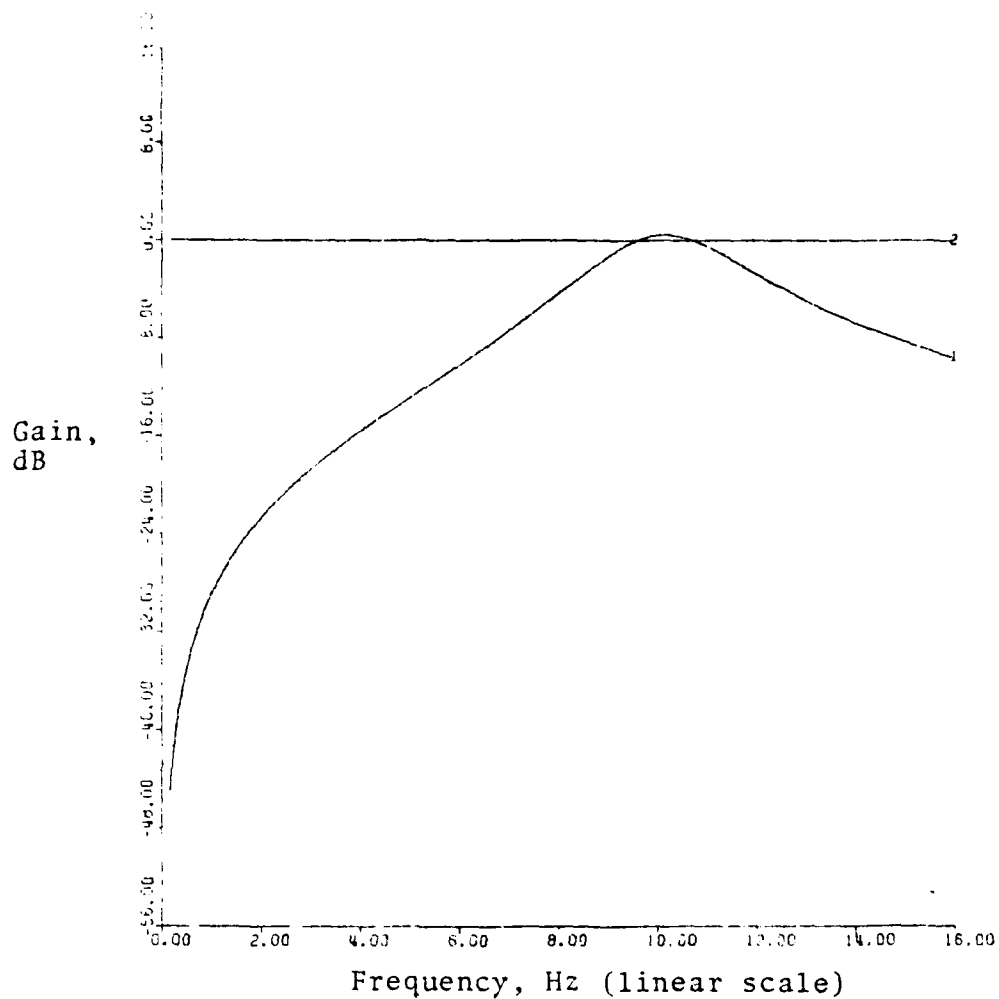


Figure 3-3 Frequency Response of the First Section of the High Frequency Digital Bandpass Filter



The pole and zero configuration of  $H_2(Z)$  is shown in Figure 3-4. The frequency response of  $H_2(Z)$  is shown in Figure 3-5.

Figure 3-6 shows the flow graph of the algorithm for the implementation of the two cascaded sections and Figure 3-7 shows the resulting frequency response of the cascaded sections.

Figure 3-8 shows the frequency response of the low channel bandpass filter designed in the same manner. Figure 3-9 illustrates the resulting band coverage of each channel.

The possibility of a bending mode occurring at the eight-hertz cross-over frequency between channels causing both channels to lock on that frequency and leaving one bending mode unattenuated is compensated for by initializing both notch filters at the cross-over frequency, thereby attenuating a bending mode at eight-hertz immediately and freeing either channel to track and remove the unattenuated bending mode.

## 2. The Zero Crossing Detector Module

The zero crossing detector is based on a linear estimate of the crossing time if the amplitude of the output of the bandpass filter changes signs between samples. Linear estimation of the crossing time is a feature incorporated into the digital simulation language program (DSL) as the cross function but could also be programmed using the algorithm shown in Figure 3-10. The potential for using

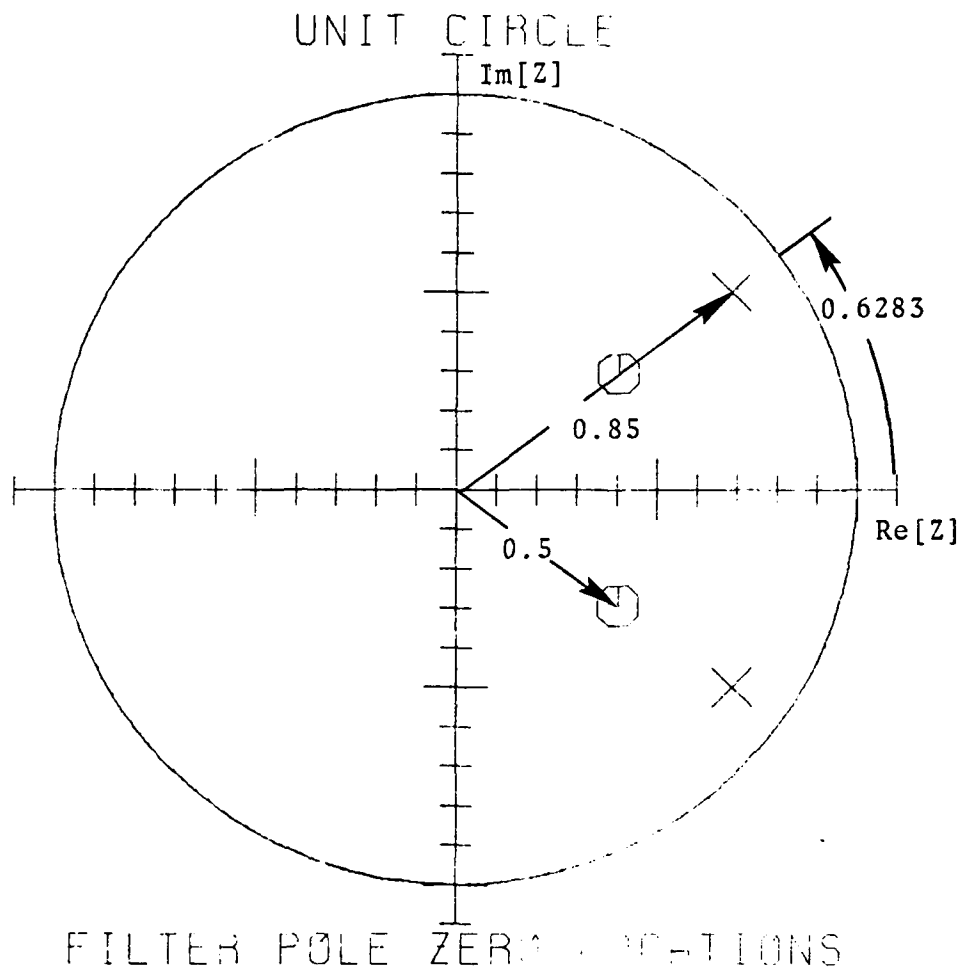


Figure 3-4 Discrete Bandpass Filter  
Pole/Zero Locations

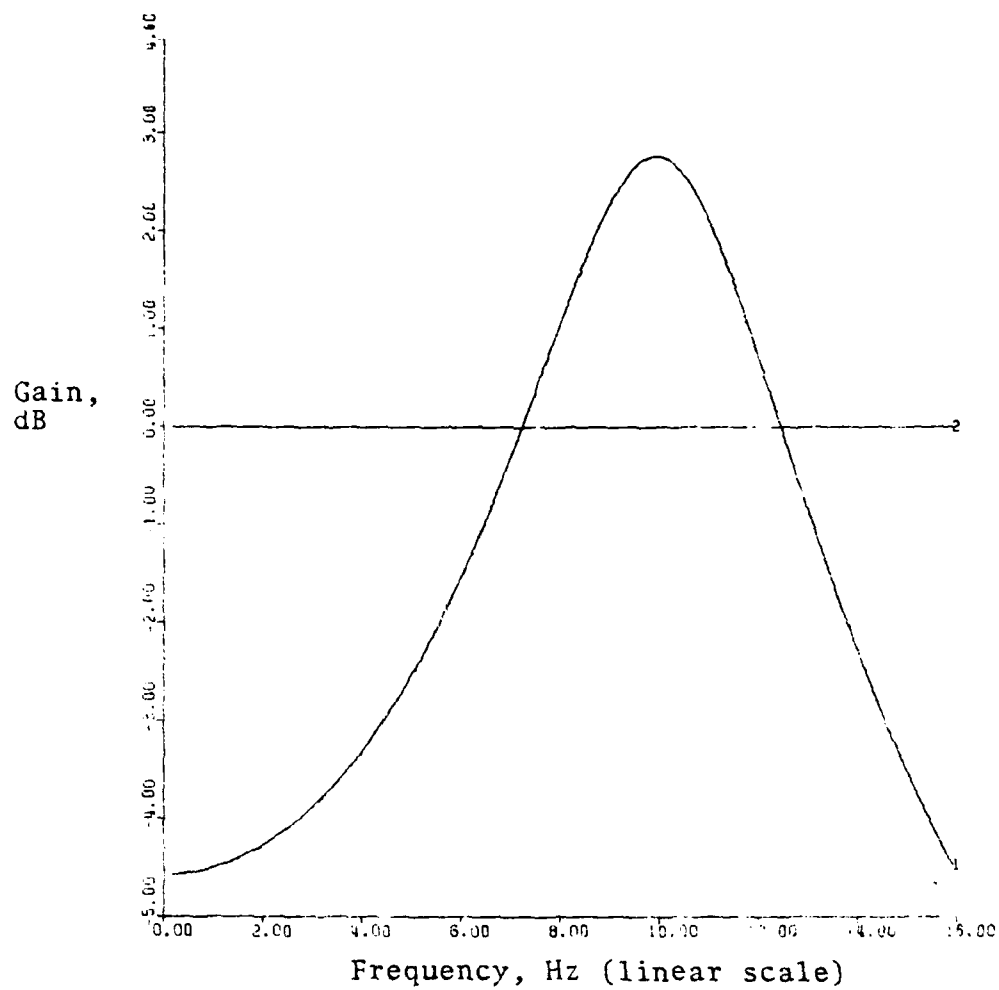


Figure 3-5 Frequency Response of the Second Section of the High Frequency Digital Bandpass Filter

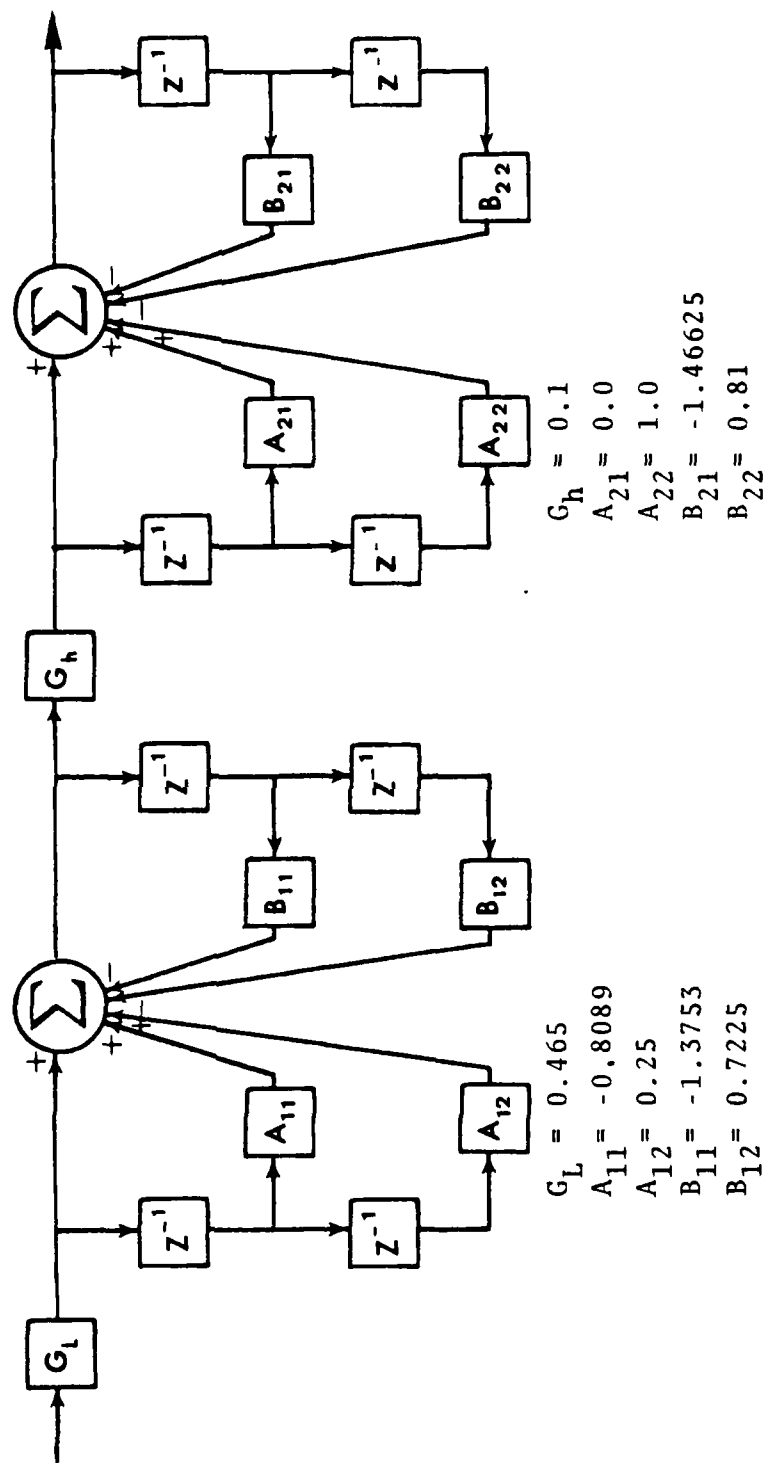


Figure 3-6 Digital Filter Implementation

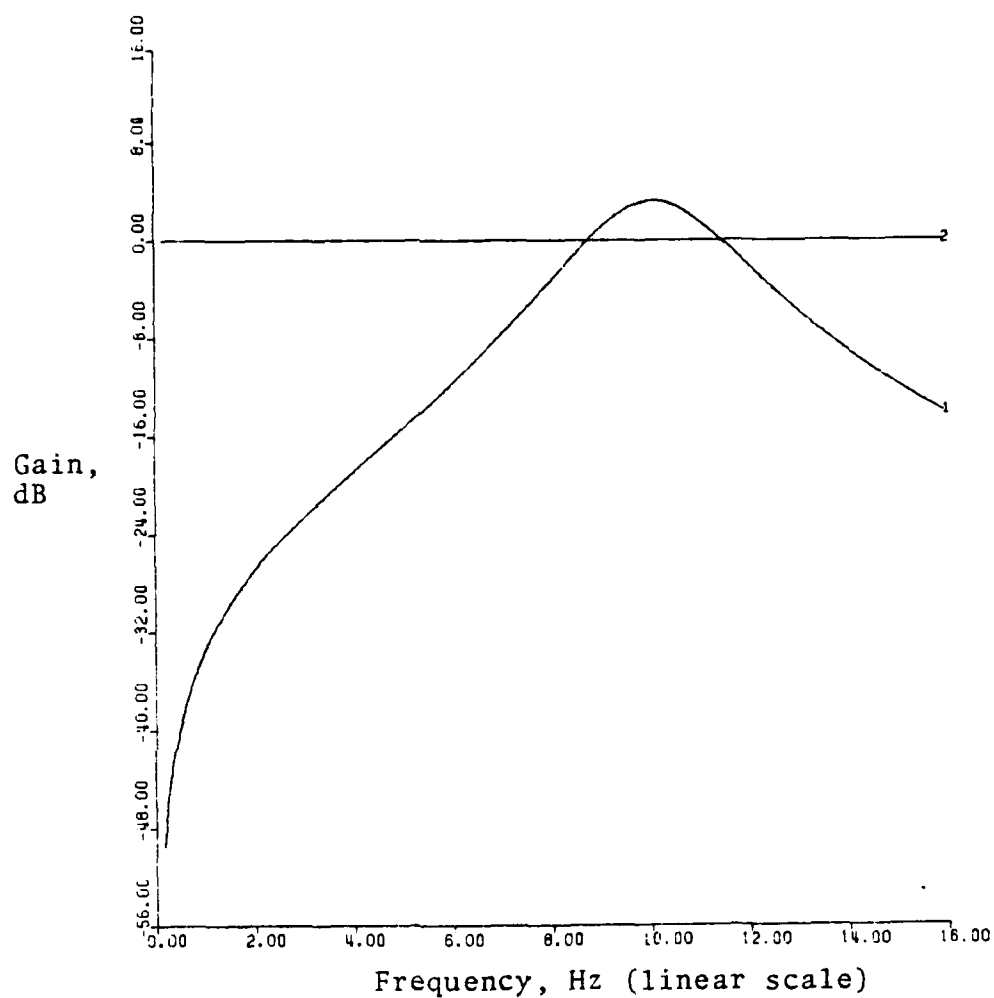


Figure 3-7 Frequency Response of Cascaded Filter Sections of the High Frequency Bandpass Filter

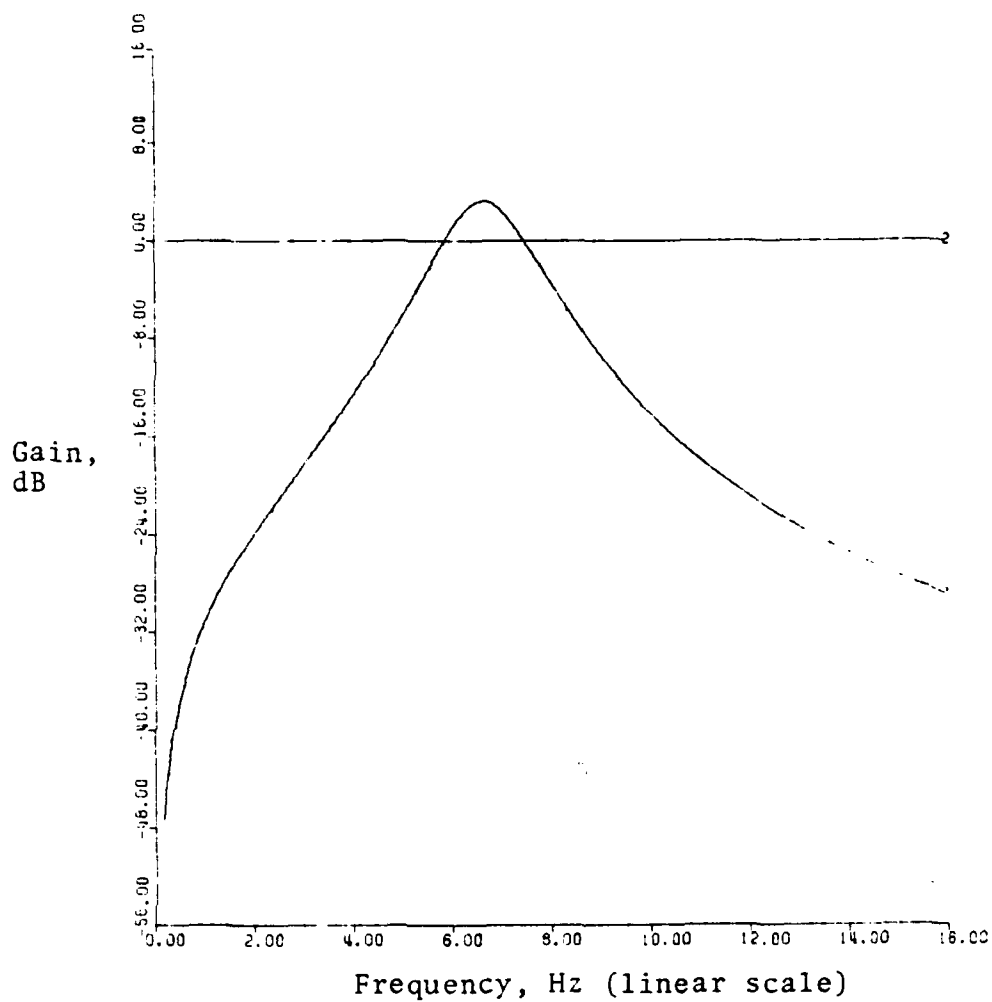


Figure 3-8 Frequency Response of Low Frequency Digital Bandpass Filter

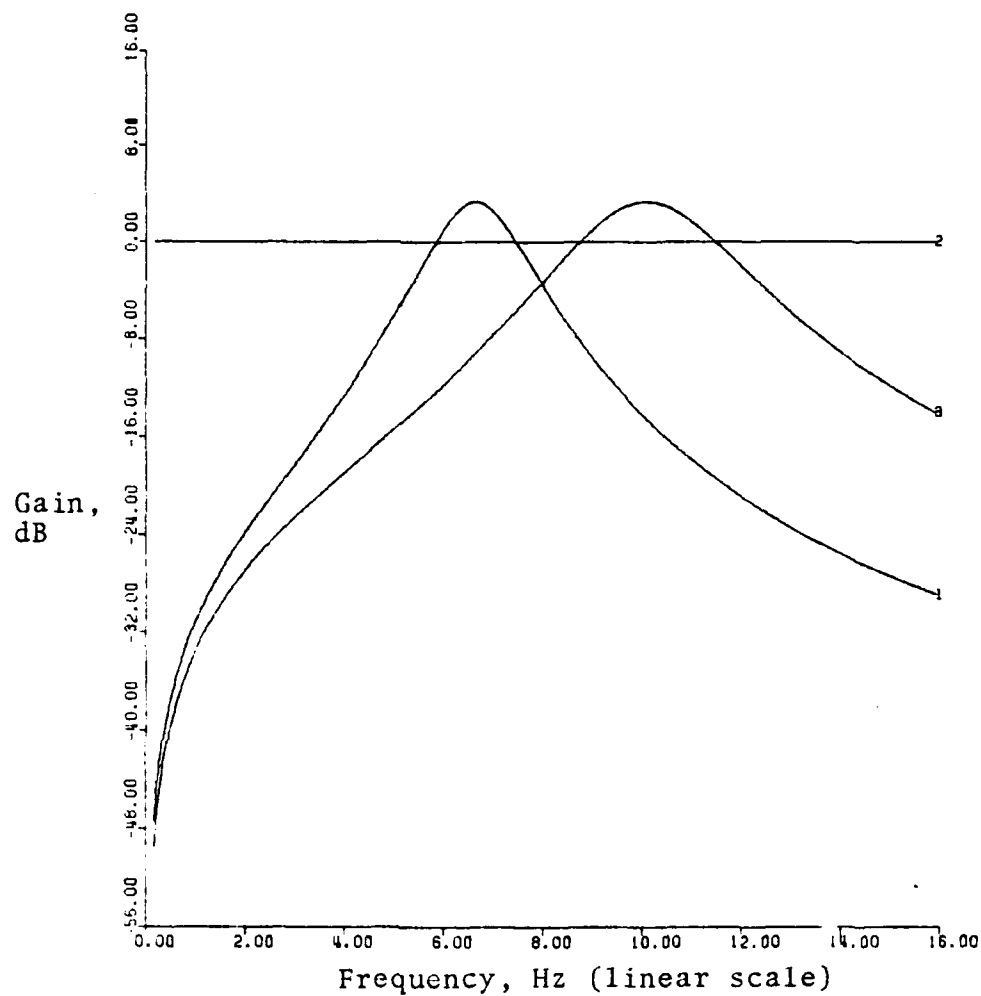
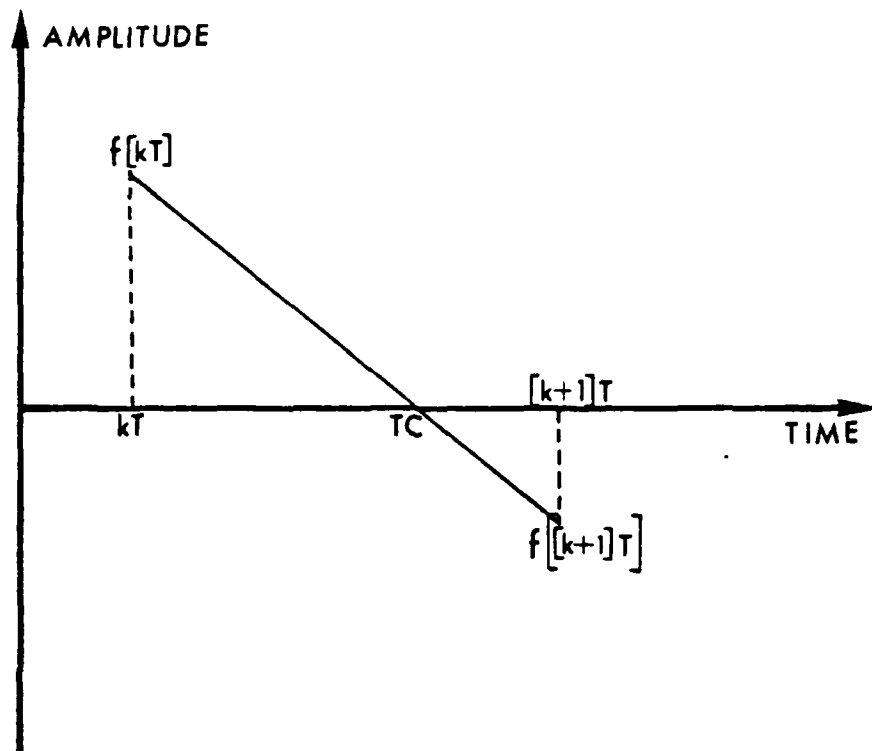


Figure 3-9 Frequency Coverage of High and Low Frequency Digital Bandpass Filter



$$TC = \frac{-f[kT]}{f[(k+1)T] - f[kT]} + kT$$

Figure 3-10 Zero Crossing Time Algorithm



a sinusoidal curve estimation rather than a linear estimation was considered and dismissed because any increase in the accuracy of the estimate of the zero crossing time was offset by the jitter in the actual crossing time caused by leakage into the channel of the adjacent bending mode and plant frequencies.

The major deficiency in the use of a zero crossing detector as a frequency measuring device is the nonlinear error in the frequency estimate as a function of the actual frequency. For example, if the frequency being measured is 5.0 hertz the half-period measured should be 0.1 seconds. If noise caused a 0.01 second measurement error and the measured half-period was 0.09 seconds then the frequency detector would estimate the input frequency to be 5.55 hertz. If the input frequency was 10.0 hertz the same 0.01 second error would result in an estimate of the input frequency of 12.5 hertz, a five times greater error for the same measurement error.

The effect of the nonlinear quality of the estimated frequency in the presence of noise causes a much greater variation in the estimate of the higher frequency bending modes and contributes to the limit cycle problem described below.

### 3. The Frequency Averaging Module

The primary source of limit cycle behavior in the tracking algorithm appears to be due to leakage of an

adjacent bending mode frequency into the zero crossing detector causing a periodic error in the frequency determination. The frequency averaging module simply determines the mean of the last detected frequency from the frequency detector and the current notch filter center frequency. The mean of the two frequencies becomes the new notch filter center frequency. The process of averaging the last detected frequency with the current notch filter center frequency reduces the amplitude of the limit cycle but does not eliminate it. To further reduce the amplitude of the limit cycle, several approaches may be taken:

(a) Greatly improve the stopband attenuation and roll-off characteristics of the bandpass filters. This approach is discussed in the conclusions contained in Chapter Five.

(b) Average the detected frequency over a sufficient number of zero crossings before moving the notch. This approach was found to significantly reduce the amplitude of the limit cycle but was so slow in moving the notch to the correct frequency that the bending modes would increase to such an amplitude that the missile would be destroyed

#### 4. Design of the Notch Filter Module

The design of a discrete notch filter and the calculation of the coefficients is simple and efficient. Figure 3-11 illustrates the pole and zero location of a second-order notch filter on the Z-plane. Since the zero is located on the unit circle, the center frequency  $\omega_c$  of the notch is completely specified by the angle  $\Omega_c$ .

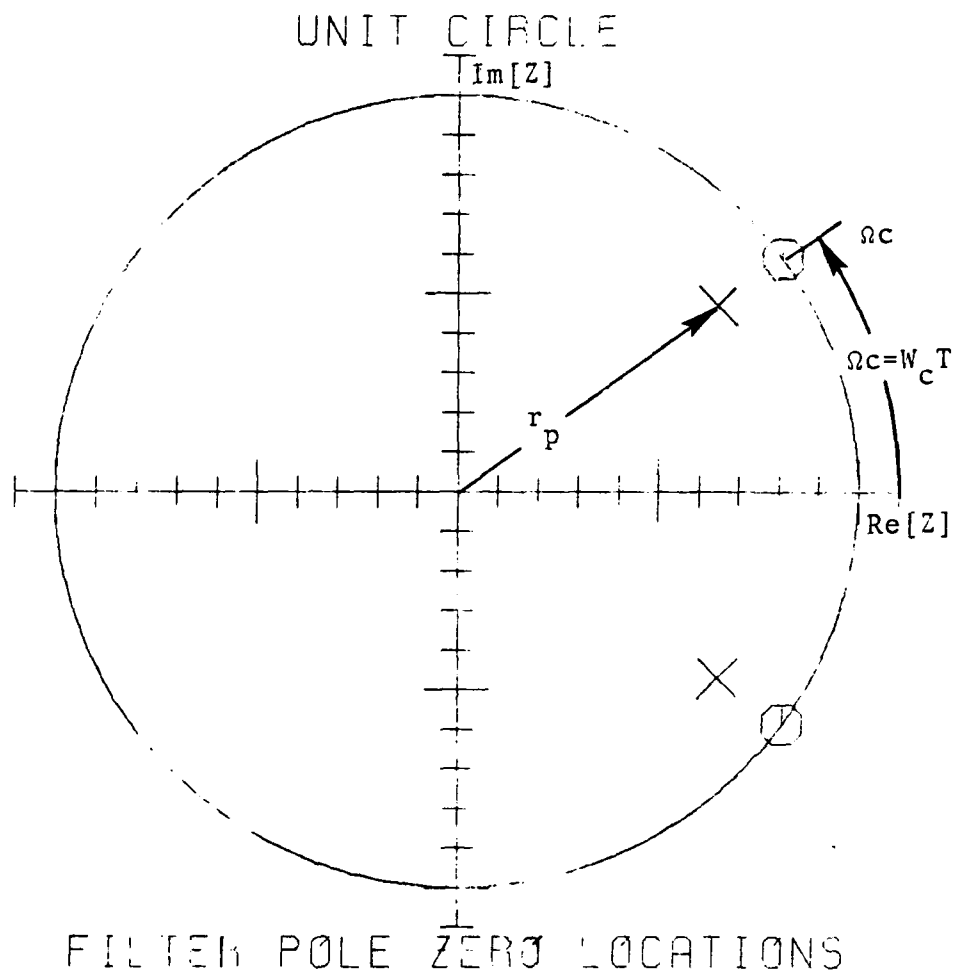


Figure 3-11 General Pole/Zero Locations  
for a Second-Order Discrete  
Notch Filter

The angle  $\Omega_c$  is referred to as the discrete frequency and is defined as the angle from the positive real axis to the zero such that:

$$\Omega_c = W_c T$$

where:

$W_c$  is the desired notch center frequency in rad/sec

$T$  is the sampling period in seconds

The location of the zero on the unit circle at a selected discrete frequency,  $\Omega_c$ , ensures that the center of the notch will be at the desired frequency completely independent of the selected location of the poles. The location of the poles on the same radial (discrete frequency) as the zero maintains the approximate symmetry of the notch. The radius of the poles determines the bandwidth of the notch. The closer the poles are to the unit circle, the narrower the notch will be and the longer the settling time.

The transfer function  $H_N(Z)$  for the notch filter is of the form:

$$H_N(Z) = \frac{G(Z^2 - A1 Z + 1)}{Z^2 - B1 Z + B2}$$

where the coefficients are defined by the following formulas:

$$A1 = 2 \cos (W_c T)$$

$$B1 = 2 r_p \cos (W_c T)$$

$$B2 = r_p^2$$

$r_p$  is the radius of the poles

$W_c$  is the desired center frequency of the notch in rad/sec

$G$  is the gain

For unity DC gain  $H(Z)|_{Z=+1}=1$  yields the formula

$$G = \frac{1 - B_1 + B_2}{2 - A_1}$$

The relationship between the pole radius and the 3 dB bandwidth of the notch filter is a function of center frequency but can be approximated by making certain simplifying assumptions. Figure 3-12 shows the geometry on the unit circle when the discrete frequency,  $W_D T$  is at the 3 dB cutoff frequency. The gain at the cutoff frequency is:

$$G = \frac{|Z_1| |Z_2|}{|P_1| |P_2|} = 0.707 \quad (7)$$

In this application it is reasonable to assume that  $|Z_2| \approx |P_2|$ , the poles are close to the unit circle, and the bandwidth of the filter is small ( $W_c T \approx W_D T$ ). With the above assumptions, equation (7) then reduces to:

$$G = \frac{|Z_1|}{|P_1|} = 0.707 \quad (8)$$

Using the pythagorean theorem and substituting  $Z_1^2 = 0.5 P_1^2$  from equation (8) the following relationship can be found:

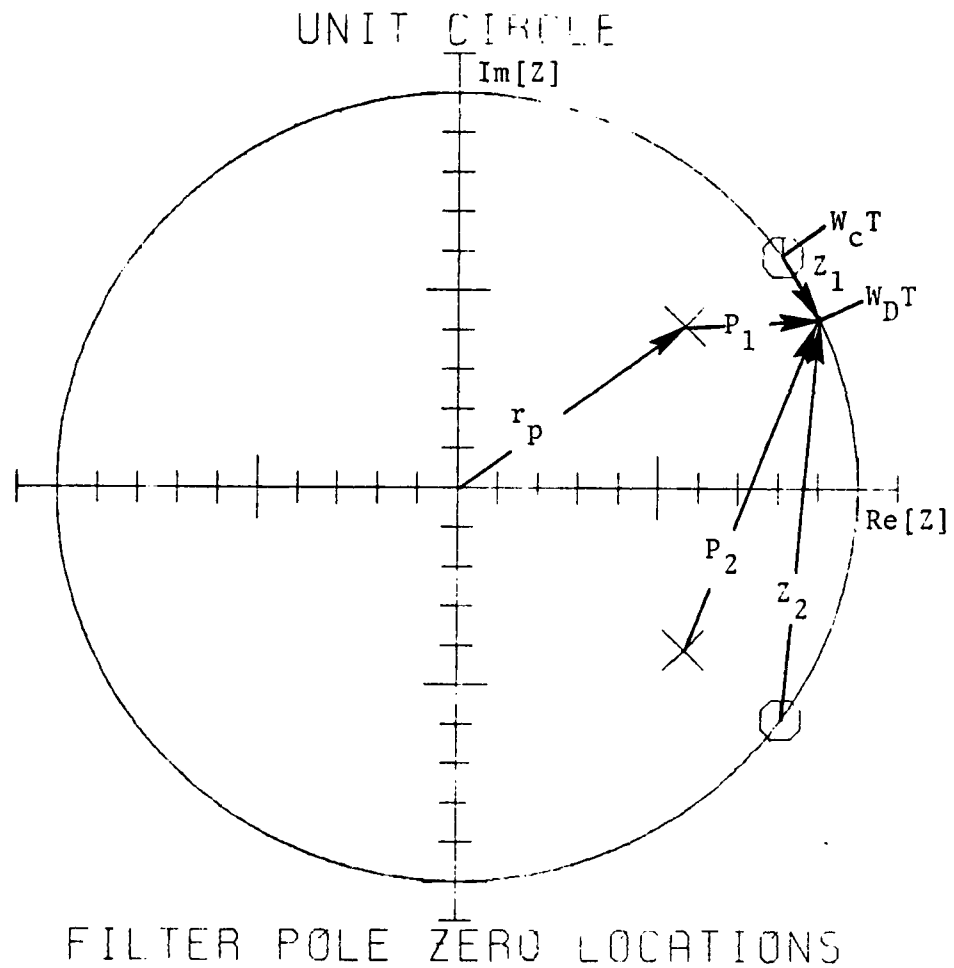


Figure 3-12 Vectors Used to Calculate  
Notch Filter Bandwidth

$$(1 - r_p) = Zl \quad (9)$$

For small angles the cord can be assumed to be equal to the ARC length, therefore:

$$Zl = W_c T - W_D T = 0.5 B_D = 0.5 B_W T \quad (10)$$

where:

$B_D$  is the discrete bandwidth in rad

$B_W$  is the analog bandwidth in rad/sec

Substituting equation (10) into equation (9) and solving for  $B_W$  yields the approximate relationship between the notch filter analog frequency bandwidth and the pole radius in the discrete domain.

$$B_W = \frac{2(1 - r_p)}{T} \quad (11)$$

The numerical data associated with the frequency response curves for the notch filters indicates that equation (11) yields bandwidths that are larger than the desired bandwidths but the error is less than 10 percent in the frequency range of 5 to 15 hertz.

Figure 3-13 shows the gain vs frequency response of the low channel notch filter with a center frequency of 6.0 hertz and a pole radius of 0.9. This configuration has a

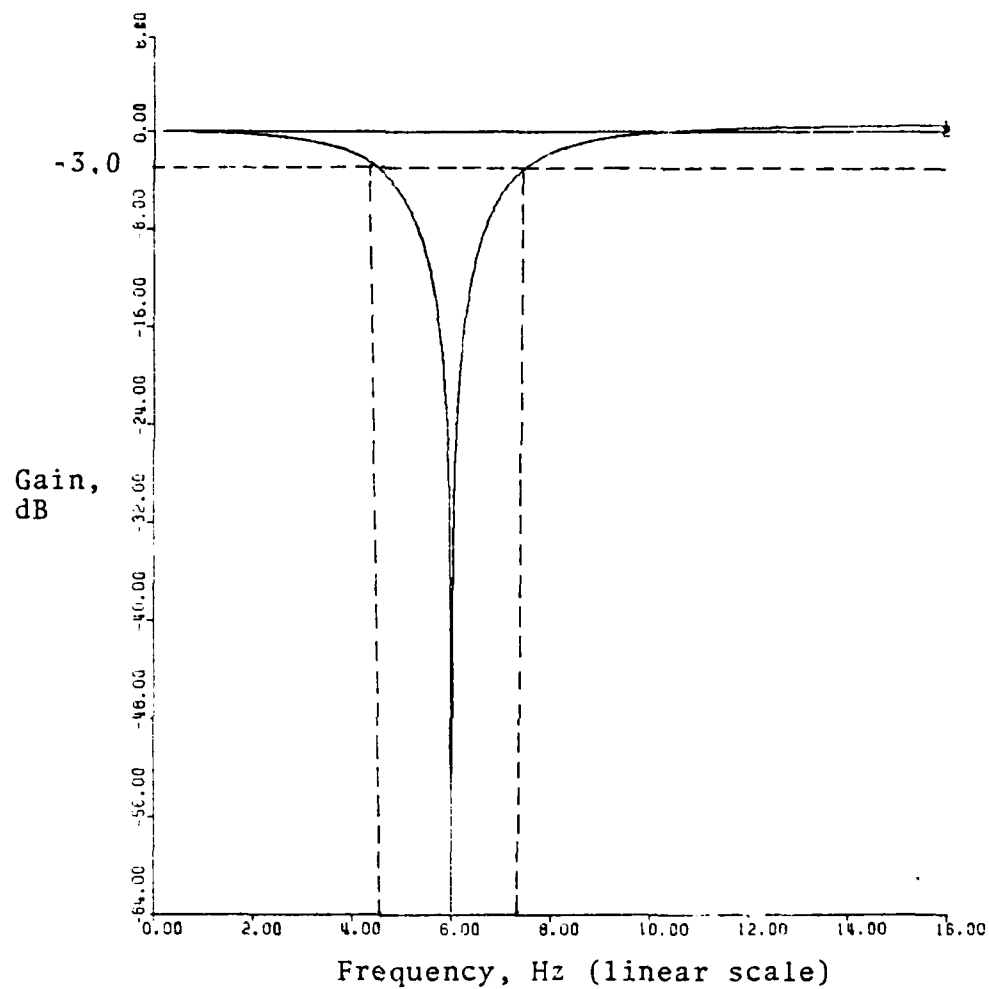


Figure 3-13 Frequency Response of Digital Notch Filter with 0.9 Pole Radius Centered at 6 Hz



3 dB bandwidth of 2.95 hertz. Figure 3-14 shows the phase vs frequency response of the same notch filter.

Figure 3-15 shows the gain vs frequency response of the high channel notch filter with a center frequency of 10.0 hertz and a pole radius of 0.8. This configuration has a 3 dB bandwidth of 5.9 hertz. Figure 3-16 shows the phase vs frequency response of the same notch.

The argument used to create Figure 2-6 established that the higher of the two bending modes would have a wider bandwidth than the lower frequency bending mode, therefore the bandwidth of the notch filter for the high channel was designed to be wider than the low channel. There is a limit to which the notch bandwidth can be increased without inducing excessive phase loss at the plant operating frequency of two-hertz. For the notch bandwidths used in this algorithm the high channel, with the notch centered at 10.0 hertz, introduces a phase loss of 7.75 degrees at two-hertz and the low channel, with the notch centered at 6.0 hertz, introduces a phase loss of 11.0 degrees at two-hertz. The combined phase loss introduced by the notch filters used in this algorithm does not have a pronounced effect on the stability of the plant.

##### 5. Flow Chart of the Algorithm

Figure 3-17 provides a flow chart of the entire algorithm. The "prime time" computations are the processing of the error signal and outputting the filtered value to the

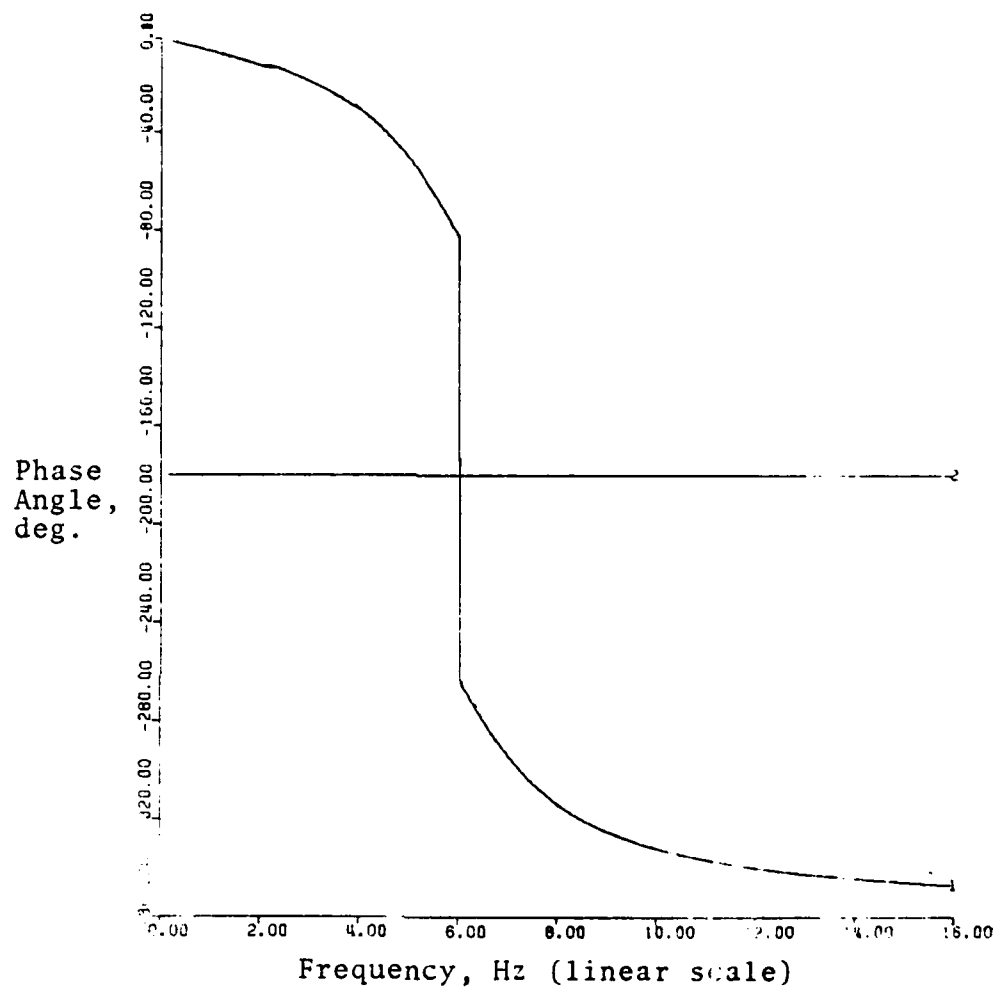


Figure 3-14 Frequency Response of Digital Notch Filter with 0.9 Pole Radius Centered at 6 Hz

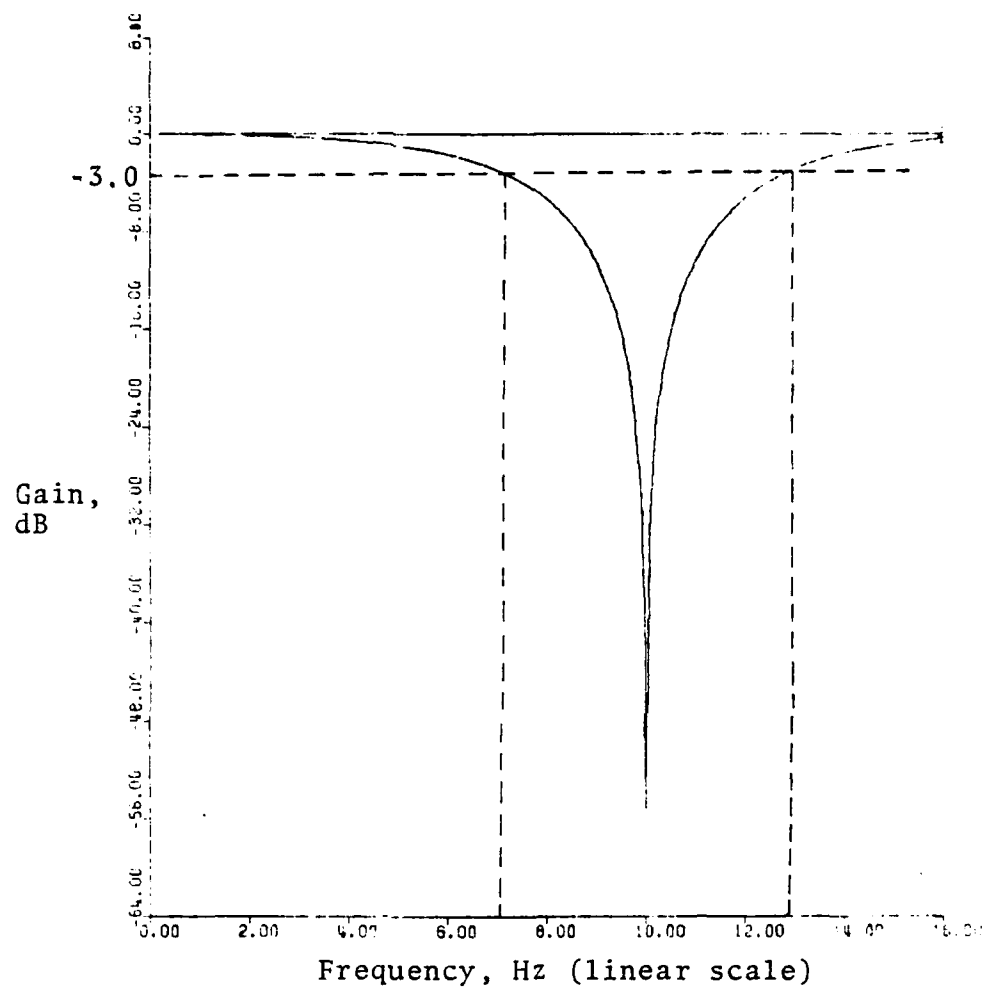


Figure 3-15 Frequency Response of Digital Notch Filter with 0.8 Pole Radius Centered at 10 Hz

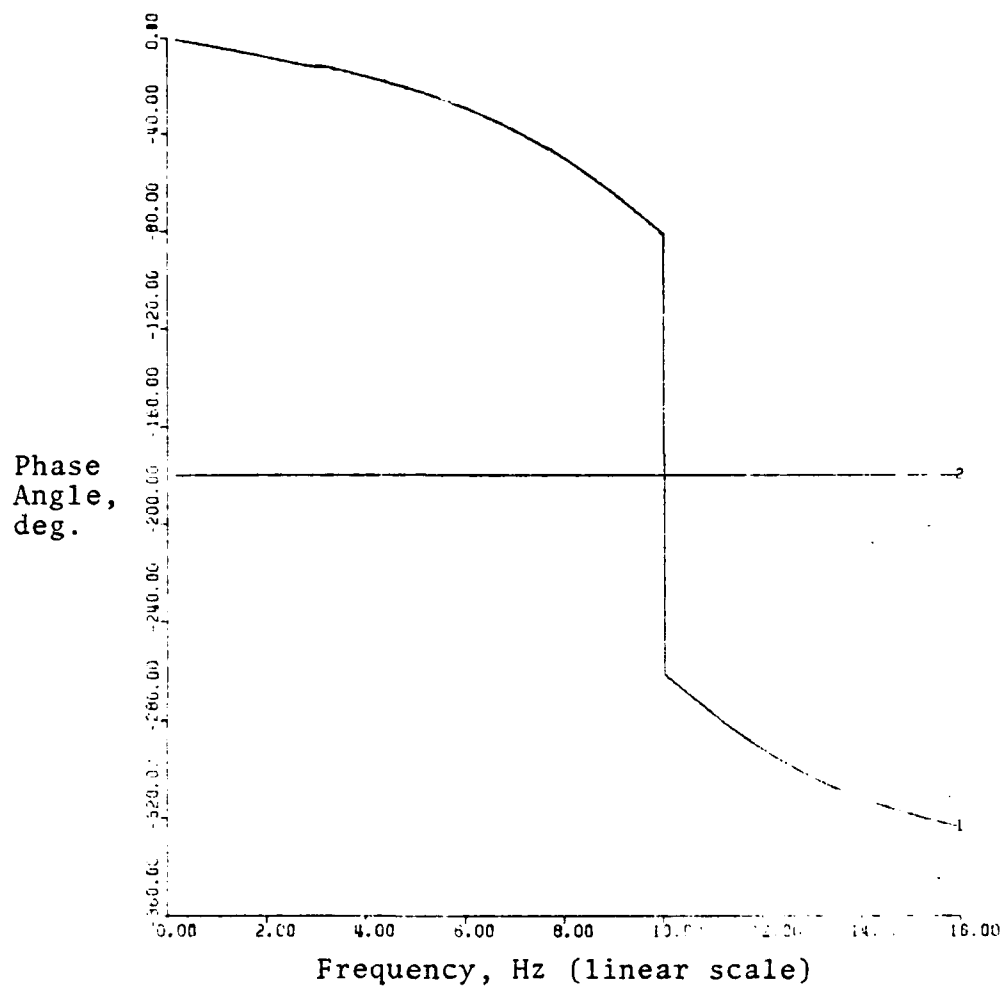


Figure 3-16 Frequency Response of Digital Notch Filter with 0.8 Pole Radius Centered at 10 Hz

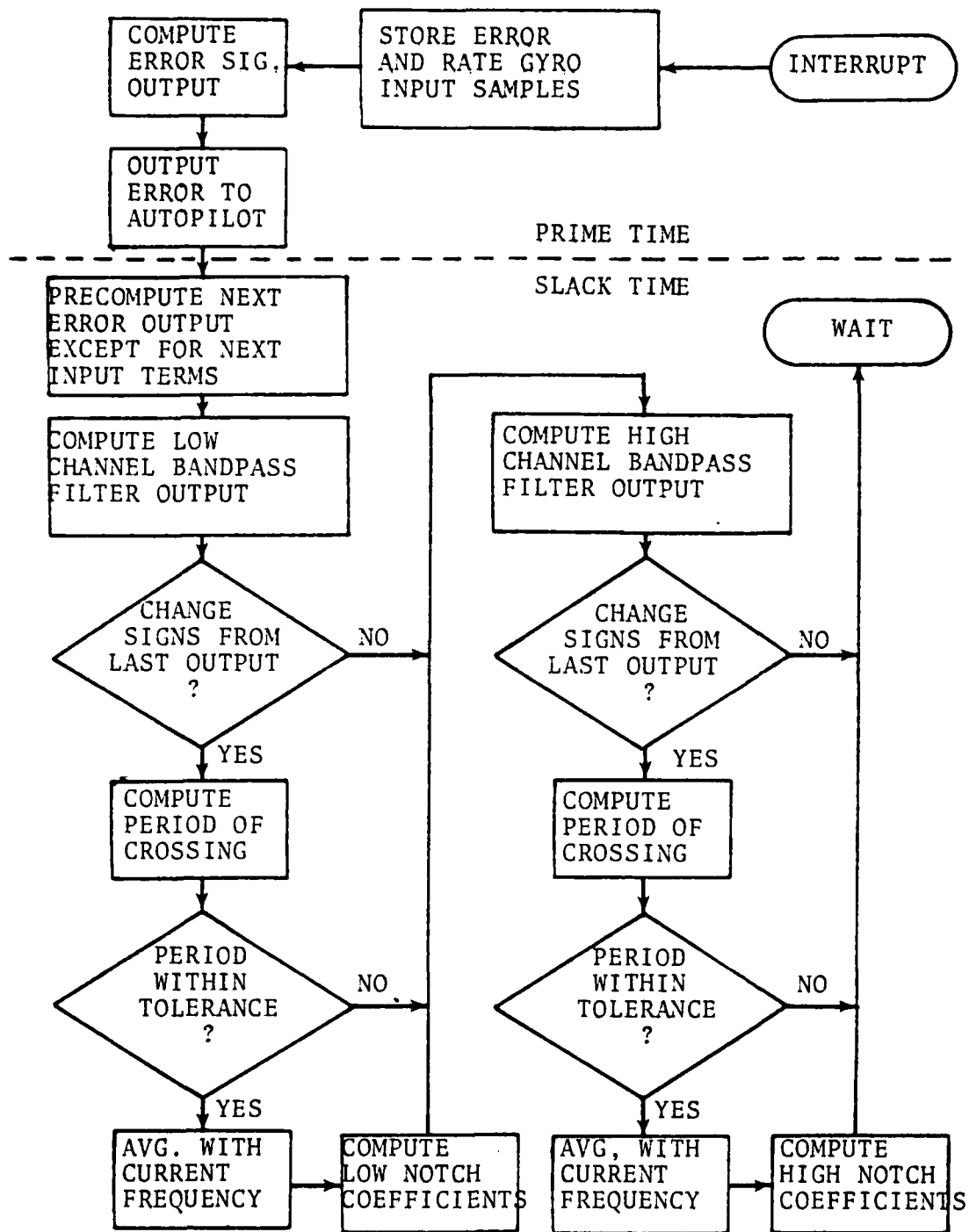


Figure 3-17 Algorithm Flowchart

autopilot with minimum processing delay. The "slack time" computations are the computations performed after the error signal has been processed and which do not introduce processing delay in the control system. With a 100 hertz sampling frequency, sufficient time should be available to complete all slack time calculations every cycle, with currently available microprocessors.

#### C. TEST OF THE ALGORITHM

The algorithm was first tested as shown in Figure 3-18. An input signal consisting of the sum of equal amplitude 2.0, 6.0 and 10.0 hertz sine waves initially in phase was used to simulate the rate gyro output signal with bending mode contamination. The signal was first passed through the tracking notch filter modules and the result was then used as an input to the two channels of the bending mode frequency determination, tracking and filtering algorithm. The unusual process of passing the input signal through the notch filters first was done to allow the effects of feedback to be observed as the notch filters remove the very signals that the remainder of the algorithm is trying to track.

Figure 3-19 shows the two-hertz input signal (line 3) to the notch filters and the resulting output signal (line 2, accentuated). The notch filters were reasonably able to filter out the 6 and 10 hertz components and pass the

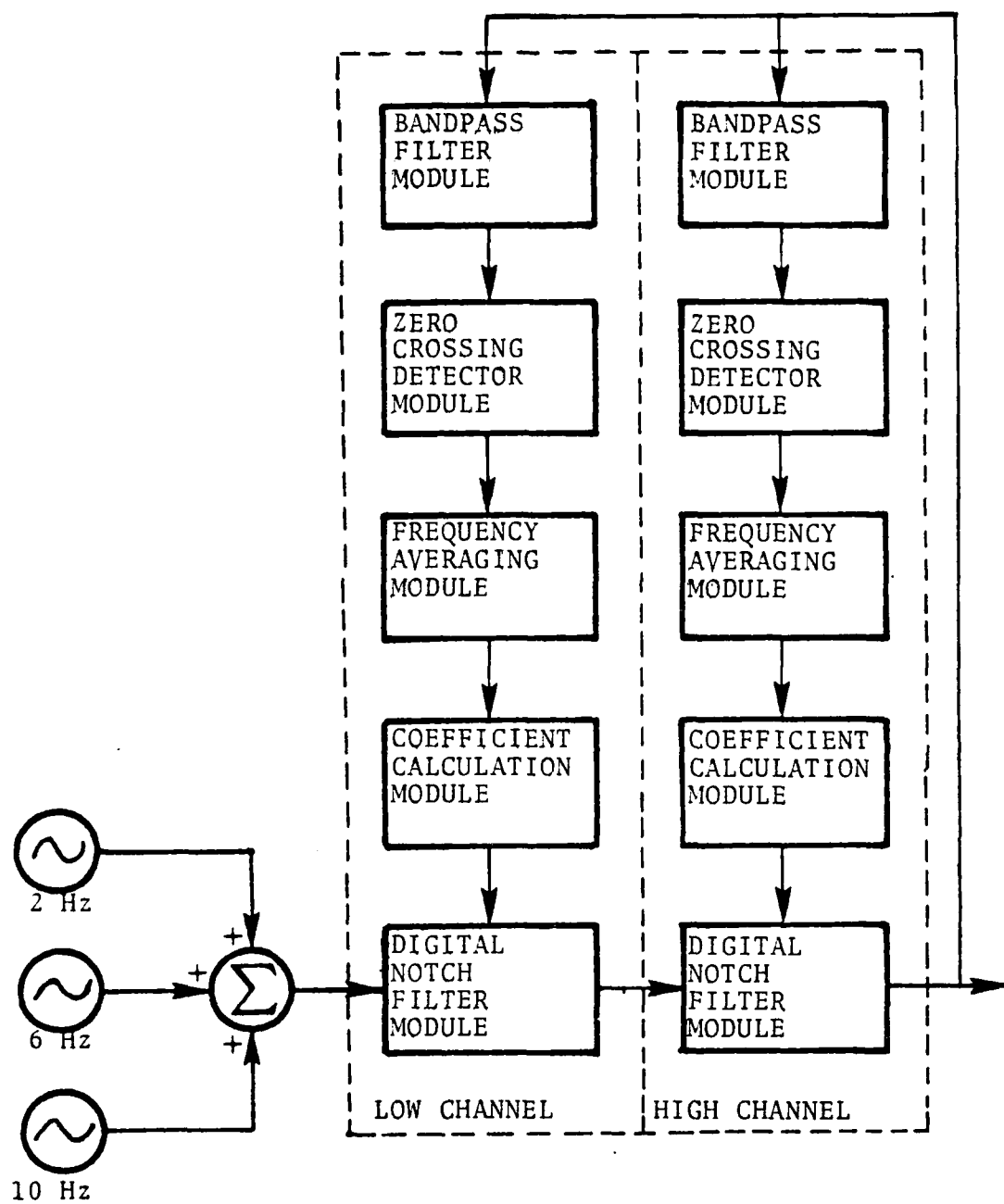
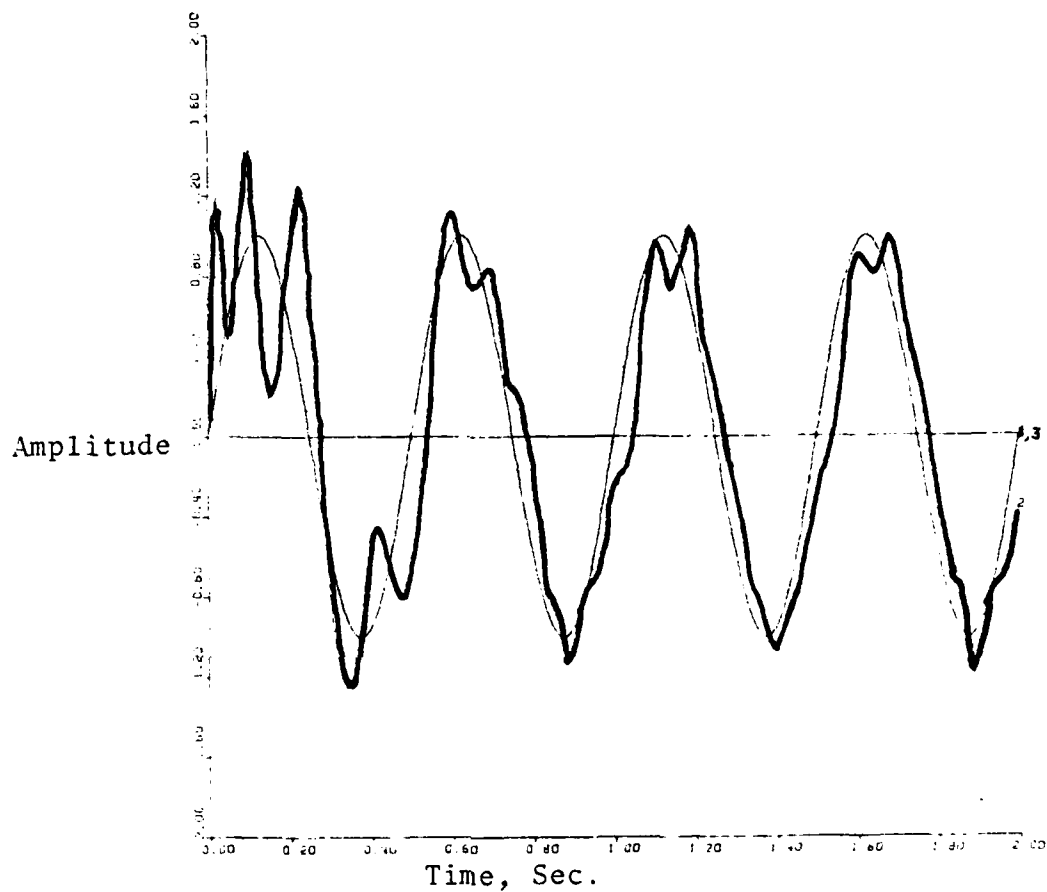


Figure 3-18 Adaptive Notch Filter  
Algorithm Test Arrangement



Line 1 is zero amplitude reference

Line 2 is the output of the adaptive digital notch filters

Line 3 is 2 Hz input signal

Figure 3-19 Output of the Adaptive Digital Notch Filters



two-hertz. The numerical data associated with Figure 3-19 indicates an average phase loss of 18 degrees was experienced over the 2 seconds of simulation.

Figure 3-20 shows the tracking history of each of the channels. The low channel locked on the six-hertz frequency (actual lock on frequency was 6.0546 Hz) after 0.56 seconds and remained locked on for the remainder of the simulation. The high channel went into a four cycle per second limit cycle with an average frequency of 9.85 hertz. The cause of the limit cycle is leadage of the two-hertz signal when the amplitude of the two-hertz reaches near maximum amplitudes. The limit cycle has a minimum effect on the output of the notch filters since the high channel notch bandwidth is nearly six-hertz and the magnitude of the limit cycle is only 1.65 hertz.

Figure 3-21 shows the input (line 1) and output (line 2, accentuated) of the low frequency channel bandpass filter. Figure 3-22 shows the input (line 1) and the output (line 2, accentuated) of the high channel bandpass filter. The effects of the leadage of the two-hertz signal can be seen in the output of both filters.

AD-A094 554

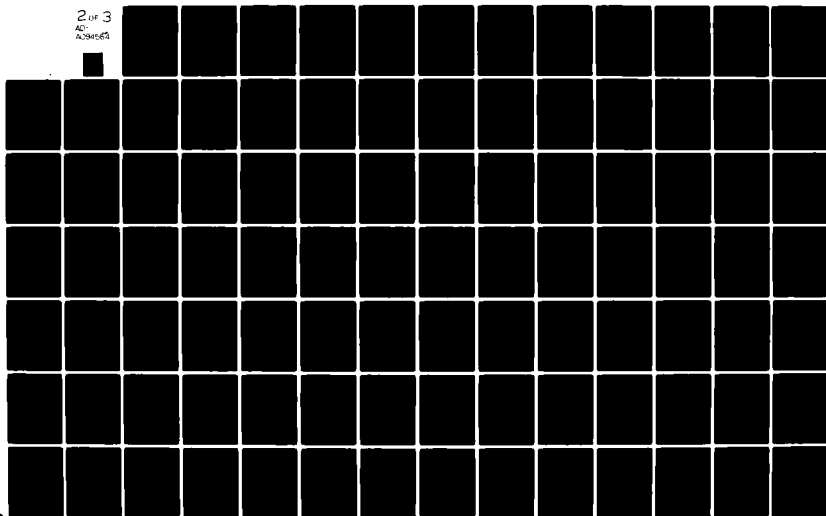
NAVAL POSTGRADUATE SCHOOL MONTEREY CA  
ADAPTIVE NOTCH FILTER SUPPRESSION OF BENDING MODES.(U)  
DEC 80 W L MARKS

F/6 9/2

UNCLASSIFIED

NL

2 of 3  
AD-  
A094563



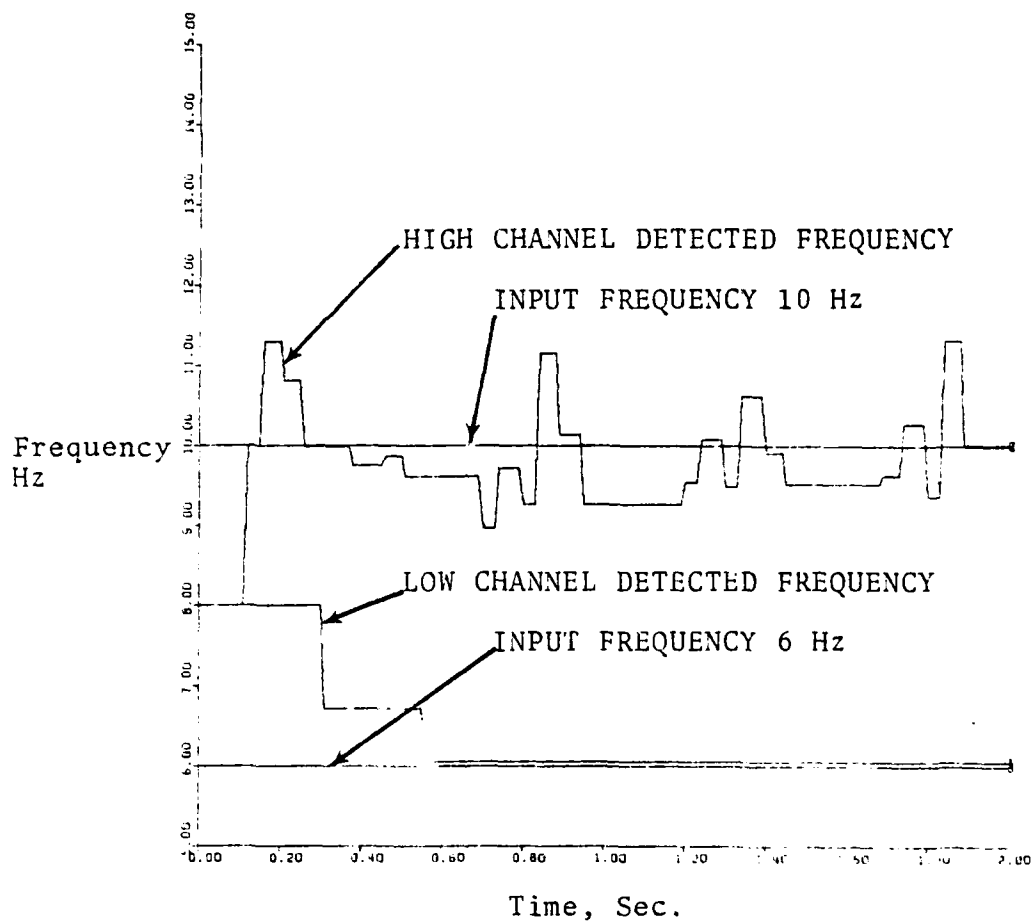
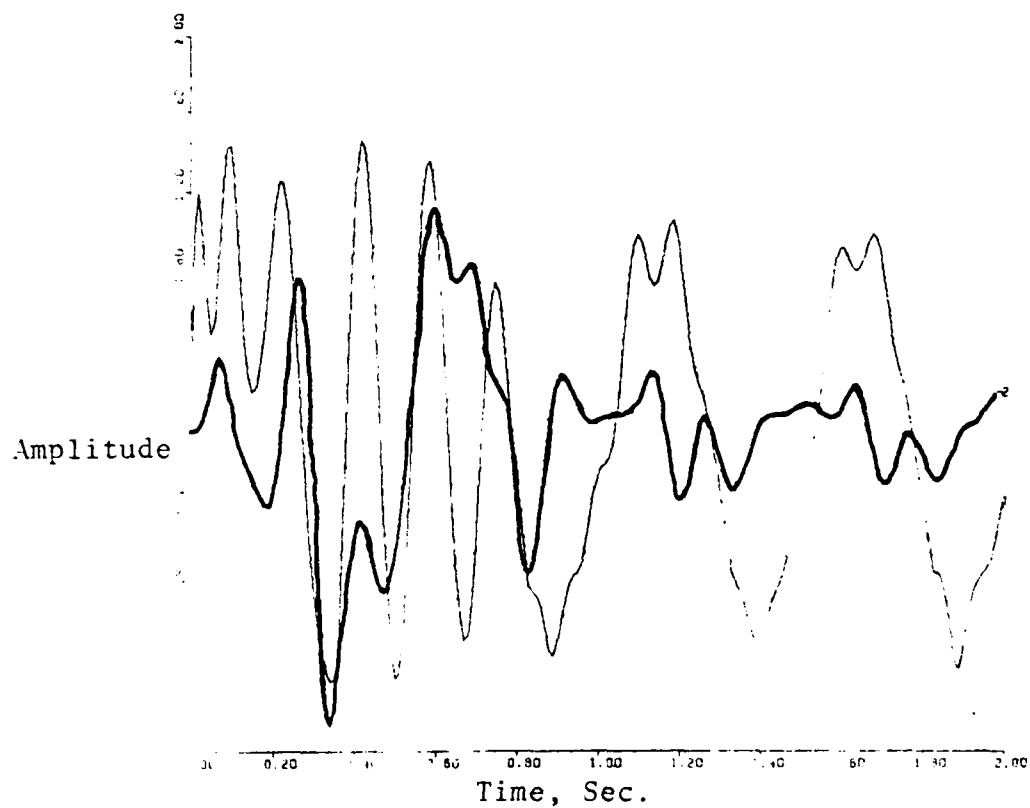


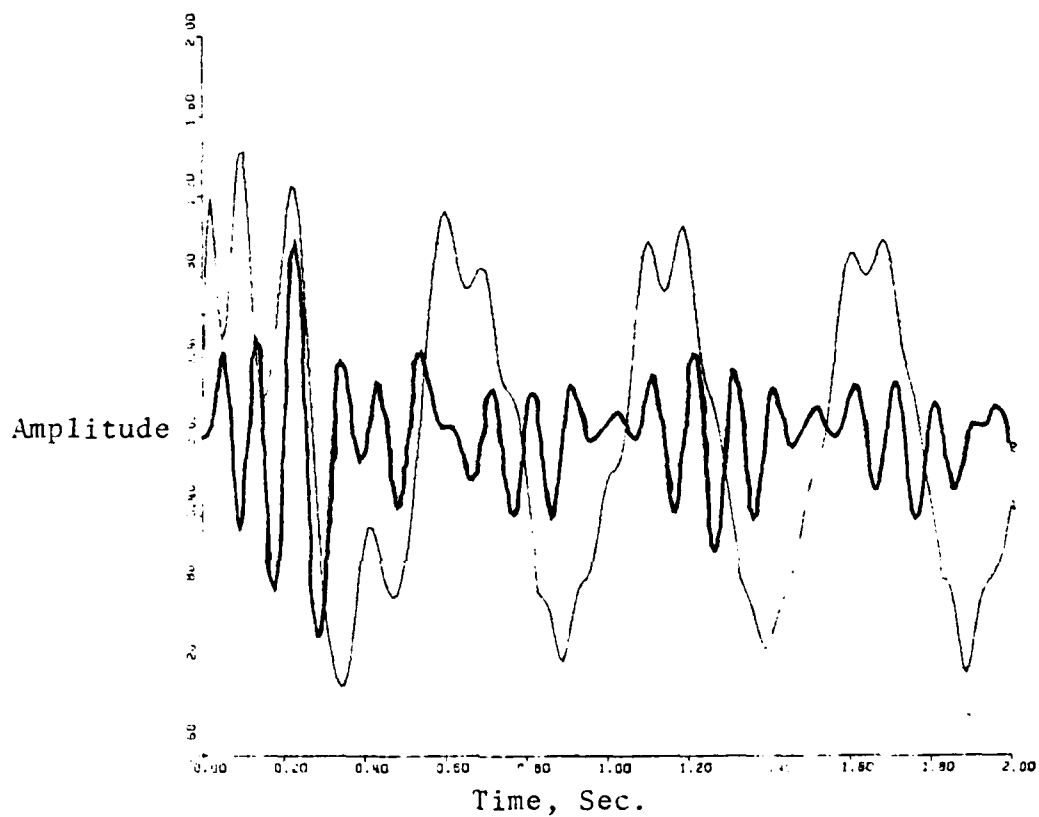
Figure 3-20 Frequency Detector Output for 6 and 10 Hz Input



Line 1 is the output from the adaptive notch filter

Line 2 is the output from the low channel bandpass filter

Figure 3-21 Low Channel Bandpass Filter Output



Line 1 is the output from the adaptive notch filters

Line 2 is the output from the high channel bandpass filter

Figure 3-22 Output from the High Channel Bandpass Filter

#### IV. SIMULATION STUDIES

##### A. DIGITAL SIMULATION LANGUAGE (DSL/360)

The programming languages used throughout this thesis are the IBM Digital Simulation Language (DSL/360) [9] and FORTRAN IV. DSL/360 has not been released for general use by the IBM Corporation but was used in this thesis for the simulation studies due to its enhanced capabilities. The exclusive features of DSL/360 were used only in modeling of the continuous systems. The modules of the adaptive digital filter are programmed exclusively in FORTRAN IV and may be used with any continuous systems simulation language that will accept FORTRAN subroutines.

##### B. BLOCK DIAGRAM OF THE SIMULATION MODEL

Figure 4-1 illustrates the block diagram of the system used to develop Program 4-2. The block diagram forms the core program for all the simulation studies in this chapter with the only changes being the addition of a ramp function for the input command in Program 4-3 and ramp functions to create dynamic bending mode frequencies in Programs 4-10 and 4-12.

##### C. SIMULATION CONDITIONS

The parameters of the plant selected for all the following simulation studies are from Table 2-1 at time = 40 seconds.

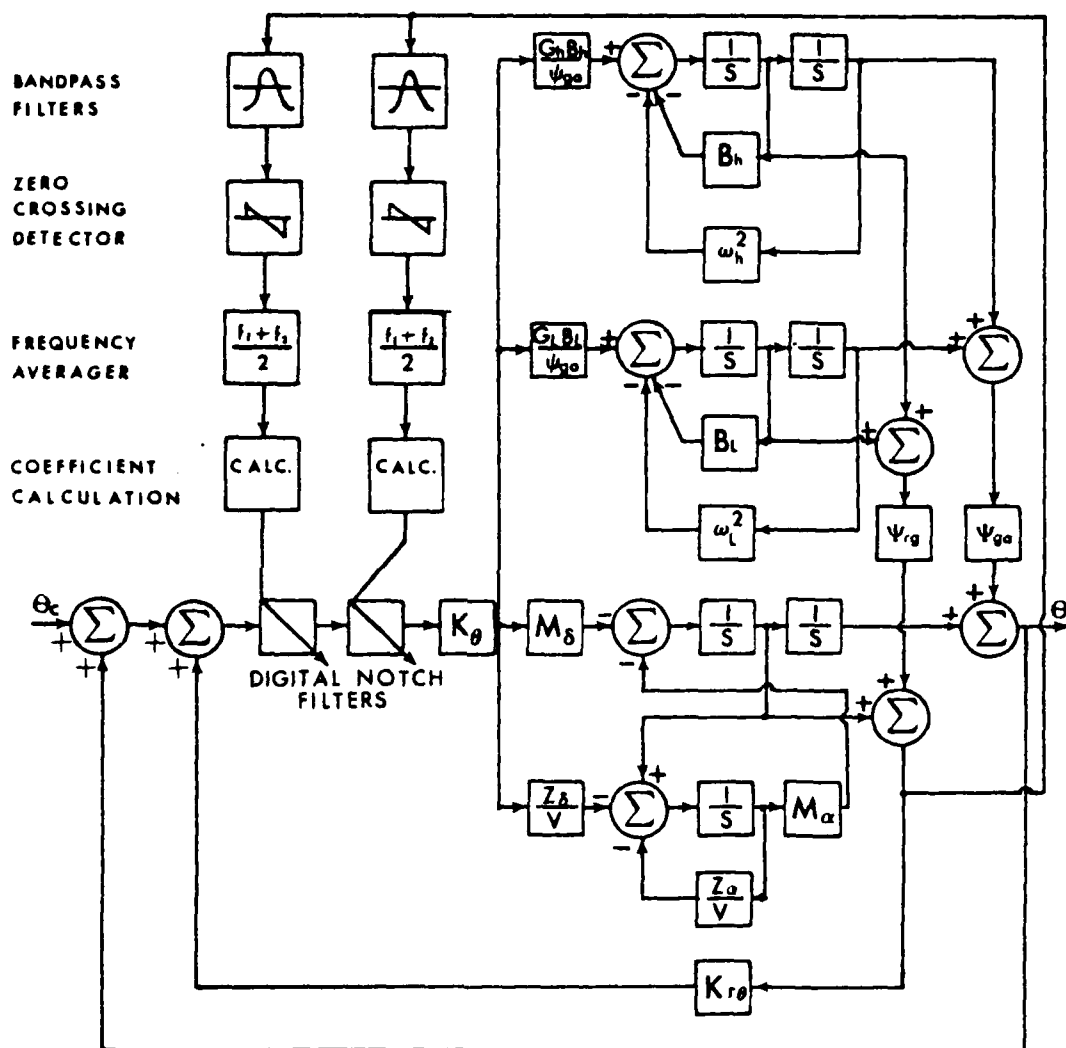


Figure 4-1 Simulation Study Model

The selected plant parameters represent the values when the missile passes through the point of maximum dynamic pressure ( $\max Q$ ) and is the least stable even without the presence of bending modes. When simulation studies were conducted with plant parameters yielding a more stable plant the results indicated the proposed adaptive digital filtering technique functioned essentially the same and therefore only the worst case conditions are presented.

Two pitch commands from the guidance system were selected for simulation: a 0.1 radian step input and a 0.05 radian per second ramp. The step command simulates a command from the autopilot which would normally occur at water exit, staging, or inflight restart of the guidance system after a failure. The simulation studies with a step input are intended to simulate the condition of a guidance system restart at the point in the flight when the missile has the least stability, a highly unlikely but undoubtedly severe condition. The ramp input simulates a more normal condition where the autopilot responds to wind shear at the point of least stability. The ramp input response serves to demonstrate that although the bending modes are not excited as violently as they are with a step input, the adaptive digital filters successfully detect their presence and provide the proper filtering. The ramp input again includes the simulation of an inflight restart of the guidance system since



the simulation is started with no history available to the adaptive digital filters or frequency detector algorithms.

The bending mode frequencies were the primary variable in the simulation studies. The first two studies have fixed bending mode frequencies centered at 6.0 and 10.0 hertz. The third study has the bending mode frequencies again fixed but at 7.0 and 9.0 hertz to ensure that the algorithm can separate two close bending mode frequencies. The fourth study has the bending modes fixed at 5.5 and 14.0 hertz to test the ability of the algorithm to properly filter two widely separated bending mode frequencies. The final two studies have dynamic bending modes with the upper bending mode changing at the rate of 1.5 hertz per second and the lower bending mode changing at 1.0 hertz per second. The rates of change far exceed the rates of change anticipated but were included as a demonstration of the capability of the algorithm to track very high rates of change in the bending mode frequencies. The final two studies illustrate the response of the system with the bending mode frequencies converging and diverging.

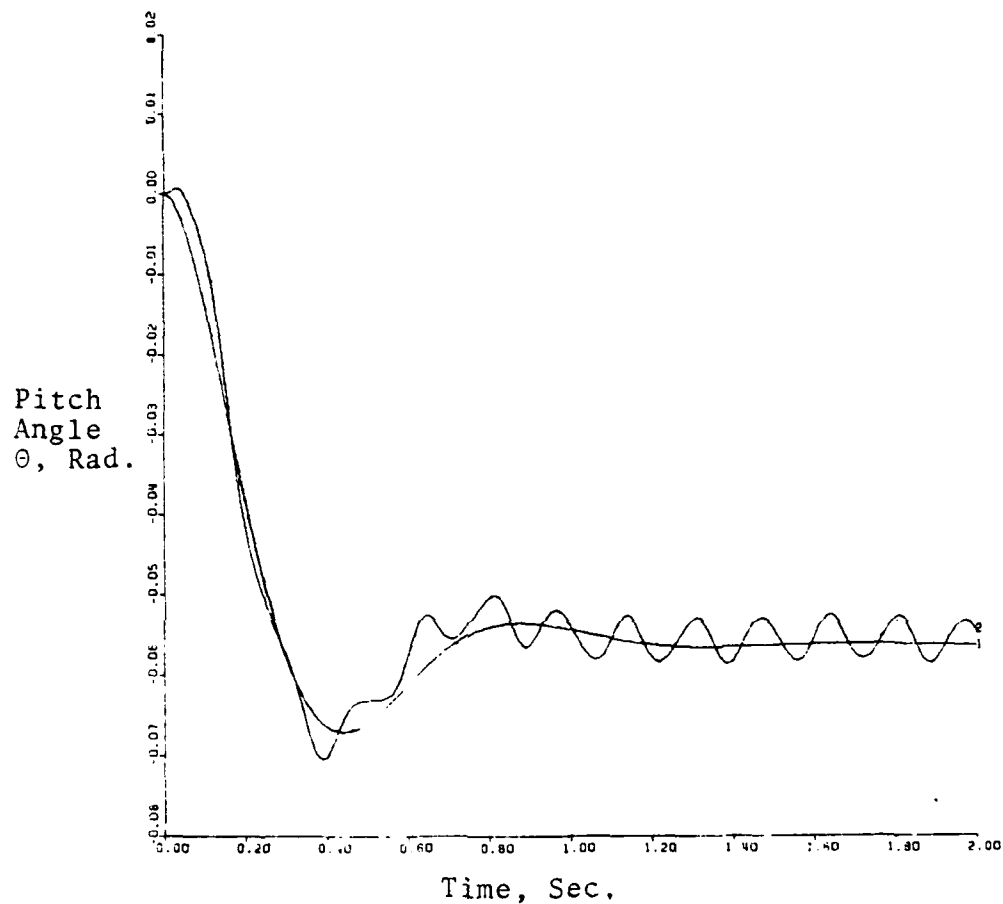
Table 4-1 provides a summary of the conditions used in the six simulation studies.

#### D. SIMULATION RESULTS

Figures 4-2 and 4-3 illustrate the system response for a 0.1 radian step pitch command with the bending mode frequencies fixed at 6.0 and 10.0 Hz. Line 1 in Figure 4-2 is

TABLE 4-1

FIGURES	INPUT	BENDING MODES
4-2	0.1 rad	6.0 Hz and 10.0 Hz
4-3	STEP	FIXED
4-4	0.05*T rad/sec	6.0 Hz and 10.0 Hz
4-5	RAMP	FIXED
4-6	0.1 rad	7.0 Hz and 9.0 Hz
4-7	STEP	FIXED
4-8	0.1 rad	5.5 Hz and 14.0 Hz
4-9	STEP	FIXED
4-10	0.1 rad	6.0 Hz + 1.0 Hz/sec
4-11	STEP	DYNAMIC
4-12	0.1 rad	8.0 Hz - 1.0 Hz/sec
4-13	STEP	9.0 Hz + 1.5 Hz/sec DYNAMIC



System: Third order missile model with fixed bending modes at 6 and 10 Hz

Input: 0.1 radian step command

Line 1 is the nominal missile response without bending modes

Line 2 is the missile response with bending modes

Figure 4-2 Missile Step Response with Fixed 6 and 10 Hz Bending Modes

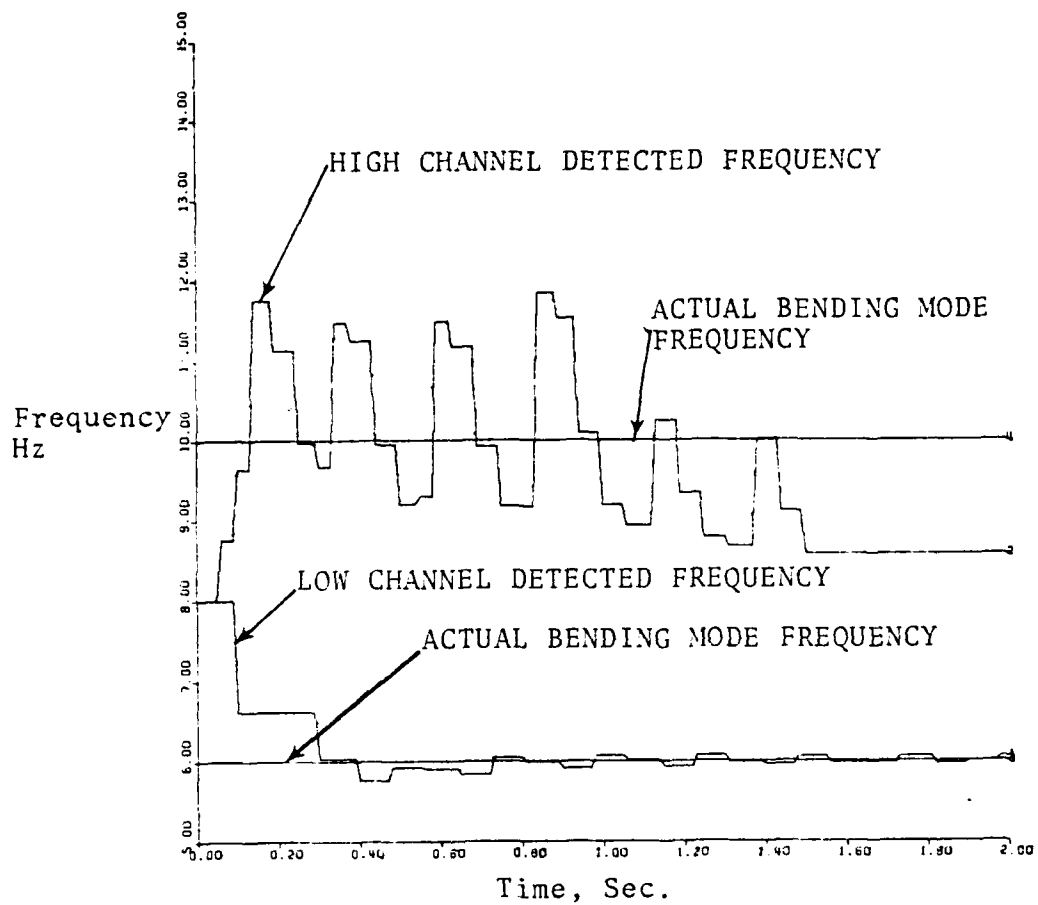


Figure 4-3 Frequency Detector Output for Fixed 6 and 10 Hz Bending Modes

the nominal response of the plant without bending modes to the same input. It is provided as a standard by which the effectiveness of the adaptive digital notch filtering may be evaluated. Line 2 in Figure 4-2 is the response of the system with the bending modes and the adaptive digital notch filters.

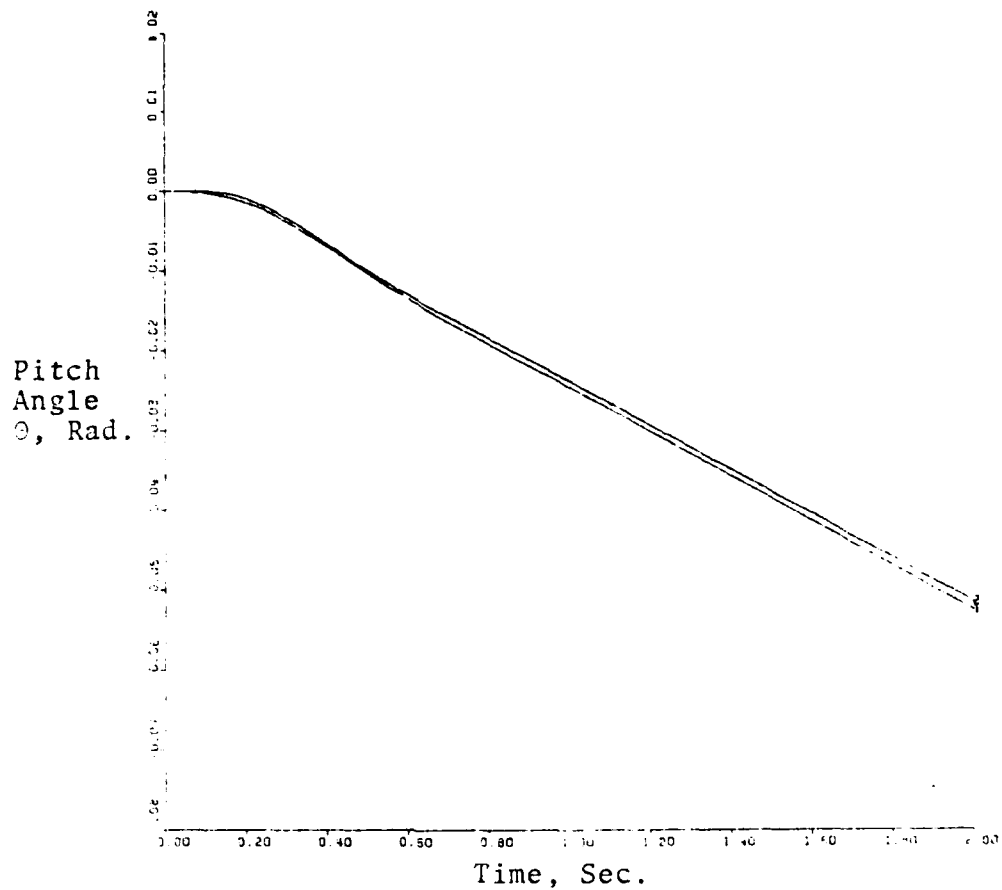
Figure 4-3 provides a history of the center frequency of the high and low channel notch filters. Line 1 is the history of the low channel (5.0-8.0 Hz) notch center frequency and Line 2 is the history of the high channel (8.0-12.0 Hz) notch center frequency. Lines 3 and 4 indicate the actual bending mode center frequencies.

Figure 4-2 must be compared with Figure 2-17 to gain the proper perspective on the degree to which the system has been stabilized by the adaptive notch filters. Figure 2-17 is precisely the same system and the same input except the adaptive digital notch filters were not in the system simulated in Figure 2-17. The amount of leakage of the 6.0 hertz bending mode frequency through the notch filter is due to the relatively low precision coefficients used in the notch filters. Simulation with double precision coefficients reduced the leakage considerably but the implementation of the notch filter with this precision was not considered practical for implementation with a microprocessor and therefore not pursued.

Figure 4-3 illustrates that the algorithm can rapidly and accurately track the 6.0 hertz bending mode frequency but exhibits limit cycle behavior when tracking the 10.0 hertz bending mode. The limit cycle behavior can be attributed to the low frequencies associated with the plant dynamics causing errors in the frequency detector as discussed in Chapter Three. The limit cycle does not appear to diminish the high channel's effectiveness in eliminating the 10.0 Hz bending mode in that there is no evidence of the 10.0 hertz bending mode in the output and it is attenuated to the point that the frequency detector can no longer track it after 1.5 seconds.

Figures 4-4 and 4-5 show the response of the system for a  $0.05 \cdot T$  ramp pitch command with bending modes centered at 6.0 and 10.0 hertz. Comparing Figure 4-4 with Figure 2-23 it is evident that when the adaptive digital notch filters are included in the system the response is essentially the same as if no bending modes were present. Figure 4-5 shows the ability of the high channel to much more accurately lock onto the 10.0 hertz bending mode when the high plant rates are not present. The very satisfactory performance for a ramp input indicated that this input did not stress the ability of the adaptive digital notch filter algorithm and it was therefore not used in the remainder of the simulation studies.

Figures 4-6 and 4-7 show the response of the system for a 0.1 radian step input when the bending mode frequencies



System: Third order missile model with fixed bending modes at 6 and 10 Hz

Input: 0.05 radian/sec ramp command

Line 1 is the nominal missile response without bending modes

Line 2 is the missile response with bending modes

Figure 4-4 Missile Ramp Response with Fixed 6 and 10 Hz Bending Modes

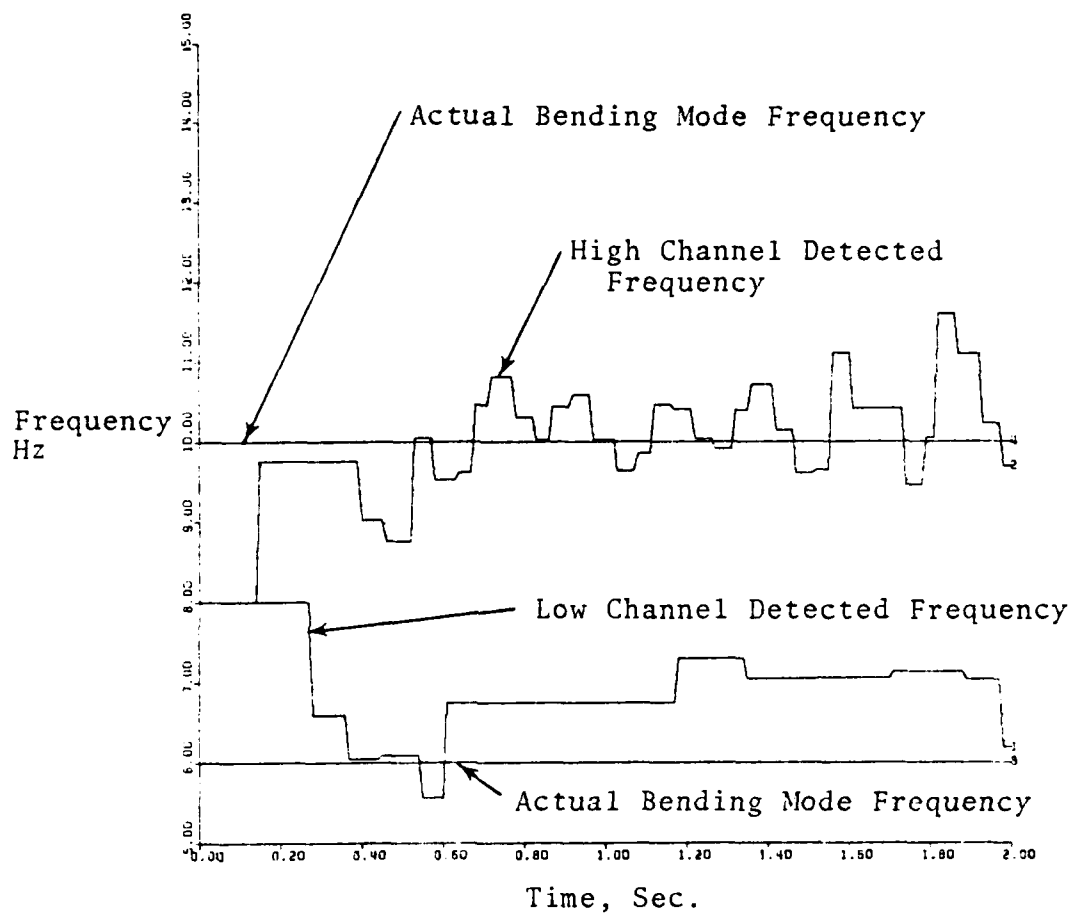
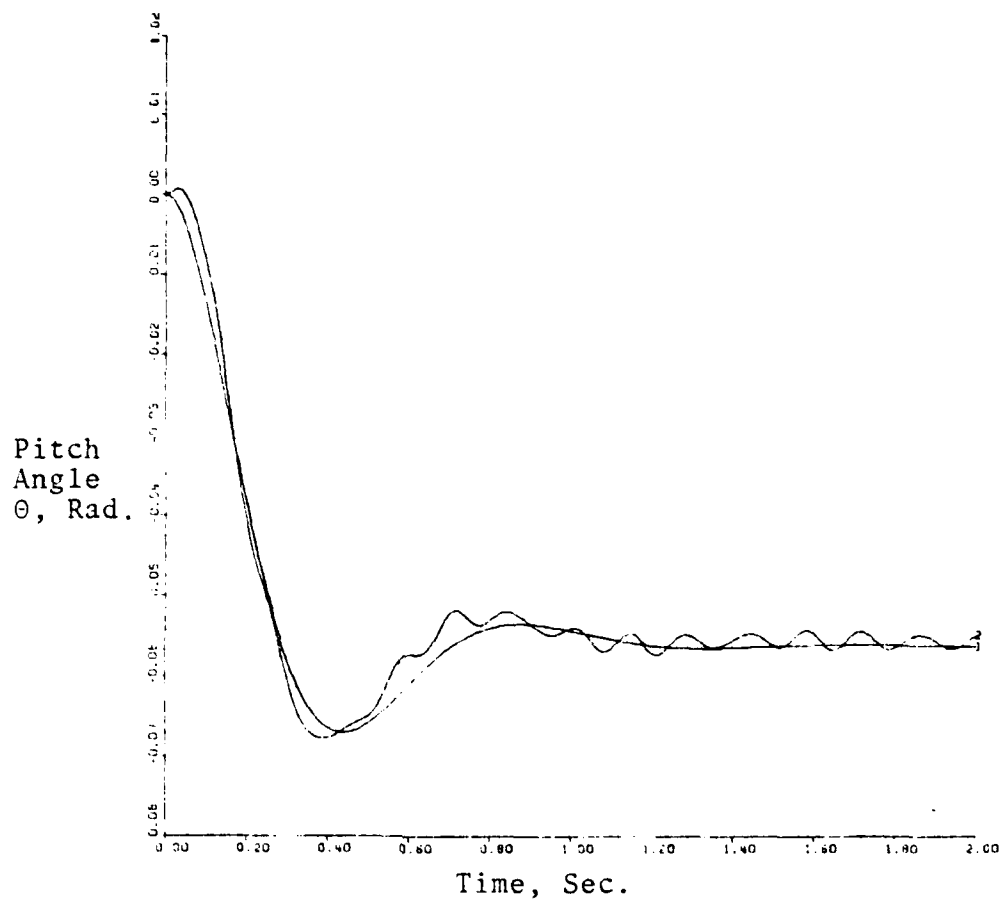


Figure 4-5 Frequency Detector Output for Fixed 6 and 10 Hz Bending Modes





System: Third order missile model with fixed bending modes at 7 and 9 Hz

Input: 0.1 radian step command

Line 1 is the nominal missile response without bending modes

Line 2 is the missile response with bending modes

Figure 4-6 Missile Step Response for Fixed 7 and 9 Hz Bending Modes

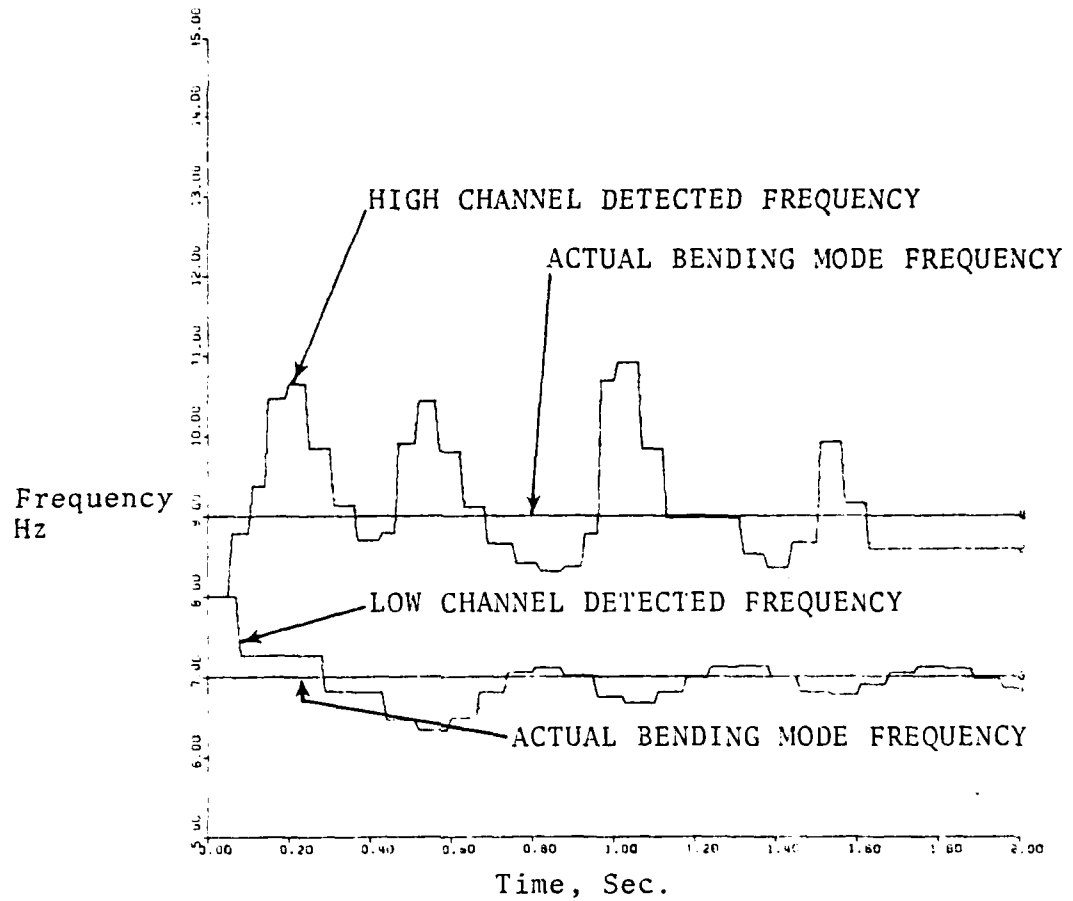


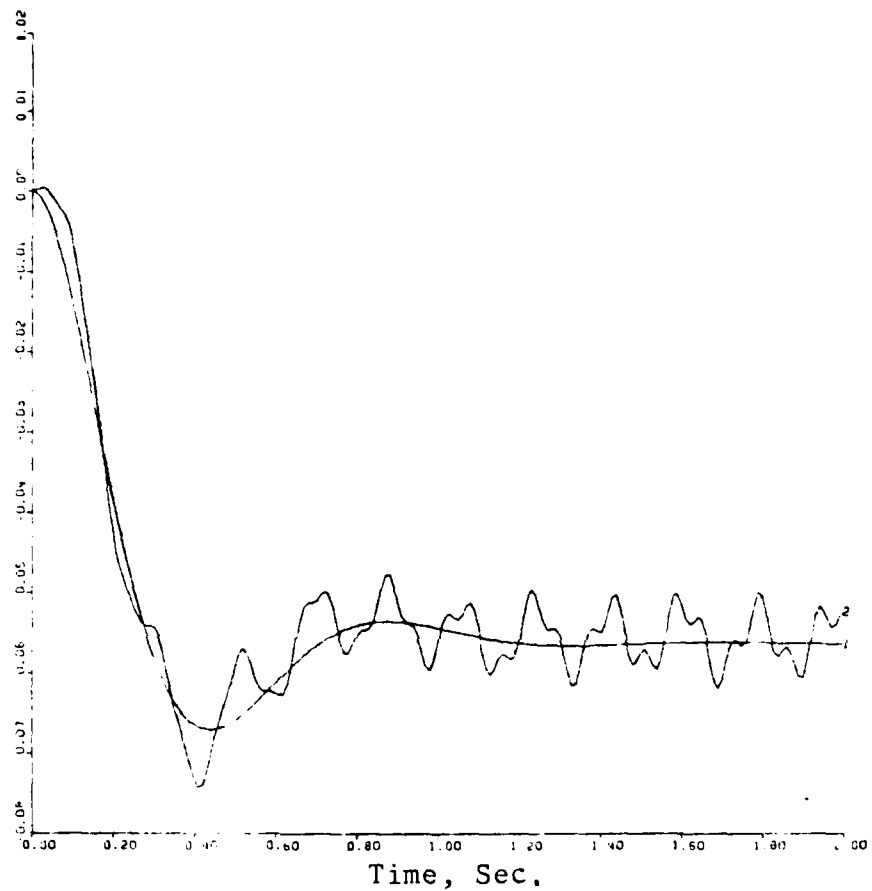
Figure 4-7 Frequency Detector Output for Fixed 7 and 9 Hz Bending Modes

were fixed and only separated by 2.0 hertz. The system response is very close to the nominal plant with some evidence of both bending modes present in the output. The cross channel leakage can be seen to cause oscillations in both of the frequency detectors.

Figures 4-8 and 4-9 show the response of the system to a 0.1 radian step input with the bending modes separated by 7.5 hertz. The lower frequency bending mode is at 5.5 hertz or 0.5 hertz above the lower limit to which the algorithm is allowed to track and the upper frequency bending mode is 14.0 hertz. The upper bending mode frequency is outside of the passband for the high channel frequency detector but within the 15.0 hertz that the high channel is allowed to track a bending mode. The performance of the system is marginal at best. This simulation clearly illustrates the inability of the algorithm to reliably acquire or track a bending mode higher than 12.0 hertz. The problem is not accentuated by the bandpass filter in the high channel attenuating frequencies above 12.0 hertz. Increasing the bandwidth of the high channel to 15.0 hertz did not enhance the ability of the algorithm to reliably identify a frequency above 12.0 hertz.

Figures 4-10 and 4-11 show the system response for a 0.1 radian step input with dynamic, converging bending mode frequencies. The high frequency bending mode starts at 12.0 hertz and decreases at 1.5 hertz per second to 9.0 hertz.

Pitch  
Angle  
 $\theta$ , Rad.



System: Third order missile model with fixed bending modes at 5.5 and 14.0 Hz

Input: 0.1 radian step command

Line 1 is the nominal missile response without bending modes

Line 2 is the missile response with bending modes

Figure 4-8 Missile Response with Fixed 5.5 and 14.0 Hz Bending Modes

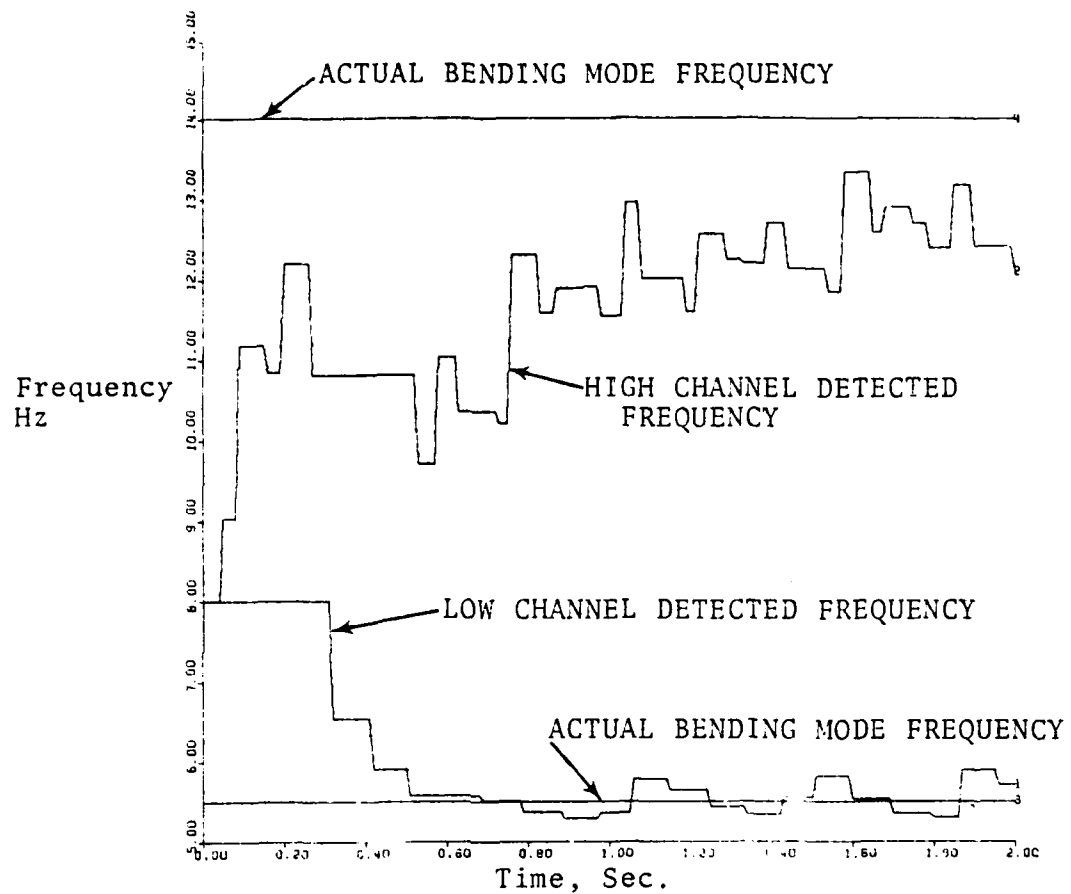
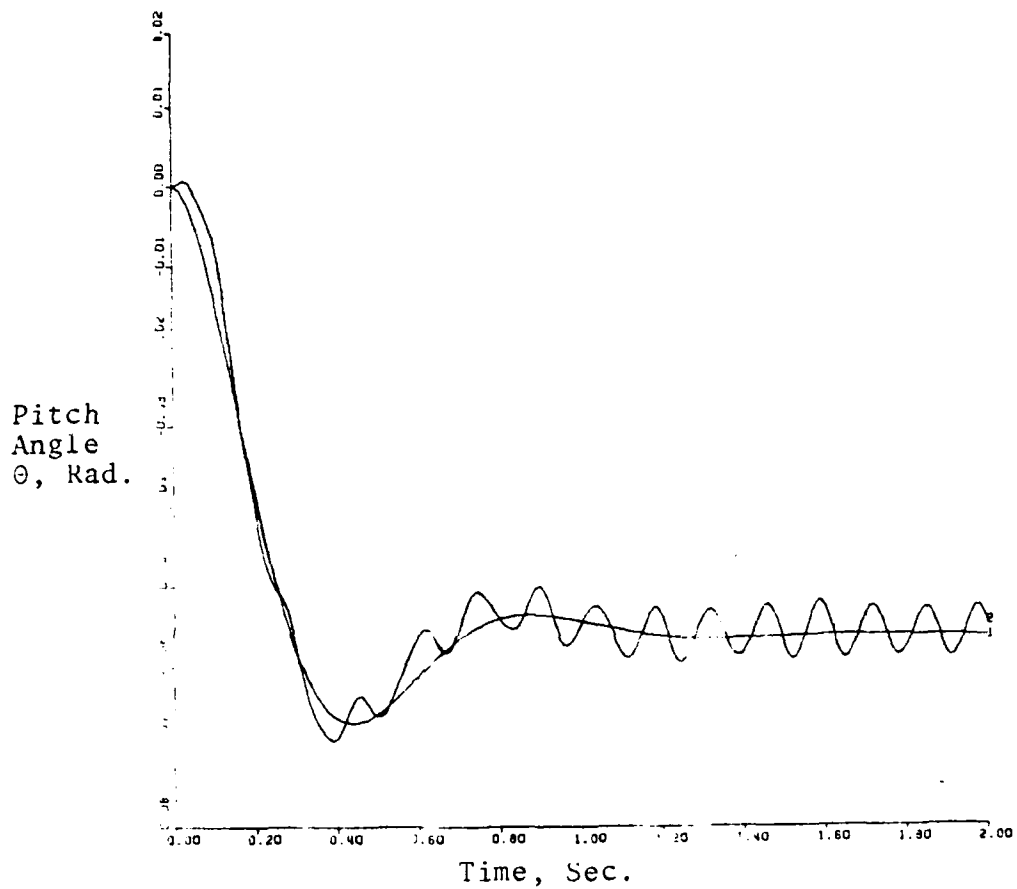


Figure 4-9 Frequency Detector Output for Fixed 5.5 and 14.0 Hz Bending Modes



System; Third order missile mode with converging dynamic bending modes

Input: 0.1 radian step command

Line 1 is the nominal missile response without bending modes

Line 2 is the missile response with bending modes

Figure 4-10 Missile Step Response with Converging Dynamic Bending Modes

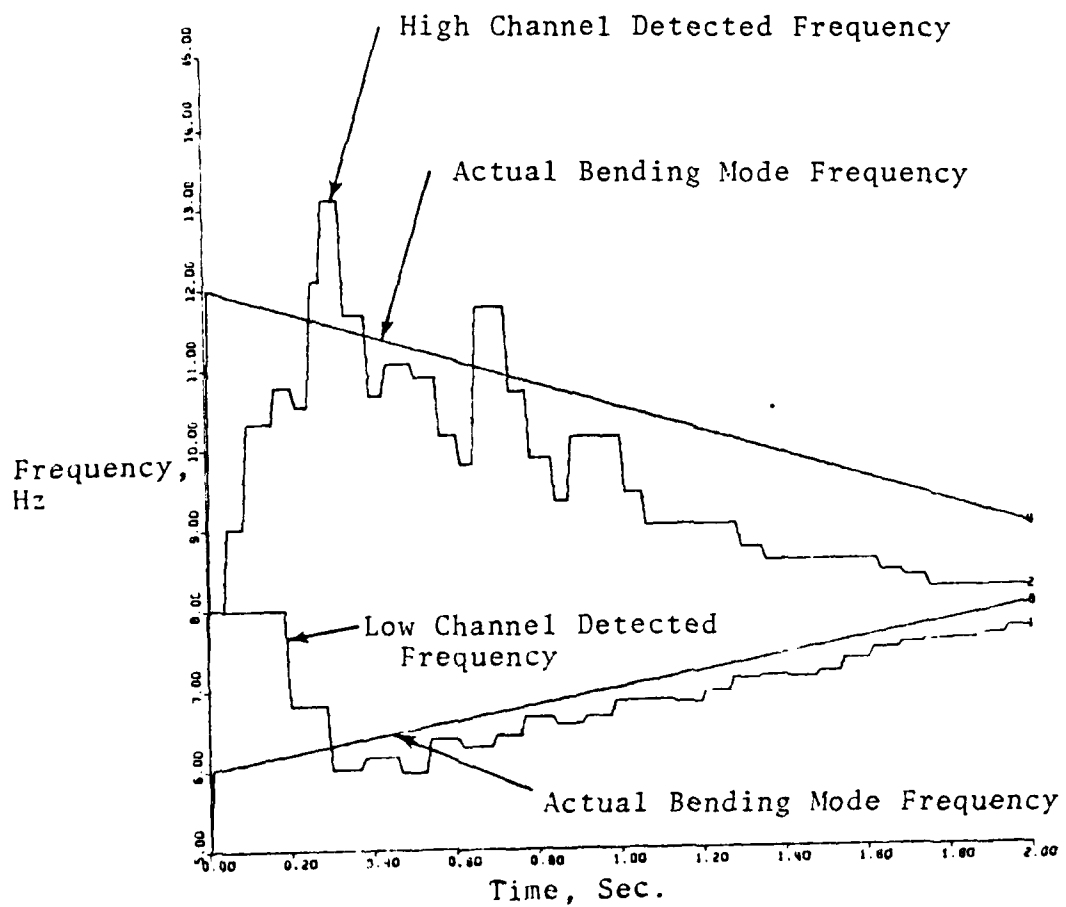
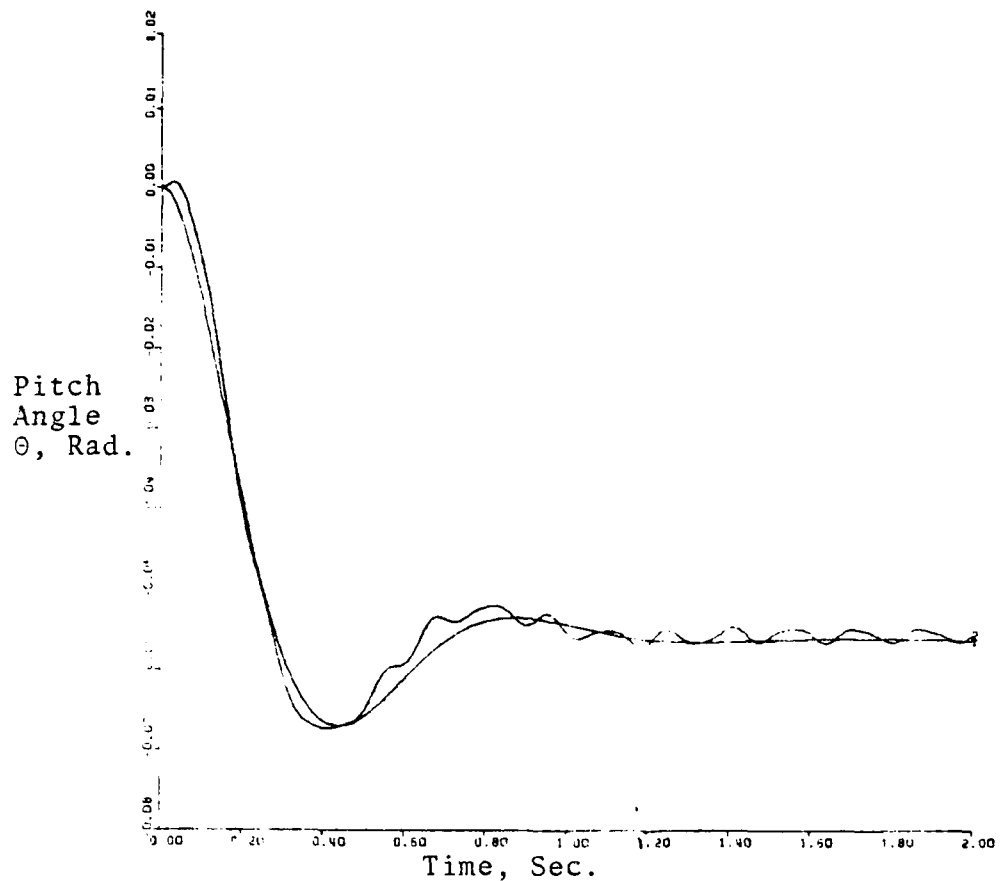


Figure 4-11 Frequency Detector Output for Converging Dynamic Bending Modes

The low frequency bending mode starts at 6.0 hertz and increases at 1.0 hertz per second to 8.0 hertz. The ability of the adaptive digital notch filters to stabilize the system with such high rates of change was not expected. When higher rates of change were simulated for the converging case, the error in the high frequency estimate became so poor that the system became unstable at the frequency of the high bending mode. A rate of 1.5 hertz per second is felt to be the limit on the rate of change of either bending mode frequency.

Figures 4-12 and 4-13 show the system response to a 0.1 radian step input with dynamic diverging bending mode frequencies. The upper bending mode frequency starts at 9.0 hertz and increases at the rate of 1.5 hertz per second to 12.0 hertz. The lower frequency bending mode starts at 8.0 hertz and decreases at the rate of 1.0 hertz per second to 6.0 hertz. The very good performance of the system is probably due to the notch filters being initialized at 8.0 hertz. The inability of the high channel to track a bending mode frequency greater than 12.0 hertz is evident as the high bending mode frequency increases.





System: Third order missile model with diverging dynamic bending modes

Input: 0.1 radian step command

Line 1 is the nominal missile response without bending modes

Line 2 is the missile response with bending modes

Figure 4-12 Missile Step Response with Diverging Dynamic Bending Modes

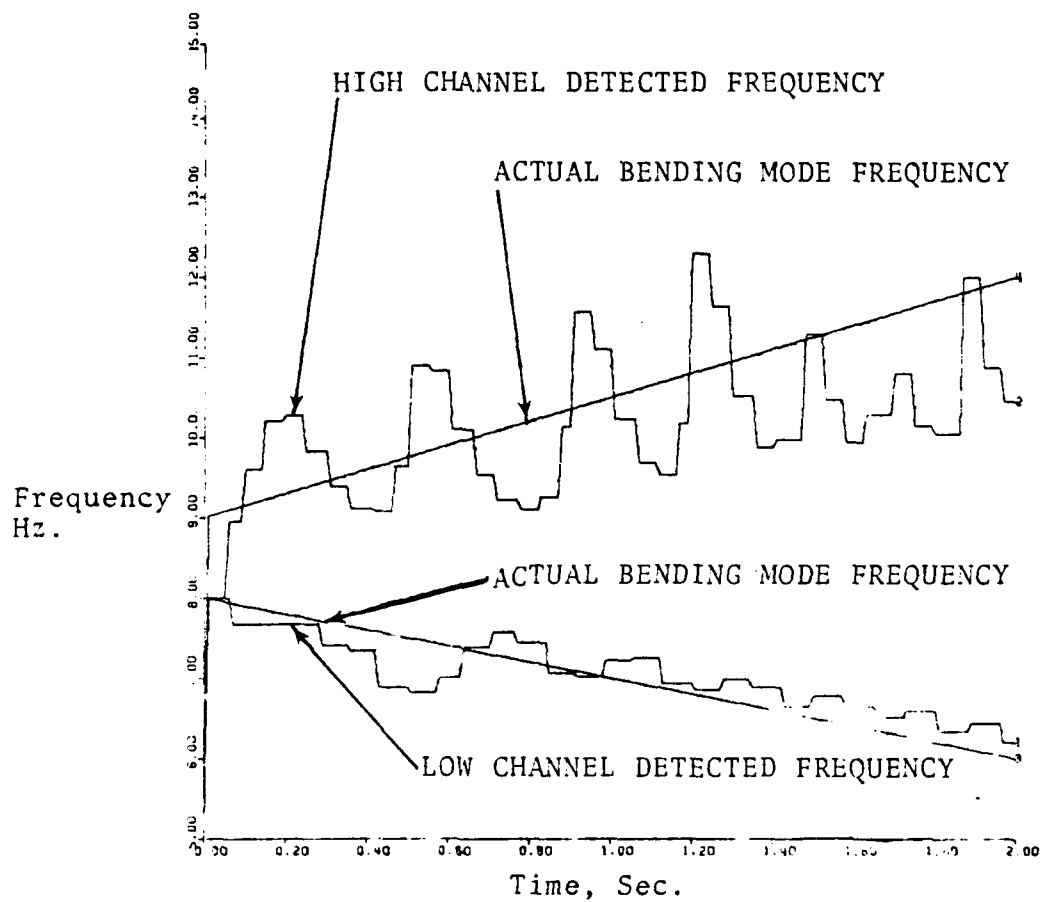


Figure 4-13 Frequency Detector Output for Diverging Dynamic Bending Modes

## V. CONCLUSIONS AND RECOMMENDATIONS

### A. CONCLUSIONS

The feasibility of implementing an adaptive digital notch filter to stabilize the Trident Missile Control System when two dynamic bending modes are present has been demonstrated. The conditions simulated in Chapter Four represent the worst case conditions and the performance of the algorithm under these conditions was satisfactory considering the very desirable response to less violent and more likely commands as shown in Figure 4-4.

The algorithms used in the simulation studies contained in Chapter Four were developed with the ability to implement them in a microprocessor program as a primary concern. Simplicity of the algorithm was maintained, perhaps at the expense of performance, to ensure that the algorithm could be implemented on a microprocessor for subsequent real-time studies. The time varying, nonlinear characteristics of the system when the adaptive digital notch filters are tracking dynamic bending modes with varying input commands deny an analytical approach and therefore require extensive simulation to optimize the algorithm.

## B. RECOMMENDATIONS FOR FURTHER STUDIES

The simplicity of the digital bandpass filters allows an excessive amount of out of band interference. The performance of the bandpass filters could be significantly improved without an appreciable increase in the order of the filters by using more sophisticated types of filters such as a Chebyshev or an elliptical filter. The temptation to enhance the performance of the bandpass filter in nonreal-time simulations without considering the implementation problem on a microprocessor must be resisted.

The direct realization of the bandpass and notch digital filters did not minimize memory, noise due to finite precision coefficients or the number of multiplications required for each output. The structure of the filters needs to be examined with a specific microprocessor's capabilities considered. The ZILOG Z-8000 microprocessor capabilities were considered during the development of the algorithm as a current state-of-the-art microprocessor.

The algorithm must be evaluated on the six degree of freedom model of the Trident Missile available at Lockheed Missile and Space Company, Sunnyvale, California. The results of the simulation studies contained in Chapter Four are only as valid as the assumptions made in modeling the bending modes and in simplifying the plant. It must be emphasized that the algorithm contained in this thesis will not perform satisfactorily with the bending mode frequencies

present in the current Trident Missile. The algorithm in this thesis was designed to identify, track and attenuate bending modes that are a full octave below those of the current Trident Missile.

A phaselock loop scheme should be reconsidered as a frequency detector. The phaselock loop has precisely the desired characteristic of seeking out and locking onto a frequency within its predetermined acquisition range and seems ideally suited for the task of identifying and tracking the bending mode frequencies. It is recommended that future studies of the application of phaselock loops in this application use actual phaselock loops rather than computer simulation due to the inability to properly simulate the non linear behavior of the phaselock loop with algorithms known to the author. The feasibility of prefiltering the input to the phaselock loop with a bandpass filter to attenuate out of track range signals and thereby reduce the lock-on time should be considered.



# PROGRAM CONTROL AND PLOTTER CONTROL

0.0	0.2	-0.08	0.01	10.0	10.0





MODEL OF THE THIRD ORDER SYSTEM

```

***
PE=PC+PQ
GAMA=PE+P8
P1=GAMA*KTHETA
P2=MDelta*P1
P3=-P2-MA
MA=MALFA*ALFA
P4=ZDelta*P1/VEL
P5=PR-P4-P6
P6=ZALFA*ALFA/VEL
P7=PR
P8=KRTHET*P7
P9=INTGRL(0.0,PR)
PQ=P9
PR=INTGRL(0.0,P3)
ALFA=INTGRL(0.0,P5)

PROGRAM CONTROL AND PLOTTER CONTROL

***
SAMPLE CALL DRWG(1,1,TIME,P0)
TERMINAL
CALL ENDRWINPLOT)
CONTRL FINTIM=2.0 , DELT=0.01, DELS=0.01
PRINT 0.01,P0,PC
END
STOP
//C.SYSPRINT DD DSN=,SYSDUT=A
//PLOT.STEPLIB DD DSN=C0044.Q,UNIT=3330,VOL=SER=DISK02,DISP=SHR
//PLOT.PLOTPARM DD *
&PLOT SCALE=Q.45 &END
//PLOT.SYSIN DD *
0.0 0.2 -0.08 0.01 10.0 10.0

```

PROGRAM 2-10  
ASSOCIATED FIGURE 2-10

PROGRAM CONTROL PARAMETERS

COMPLEX S,D,N,G,H,BL,BH,P,T  
COMMON/CAREA/S,D,N,G,H,BL,BH,P,T

## SYSTEM PARAMETERS

*PARAM	GAINL=240.0
*PARAM	PSI=0.06
*PARAM	MD=24.17
*PARAM	MA=28.625
*PARAM	ZA=180.0
*PARAM	ZD=113.75
*PARAM	V=2500.0
*PARAM	KRT=1.48
*PARAM	WL=37.7
*PARAM	BWL=62.83
*PARAM	BWH=0.1
**	BWH=1.19

```

INITIAL
**
**      DBZERO=0.0
**
** DYNAMIC
**
**      W=RAMP(0.0)+1
**      HZ=W/6.28
**      S=CMPLX(0.0,W)
**
** SYSTEM DYNAMICS
**
**      BL=(GAINL*BWL/PSI)/((S**2+BWL*S+WL**2)
**      BH=(GAINH*BWH/PSI)/((S**2+BWH*S+WH**2)
**      P=(-MD*S+(ZD*MA/V-ZA*MD/V))/((S**2+ZA/V*S+MA))
**      G=P
**      MAG=CABS(G)
**      MDB=20.*ALOG10(MAG)
**
** PROGRAM AND PLOTTER CONTROL
**
** SAMPLE
**      CALL DRWG(1,1,W/6.28,MDB)
**      CALL DRWG(1,2,W/6.28,DBZERO)
**
** TERMINAL
**      CALL ENDRW(NPLOT)
**      CONTROL FINIM=99.0,DELT=0.1,DELS=0.1
**      PRINT 0.1,W,HZ,MDB
**      END
**      STOP
**      //C.SYSPRINT DD DSN=,SYSOUT=A
**      //PLOT.STEPLIB DD DSN=C0044.Q,UNIT=3330,VOL=SER=DISK02,DISP=SHR
**      //PLOT.PLOTARM DD *
**      &PLOT.SCALE=0.55 &END
**      //PLOT.SYSIN DD *

```

```

0.0      2.0      -30.0      10.0      8.0      7.0

```

PROGRAM 2-11  
ASSOCIATED FIGURE 2-11

## SYSTEM PARAMETERS

PARAM	GAINL=240.0
PARAM	GAINH=20.0
PARAM	PSI=0.06
PARAM	MD=24.17
PARAM	MA=28.625
PARAM	ZA=180.0
PARAM	ZD=113.75
PARAM	V=2500.0
PARAM	KRT=1.48
PARAM	WL=0.2
PARAM	WH=37.7
PARAM	BWL=62.83
PARAM	BWL=0.1
PARAM	BWL=1.19



PROGRAM	2-12
ASSOCIATED FIGURE	2-12

## PROGRAM CONTROL PARAMETERS

COMPLEX S,D,N,G,H,BL,BH,P,T  
COMMON/CAREA/S,D,N,G,H,BL,BH,P,T

## SYSTEM PARAMETERS

**INITIAL**

```

**          DBZERO=0.0
**
** DYNAMIC
**
W=RAMP(0.0)+1
HZ=W/6.28
S=CMPLX(0.0,W)

** SYSTEM DYNAMICS
**
BL=(GAINL*BWL/PSI)/((S**2+8WL*S+WL**2)
BH=(GAINH*BWH/PSI)/((S**2+8WH*S+WH**2)
P=(-MD*S+(ZO*MA/V-ZA*MD/V))/((S*(S**2+ZA/V*S+MA))
T=(P+PSI*(BL+BH))

G=P+PSI*BL
MAG=CABS(G)
MDB=20.*ALOG10(MAG)

** PROGRAM AND PLOTTER CONTROL
**
**
SAMPLE
CALL DRWG(1,1,W/6.28,MDB)
CALL DRWG(1,2,W/6.28,DBZERO)
TERMINAL
CALL ENDRW(NPLOT)
CONTRL FINTIM=99.0,DELT=0.1,DELS=0.1
PRINT 0.1,W,HZ,MDB
END
STOP
//C.SYSPRINT DD DSN=,SYSOUT=A
//PLOT.STEPLIB DD DSN=C0044.Q,UNIT=3330,VOL=SER=DISK02,DISP=SHR
//PLOT.PLOTPARM DD *
//PLOT.SCALE=0.55 &END
//PLOT.SYSIN DD *
0.0      2.0      -30.0      10.0      8.0      7.0

```

PROGRAM	2-13
ASSOCIATED FIGURE	2-13

## SYSTEM PARAMETERS

*PARAM	GAINL=240.0
PARAM	GAINH=20.0
PARAM	PSI=0.06
PARAM	MD=24.17
PARAM	MA=28.625
PARAM	ZA=180.0
PARAM	ZD=113.75
PARAM	V=2500.0
PARAM	KRT=1.48
PARAM	WL=37.7
PARAM	WH=62.83
PARAM	BWL=0.1
PARAM	BWH=1.19

**INITIAL**



```

**          DBZERO=0.0
**
** DYNAMIC
**
W=RAMP(0.0)+1
HZ=W/6.28
S=CMPLX(0.0,W)

** SYSTEM DYNAMICS
**
BL=(GAINL*BWL/PSI)/((S**2+BWL*S+WL**2)
BH=(GAINH*BWH/PSI)/((S**2+BWH*S+WH**2)
P=(-MD*S+(ZD*MA/V-ZA*MD/V))/(S*(S**2+ZA/V*S+MA))
T=(P+PSI*(BL+BH))

*
G=BH
MAG=CABS(G)
MDB=20.*ALOG10(MAG)

** PROGRAM CONTROL AND PLOTTER CONTROL
**
SAMPLE CALL DRWG(1,1,W/6.28,MDB)
        CALL DRWG(1,2,W/6.28,DBZERO)
TERMINAL
        CALL ENDRW(NPLOT)
CONTRL  FINTIM=99.0,DELT=0.1,DELS=0.1
PRINT  0.1,W,HZ,MDB
END
STOP
//C.SYSPRINT DD DSN=,SYSDAT=A
//PLOT.STEPLIB DD DSN=C0044.Q,UNIT=3330,VOL=SER=DISK02,DISP=SHR
//PLOT.PLOTARM DD *
&PLOT.SCALE=0.55 &END
//PLOT.SYSIN DD *
0.0      2.0      -30.0      10.0      8.0      7.0

```

PROGRAM 2-14

ASSOCIATED FIGURE 2-14

# PROGRAM CONTROL PARAMETERS

COMPLEX S, D, N, G, H, BL, BH, P, T  
COMMON/ CAREA/ S, D, N, G, H, BL, BH, P, T

## SYSTEM PARAMETERS

**INITIAL**

```

* *
* * DBZERO=0.0
* *
* * DYNAMIC
* *
* * W=RAMP(0.0)+1
* * HZ=W/6.28
* * S=CMPLX(0.0,W)
* *
* * SYSTEM DYNAMICS
* *
* * BL=(GAINL*BWL/PSI)/(S**2+BWL*S+WL**2)
* * BH=(GAINH*BWH/PSI)/(S**2+BWH*S+WH**2)
* * P=(-MD*S+(ZU*MA/V-ZA*MD/V))/(S*(S**2+ZA/V*S+MA))
* * T=(P+PSI*(BL+BH))
* *
* * G=P+PSI*BH
* * MAG=CABS(G)
* * MDB=20.*ALOG10(MAG)
* *
* * PROGRAM AND PLOTTER CONTROL
* *
* * SAMPLE
* * CALL DRWG(1,1,W/6.28,MDB)
* * CALL DRWG(1,2,W/6.28,DBZERO)
* *
* * TERMINAL
* * CALL ENDRW(NPLOT)
* * CTRL FINTIM=99.0,DELT=0.1,DELS=0.1
* * PRINT 0.1,W,HZ,MDB
* * END
* * STOP
* * //C.SYSPRINT DD DSN=,SYSOUT=A
* * //PLOT.STEPLIB DD DSN=C0044.Q,UNIT=3330,VOL=SER=DISK02,DISP=SHR
* * //PLOT.PLOTARM DD *
* * &PLOT.SCALE=0.55 &END
* * //PLOT.SYSIN DD *

```

0.0	2.0	-30.0	10.0	8.0	7.0
-----	-----	-------	------	-----	-----



```
* * DBZERO=0.0
* *
* * DYNAMIC
* *
W=RAMP(0.0)+1
HZ=W/6.28
S=CPLX(0.0,W)
* *
* * SYSTEM DYNAMICS
* *
BL=(GAINL*BWL/PSI)/((S**2+BWL*S+WL**2)
BH=((GAINH*BWH/PSI)/((S**2+BWH*S+WH**2)
P=(-MD*S+(ZD*MA/V-ZA*MD/V))/((S**2+ZA/V*S+MA))
T=(P+PSI*(BL+BH))
G=T
*
MAG=CABS(G)
MDB=20.*ALOG10(MAG)
*
* PROGRAM AND PLOTTER CONTROL
*
SAMPLE CALL DRWG(1,1,W/6.28,MDB)
CALL DRWG(1,2,W/6.28,DBZERO)
TERMINAL CALL ENDRW(NPLOT)
CONTROL FINITIM=99.0,DELT=0.1,DELS=0.1
PRINT 0.1,W,HZ,MDB
END
STOP
//C.SYSPRINT DD DSN=,SYSDOUT=A
//PLOT.STEPLIB DD DSN=C0044.Q,UNIT=3330,VOL=SER=DISK02,DISP=SHR
//PLOT.PLOTPARM DD *
&PLOT SCALE=0.55 &END
//PLOT.SYSDD *
```



```

**
** INPUT COMMAND
**
** PARAM PC=0.1
**
** DERIVATIVE
**
** MODEL OF THE THIRD ORDER PLANT WITH BENDING MODE
**
** PE=PC+PO
** GAMA=PE+P8
** P1=GAMA*KTHETA
** P2=MDELTA*P1
** P3=-P2-MA
** MA=MALFA*ALFA
** P4=ZDELTA*P1/VEL
** P5=PR-P4-P6
** P6=ZALFA*ALFA/VEL
** P7=PR+P11
** P8=KRTHET*P7
** P9=INTGRL(0.0,PR)
** P0=P9+P10
** P10=PSIRG*80
** P11=PSIGA*8R
** PK=INTGRL(0.0,P3)
** ALFA=INTGRL(0.0,P5)
**
** NARROW BAND MODEL OF LOW BAND BENDING MODE
**
** BL1=GAIN/PSIGA*P1
** BL2=ZETABL*BL1
** BL3=BL2-ZETABL*BL4-BL5*WBL**2.0
** BL4=INTGRL(0.0,BL3)
** BL5=INTGRL(0.0,BL4)
**
** NARROW BAND MODEL OF HIGH BAND PASS BENDING MODE
**
** BH1=GAINH/PSIGA*P1
** BH2=ZETABH*BH1
** BH3=8H2-ZETABH*BH4-8H5*WBH**2.0

```

```

BH4=INTGRL(0.0,BH3)
BH5=INTGRL(0.0,BH4)
BR=BH4+BL4
BO=BH5+BL5

```

```

MODEL OF THE PLANT WITHOUT BENDING MODES
TO ESTABLISH NOMINAL PERFORMANCE .

```

```

P21=PC+P27
P22=P21+P31
P23=KTHETA*P22
P24=MDELTA*P23
P25=-P24-MALFA*P30
P26=INTGRL(0.0,P25)
P27=INTGRL(0.0,P26)
P28=ZDELTA/VEL*P23
P29=-P28-ZALFA/VEL*P30+P26
P30=INTGRL(0.0,P29)
P31=KRTHET*P26

```

```

PROGRAM CONTROL AND PLOTTER CONTROL

```

```

** ** **
SAMPLE

```

```

CALL DRWG(1,1,TIME,P27)
CALL DRWG(1,2,TIME,PO)
CALL DRWG(2,1,TIME,PO)

```

```

TERMINAL

```

```

CALL ENDRW(NPLOT)
CONTRL FINTIM=2.0 , DELT=0.01, DELS=0.01
INTEG RKSPX
PRINT 0.01,PO,BR
END

```

```

STOP

```

```

//C .SYSPRINT DD DSN=,SYSOBT=A
//PLOT.STEPLIB DD DSN=C0044.Q,UNIT=3330,VOL=SER=DISK02,DISP=SHR
//PLOT.PLOTPARM DD *
&PLOT SCALE=0.45 &END
//PLOT.SYSIN DD *

```

0.0	0.2	-0.08	0.01	10.0	10.0	5
0.0	0.2				10.0	10







```

BH4=INTGRL(0.0,BH3)
BH5=INTGRL(0.0,BH4)
BR=8H4+8L4
BU=8H5+8L5

```

```

MODEL OF THE PLANT WITHOUT BENDING MODES
TO ESTABLISH NOMINAL PERFORMANCE .

```

```

P21=PC+P27
P22=P21+P31
P23=KTHETA*P22
P24=MDelta*P23
P25=-P24-MALFA*P30
P26=INTGRL(0.0,P25)
P27=INTGRL(0.0,P26)
P28=ZDELTA/VEL*P23
P29=-P28-ZALFA/VEL*P30+P26
P30=INTGRL(0.0,P29)
P31=KRTHET*P26

```

```

PROGRAM AND PLOTTER CONTROL

```

```

**
**
**
**
** SAMPLE
CALL ORWG(1,1,TIME,P27)
CALL DRWG(1,2,TIME,PO)
CALL DRWG(2,1,TIME,PO)
TERMINAL
CALL ENDRW(NPLOT)
CONTRL FINTIM=2.0 , DELT=0.01, DELS=0.01
INTEG RKSF
PRINT 0.01,PD,BR
END
STOP
//C.SYSPRINT DD DSN=,SYSOUT=A
//PLOT.STEPLIB DD DSN=C0044.Q,UNIT=3330,VOL=SER=DISK02,DISP=SHR
//PLOT.PLOTPARM DD *
&PLOT SCALE=0.45 &END
//PLOT.SYSIN DD *

```

0.0	0.2	-0.08	0.01	10.0	10.0
0.0	0.2				

5

10

PROGRAM	2-21
ASSOCIATED FIGURES	2-21 2-22

PLANT CONTAMINATED WITH ONE  
BENDING MODE CENTERED AT 6 HZ.  
STEP INPUT=0.1 RAD.  
NO DIGITAL FILTER

```

+ INTEGER NPLOT
+ CONST NPLOT=1

```

*PARAM	PSIGA=0.06
PARAM	PSIRC=0.06
PARAM	MDELTA=28.625
PARAM	WELFA=24.17
PARAM	ZALFA=180.0
PARAM	ZDELTA=113.75
PARAM	VEL=250.0
PARAM	WBH=62.83
PARAM	ZETABH=1.19
PARAM	GAINH=0.0
PARAM	WBL=37.7
PARAM	ZETABL=0.1
PARAM	GAINL=240.0
PARAM	KTHETA=1.48
PARAM	KRTHET=0.2

# MODEL OF THE THIRD ORDER PLANT

### NARROW BAND MODEL OF LOW BAND BENDING MODE

## NARROW BAND MODEL OF HIGH BAND BENDING MODE

BH1=GAINH/P SIGA\*PI  
BH2=ZETABH\*BHI

```

BH3=BH2-ZETABH*BH4-BH5*WBH**2.0
BH4=INTGRL(0.0,BH3)
BH5=INTGRL(0.0,BH4)
BR=BH4+BL4
BO=BH5+BL5

```

```

MODEL OF THE PLANT WITHOUT BENDING MODES
TO ESTABLISH NOMINAL PERFORMANCE .

```

```

P21=PC+P27
P22=P21+P31
P23=KTHETA*P22
P24=MDELTA*P23
P25=-P24-MALFA*P30
P26=INTGRL(0.0,P25)
P27=INTGRL(0.0,P26)
P28=ZDELTA/VEL*P23
P29=-P28-ZALFA/VEL*P30+P26
P30=INTGRL(0.0,P29)
P31=KRTHEI*P26

```

```

PROGRAM AND PLOTTER CONTROL

```

```

** ** **
SAMPLE

```

```

CALL DRWG(1,1,TIME,P27)
CALL DRWG(1,2,TIME,PO)
CALL DRWG(2,1,TIME,PO)

```

```

TERMINAL

```

```

CALL ENDRW(NPLOT)
CONTRL FINTIM=2.0 , DELT=0.01, DELS=0.01
INTEG RKSF
PRINT 0.01,PO,BR
END

```

```

STOP

```

```

//C. SYSPRINT DD DSN=,SYSOIT=A
//PLOT. STEPLIB DD DSN=C0044.Q,UNIT=3330,VOL=SER=DISK02,DISP=SHR
//PLOT. PLOTARM DD *
&PLOT SCALE=0.45 &END
//PLOT. SYSIN DD *

```

```

0.0 0.2 -0.08 0.01 10.0 10.0

```

```

5
10

```

10.0

0.2

0.0







```

BH2=ZETABH*BH1
BH3=8BH2-ZETABH*BH4-8BH5*WBH**2.0
BH4=INTGRL(0.0,BH3)
BH5=INTGRL(0.0,BH4)
BR=8BH4+BL4
BO=8BH5+BL5

```

MODEL OF THE PLANT WITHOUT BENDING MODES  
TO ESTABLISH NOMINAL PERFORMANCE .

```

P21=PC+P27
P22=P21+P31
P23=KTHETA*P22
P24=MDELTA*P23
P25=-P24-MALFA*P30
P26=INTGRL(0.0,P25)
P27=INTGRL(0.0,P26)
P28=ZDELTA/VEL*P23
P29=-P28-ZALFA/VEL*P30+P26
P30=INTGRL(0.0,P29)
P31=KRTHET*P25

```

PROGRAM CONTROL AND PLOTTER CONTROL

```

**
**
**
**
**
**
SAMPLE
CALL DRWG(1,1,TIME,P27)
CALL DRWG(1,2,TIME,PO)
CALL DRWG(2,1,TIME,PO)
TERMINAL
CALL ENDRW(NPLOT)
CONTROL FINTIM=2.0 , DELT=0.01, DELS=0.01
INTEG RKSF
PRINT 0.01,PO,BR
END
STOP
//C.SYSPRINT DD DSN=,SYSOUT=A
//PLOT.STEPLIB DD DSN=C0044.Q,UNIT=3330,VOL=SER=DISK02,DISP=SHR
//PLOT.PLOTPARM DD *
&PLOT SCALE=0.45 &END
//PLOT.SYSIN DD *

```

```

0.0      0.2      -0.08      0.01      10.0      10.0

```

10

10.0

0.2

0.0





```

END
STOP
//C.SYSPRINT DD DSN=,SYSOUT=A
//PLOT.STEPLIB DD DSN=C0044.Q,UNIT=3330,VOL=SER=DISK02,DISP=SHR
//PLOT.PLOTPARM DD *
//PLOT.SCALE=0.55 &END
//PLOT.SYSIN DD *

```

10

8.0

2.0

0.0

10

8.0

2.0

0.0



```

W=RAMP(0.0)+1.0
HZ=W/6.28
S=CMPLX(0.0,W)
Z=CEXP(S*T)

```

```

ENTER THE NUMERATOR POLYNOMIAL IN Z.
N1, N2, N3 CAN BE USED AS SUB-FUNCTIONS OF
THE NUMERATOR.

```

```

N1=(0.15*Z**2-0.12135*Z+0.0375)*3.1
N2=0.1*Z**2-0.1
N=N1

```

```

ENTER THE DENOMINATOR POLYNOMIAL IN Z.
D1, D2, D3 CAN BE USED AS SUB-FUNCTIONS OF
THE DENOMINATOR.

```

```

D1=Z**2-1.3753*Z+.7225
D2=Z**2-1.45625*Z+0.81
D=D1

```

```

G=N/D
MAG=CABS(G)
MDB=20.0*ALOG10(MAG)
RE=REAL(G)
IM=AIMAG(G)
PHI=57.3*ATAN2(IM,RE)
IF(PHI.GT.0.0) PHI=PHI-360.0

```

```

PROGRAM AND PLOTTER CONTROL

```

```

SAMPLE

```

```

CALL DRWG(1,1,W/6.28,MDB)
CALL DRWG(1,2,W/6.28,DBZERO)
CALL DRWG(2,1,W/6.28,PHI)
CALL DRWG(2,2,W/6.28,PHI180)

```

```

TERMINAL

```

```

CALL ENDRW(NPLOT)
CONTRL FINTIM=99.0, DELT=0.1, DELS=0.1
PRINT 0.1,HZ,MDB,PHI
END

```



```

STOP
//C. SYSPRINT DD DSN=, SYSOUT=A
//PLOT. STEPLIB DD DSN=C0044.Q, UNIT=3330, VOL=SER=DISK02, DISP=SHR
//PLOT. PLOT Parm DD *
//PLOT. SCALE=0.55 &END
//PLOT. SYSIN DD *

```

```

0.0      2.0
0.0      2.0

```

```

8.0
8.0

```

```

10
10

```

PROGRAM 3-7	ASSOCIATED FIGURE 3-7
1. The first step in the process of identifying a problem is to recognize that a problem exists.	1. The first step in the process of identifying a problem is to recognize that a problem exists.
2. The second step is to define the problem in terms of specific, measurable, and observable criteria.	2. The second step is to define the problem in terms of specific, measurable, and observable criteria.
3. The third step is to identify the causes of the problem.	3. The third step is to identify the causes of the problem.
4. The fourth step is to develop a plan of action to solve the problem.	4. The fourth step is to develop a plan of action to solve the problem.
5. The fifth step is to implement the plan of action.	5. The fifth step is to implement the plan of action.
6. The sixth step is to evaluate the results of the plan of action.	6. The sixth step is to evaluate the results of the plan of action.
7. The seventh step is to modify the plan of action if necessary.	7. The seventh step is to modify the plan of action if necessary.

## PROGRAM CONTROL PARAMETERS

### †TITILE FREQUENCY RESPONSE OF THE HIGH FREQUENCY BANDPASS TITILE FREQUENCY DETECTOR FILTER.

ENTER THE SAMPLING INTERVAL T.

COMPLEX S,Z,N,D,N1,N2,N3,D1,D2,D3,G  
COMMON/CAREA/S,Z,N,O,N1,N2,N3,D1,D2,D3,G

PHI180=-180.0  
DBZERO=0.0

$$W = \text{RAMP}(0.0) + 1.0$$

```

* * * * *
HZ=W/6.28
S=CMPLX(0.0,W)
Z=CEXP(S*T)

ENTER THE NUMERATOR POLYNOMIAL IN Z.
N1, N2, N3 CAN BE USED AS SUB-FUNCTIONS OF
THE NUMERATOR.

N1=(0.15*Z**2-0.12135*Z+0.0375)*3.1
N2=0.1*Z**2-0.1
N=N1*N2

ENTER THE DENOMINATOR POLYNOMIAL IN Z.
D1, D2, D3 CAN BE USED AS SUB-FUNCTIONS OF
THE DENOMINATOR.

D1=Z**2-1.3753*Z+.7225
D2=Z**2-1.45625*Z+0.81
D=D1*D2

G=N/D
MAG=CABS(G)
MDB=20.0*ALOG10(MAG)
RE=REAL(G)
IM=AIMAG(G)
PHI=57.3*ATAN2(IM,RE)
IF(PHI.GT.0.0) PHI=PHI-360.0

PROGRAM AND PLOTTER CONTROL

* * * * *
SAMPLE
CALL DRWG(1,1,W/6.28,MDB)
CALL DRWG(1,2,W/6.28,DBZERO)
CALL DRWG(2,1,W/6.28,PHI)
CALL DRWG(2,2,W/6.28,PHI180)

TERMINAL
CALL ENDRW(NPLOT)
CONTRL FINTIM=99.0, DELT=0.1, DELS=0.1
PRINT 0.1,HZ,MDB,PHI
END
STOP

```

```

//C.SYSPRINT DD DSN=,SYSOBT=A
//PLOT.STEPLIB DD DSN=C0044.Q,UNIT=3330,VOL=SER=DISK02,DISP=SHR
//PLOT.PLOTARM DD *
&PLOT.SCALE=0.55 &END
//PLOT.SYSIN DD *

```

10

10

8.0

8.0

2.0

2.0

0.0

0.0



```

HZ=W/6.28
S=CMPLX(0.0,W)
Z=CEXP(S*T)

```

```

ENTER THE NUMERATOR POLYNOMIAL IN Z.
N1, N2, N3 CAN BE USED AS SUB-FUNCTIONS OF
THE NUMERATOR.

```

```

N1=0.15*Z**2-0.12354*Z+0.030375
N2=0.1*Z**2-0.1
N=N1*N2

```

```

ENTER THE DENOMINATOR POLYNOMIAL IN Z.
D1, D2, D3 CAN BE USED AS SUB-FUNCTIONS OF
THE DENOMINATOR.

```

```

D1=Z**2-1.7228*Z+.88604
D2=Z**2-1.64725*Z+0.81
D=D1*D2

```

```

G=N/D
MAG=CABS(G)
MDB=20.0*ALOG10(MAG)
RE=REAL(G)
IM=AIMAG(G)
PHI=57.3*ATAN2(IM,RE)
IF(PHI.GT.0.0) PHI=PHI-360.0

```

```

PROGRAM AND PLOTTER CONTROL

```

```

SAMPLE

```

```

CALL DRWG(1,1,W/6.28,MDB)
CALL DRWG(1,2,W/6.28,DBZERO)
CALL DRWG(2,1,W/6.28,PHI)
CALL DRWG(2,2,W/6.28,PHI180)

```

```

TERMINAL

```

```

CALL ENDRW(NPLOT)
CONTRL FINTIM=99.0, DELT=0.1, DELS=0.1
PRINT 0.1,HZ,MDB,PHI
END
STOP

```

```

//C.SYSPRINT DD DSN=,SYSCUT=A
//PLOT.STEPLIB DD DSN=C0044.Q,UNIT=3330,VUL=SER=DISK02,DISP=SHR
//PLOT.PLOTPARM DD *
&PLOT.SCALE=0.55 &END
//PLOT.SYSIN DD *

```

0.0	2.0	8.0	10
0.0	2.0	8.0	10





S=CMPLX(0.0,W)  
Z=CEXP(S\*T)

ENTER THE LOW FREQUENCY BANDPASS FILTER NUMERATOR.

N1=0.15\*Z\*\*2-0.12354\*Z+0.030375  
N2=0.1\*Z\*\*2-0.1  
N=N1\*N2

ENTER THE HIGH FREQUENCY BANDPASS FILTER NUMERATOR.

N3=(0.15\*Z\*\*2-0.12135\*Z+0.0375)\*3.1  
N4=0.1\*Z\*\*2-0.1  
NN=N3\*N4

ENTER THE LOW FREQUENCY BANDPASS FILTER DENOMINATOR.

D1=Z\*\*2-1.7228\*Z+.88604  
D2=Z\*\*2-1.64725\*Z+0.81  
D=D1\*D2

ENTER THE HIGH FREQUENCY FILTER DENOMINATOR.

D3=Z\*\*2-1.3753\*Z+0.7225  
D4=Z\*\*2-1.45625\*Z+0.81  
DD=D3\*D4

G=N/D  
MAG=CABS(G)  
MDB=20.0\*ALOG10(MAG)

GG=NN/DD  
IMAG=CABS(GG)  
IMDB=20.0\*ALOG10(IMAG)

PROGRAM AND PLOTTER CONTROL

\*\*\*\*\*

\*\*\*\*\*

\*\*\*\*\*

\*\*\*\*\*

\*\*\*\*\*

\*\*\*\*\*

\*\*\*\*\*

```

* SAMPLE      CALL DRWG(1,1,W/6.28,MDB)
              CALL DRWG(1,2,W/6.28,DBZERO)
              CALL DRWG(1,3,W/6.28,IMDB)
TERMINAL
              CALL ENDRW(NPLOT)
CONTRL FINTIM=99.0, DELT=0.1, DELS=0.1
PRINT 0.1,HZ,MDB,IMDB
END
STOP
//C.SYSPRINT DD DSN=,SYSDUT=A
//PLOT.STEPL18 DD DSN=C0044.Q,UNIT=3330,VOL=SER=DISK02,DISP=SHR
//PLOT.PLOTARM DD *
//PLOT.SCALE=0.55 &END
//PLOT.SYSIN DD *

```

0.0 2.0

8.0

10



```

HZ=W/6.28
S=CMPLX(0.0,W)
Z=CEXP(S*T)

```

```

ENTER THE NUMERATOR POLYNOMIAL IN Z.
N1, N2, N3 CAN BE USED AS SUB-FUNCTIONS OF
THE NUMERATOR.

```

```

N=0.9708*(Z**2-1.8595*Z+1.0)

```

```

ENTER THE DENOMINATOR POLYNOMIAL IN Z.
D1, D2, D3 CAN BE USED AS SUB-FUNCTIONS OF
THE DENOMINATOR.

```

```

D=Z**2-1.6736*Z+0.81

```

```

G=N/D
MAG=CABS(G)
MDB=20.0*ALOG10(MAG)
RE=REAL(G)
IM=AIMAG(G)
PHI=57.3*ATAN2(IM,RE)
IF(PHI.GT.0.0) PHI=PHI-360.0

```

```

PROGRAM AND PLOTTER CONTROL

```

```

SAMPLE

```

```

CALL DRWG(1,1,W/6.28,MDB)
CALL DRWG(1,2,W/6.28,DBZERO)
CALL DRWG(2,1,W/6.28,PHI)
CALL DRWG(2,2,W/6.28,PHI180)

```

```

TERMINAL

```

```

CALL ENDRW(NPLOT)
CONTRL FINTIM=99.0, DELT=0.1, DELS=0.1
PRINT 0.1,HZ,MDB,PHI
END

```

```

STOP

```

```

//C. SYSPRINT DD DSN=,SYSDOUT=A
//PLOT. STEPLIB DD DSN=C0044.Q,UNIT=3330,VOL=SER=DISK02,DISP=SHR
//PLOT. PLOT Parm DD *
&PLOT SCALE=0.55 &END

```

//PLOT.SYSIN DD \*

0.0 2.0

0.0 2.0

8.0

8.0

10

10

PROGRAM	3-15
ASSOCIATED FIGURES	3-15 3-16

## PROGRAM CONTROL PARAMETERS

TITLE FREQUENCY RESPONSE OF A NOTCH FILTER CENTERED  
TITLE AT 10.0 HZ. WITH A POLE RADIUS OF 0.8.

COMPLEX S,Z,N,D,N1,N2,N3,D1,D2,D3,G  
COMMON/CAREA/S,Z,N,D,N1,N2,N3,D1,D2,D3,G

PHI180=-180.0  
DBZERO=0.0

$$W = \text{RAMP}(0.0) + 1.0$$

```

HZ=W/6.28
S=CMPLX(0.0,W)
Z=CEXP(S*T)

```

```

ENTER THE NUMERATOR POLYNOMIAL IN Z:
N1, N2, N3 CAN BE USED AS SUB-FUNCTIONS OF
THE NUMERATOR.

```

```

N=0.9044*(Z**2-1.618*Z+1.0)

```

```

ENTER THE DENOMINATOR POLYNOMIAL IN Z:
D1, D2, D3 CAN BE USED AS SUB-FUNCTIONS OF
THE DENOMINATOR.

```

```

D=Z**2-1.2944*Z+0.64

```

```

G=N/D
MAG=CABS(G)
MDB=20.0*ALOG10(MAG)
RE=REAL(G)
IM=AIMAG(G)
PHI=57.3*ATAN2(IM,RE)
IF(PHI.GT.0.0) PHI=PHI-360.0

```

```

PROGRAM AND PLOTTER CONTROL

```

```

SAMPLE
CALL DRWG(1,1,W/6.28,MDB)
CALL DRWG(1,2,W/6.28,DBZERO)
CALL DRWG(2,1,W/6.28,PHI)
CALL DRWG(2,2,W/6.28,PHI180)

```

```

TERMINAL
CALL ENDRW(NPLOT)
CONTRL FINTIM=99.0, DELT=0.1, DELS=0.1
PRINT 0.1,HZ,MDB,PHI
END

```

```

STOP
//C. SYSPRINT DD DSN=, SYSOUT=A
//PLOT. STEPLIB DD DSN=C0044.Q, UNIT=3330, VOL=SER=DISK02, DISP=SHR
//PLOT. PLOTARM DD *
&PLOT SCALE=0.55 &END

```

//PLOT.SYSIN DD \*

0.0 2.0

0.0 2.0

8.0

8.0

10

10





```

** DYNAMIC
**
LHZ=6.0
HHZ=10.0

SET THE INITIAL DIGITAL FILTER PARAMETERS

IF (TIME.NE.0.0) GO TO 10

CALCULATE THE FILTER COEFFICIENTS

RADIUS=RADIUS1
A11,B11,B12,GAIN1=COEFF(F1SET,DELT,RADIUS)
RADIUS=RADIUS2
A21,B21,B22,GAIN2=COEFF(F2SET,DELT,RADIUS)
GO TO 100
CONTINUE

10
GENERATE INPUT SIGNAL COMPOSED OF 2, 6, AND 10 HZ
SINE WAVES OF EQUAL AMPLITUDE.

F1=SINE(0.0,2.0*2.0*PI,0.0)
F2=SINE(0.0,6.0*2.0*PI,0.0)
F3=SINE(0.0,10.0*2.0*PI,0.0)
FILTN=F1+F2+F3

5 TO 8 HZ DIGITAL BANDPASS FILTER AND FREQUENCY DETECTOR

BL1OUT=0.15*FILOUT-0.12354*BL11+0.030375*BL12+1.7228*BL21...
-0.88604*BL22
BL2OUT=0.1*BL1OUT-0.1*BL32+1.64725*BL41-0.81*BL42
BL12=BL11
BL11=BR21
BL22=BL21
BL21=BL1OUT
BL32=BL31
BL31=BL1OUT
BL42=BL41
BL41=BL2OUT

```

\* \* \* \* \*

8 TO 15 HZ DIGITAL BANDPASS FILTER AND FREQUENCY DETECTOR

```
BH1OUT=0.465*FILOUT-0.3761*BH11+0.1162*BH12+1.3753*BH21...
-0.7225*BH22
BH2OUT=0.1*BH1OUT-0.1*BH32+1.45625*BH41-0.81*BH42
BH12=BH11
BH11=BR
BH22=BH21
BH21=BH1OUT
BH32=BH31
BH31=BH1OUT
BH42=BH41
BH41=BH2OUT
```

\* \* \* \* \*

COMPUTE THE CENTER FREQUENCY FOR THE LOW FREQUENCY NOTCH.

```
TC1=CROSS(TIME,BH1OUT,0.0)
IF(TC1.EQ.0.0) GO TO 50
TINT1=TC1-LTINT1
LTINT1=TC1
IF(TINT1.GT.0.1) GO TO 50
IF(TINT1.LT.0.0625) GO TO 50
FREQ=1.0/(2.0*TINT1)
FREQ=(F1SET+FREQ)/2.0
RADIUS=RADIUS1
A11,B11,B12,GAIN1=COEFF(FREQ,DELT,RADIUS)
F1SET=FREQ
```

\* \* \* \* \* 50

COMPUTE THE CENTER FREQUENCY FOR THE HIGH FREQUENCY NOTCH

```
TC2=CROSS(TIME,BH2OUT,0.0)
IF(TC2.EQ.0.0) GO TO 100
TINT2=TC2-LTINT2
LTINT2=TC2
IF(TINT2.GT.0.0625) GO TO 100
IF(TINT2.LT.0.033333) GO TO 100
FREQ=1.0/(2.0*TINT2)
FREQ=(F2SET+F2SET)/2.0
RADIUS=RADIUS2
A21,B21,B22,GAIN2=COEFF(FREQ,DELT,RADIUS)
F2SET=FREQ
```









\*\*\*

5 TO 8 HZ DIGITAL BANDPASS FILTER AND FREQUENCY DETECTOR

BL1OUT=0.15\*8R-0.12354\*BL11+0.030375\*BL12+1.7228\*BL21-0.88604\*BL22  
 BL2OUT=0.1\*BL1OUT-0.1\*BL32+1.64725\*BL41-0.81\*BL42  
 BL12=BL11  
 BL11=8R  
 BL22=BL21  
 BL21=BL1OUT  
 BL32=BL31  
 BL31=BL1OUT  
 BL42=BL41  
 BL41=BL2OUT

\*\*\*\*\*

8 TO 15 HZ DIGITAL BANDPASS FILTER AND FREQUENCY DETECTOR

BH1OUT=0.465\*8R-0.3761\*BH11+0.1162\*BH12+1.3753\*BH21-0.7225\*BH22  
 BH2OUT=0.1\*BH1OUT-0.1\*BH32+1.45625\*BH41-0.81\*BH42  
 BH12=BH11  
 BH11=8R  
 BH22=BH21  
 BH21=BH1OUT  
 BH32=BH31  
 BH31=BH1OUT  
 BH42=BH41  
 BH41=BH2OUT

\*\*\*\*\*

COMPUTE THE CENTER FREQUENCY FOR THE LOW FREQUENCY NOTCH.

TCL=CROSS(TIME,BL1OUT,0.0)  
 IF(TCL.EQ.0.0) GO TO 50  
 TINT1=TCL-LTINT1  
 LTINT1=TCL  
 IF(TINT1.GT.0.1) GO TO 50  
 IF(TINT1.LT.0.0625) GO TO 50  
 FREQ=1.0/(2.0\*TINT1)  
 FREQ=(F1SET+FREQ)/2.0  
 RADIUS=RADIUS1  
 A11=BL11,BL12,GAIN1=COEFF(FREQ,DELT,RADIUS)  
 F1SET=FREQ

\*\*\*\*\*

COMPUTE THE CENTER FREQUENCY FOR THE HIGH FREQUENCY NOTCH



```

* 50
TC2=CROSS(TIME,BH2OUT,0.0)
IF(TC2.EQ.0.0) GO TO 100
TINT2=TC2-LTINT2
LTINT2=TC2
IF(TINT2.GT.0.0625) GO TO 100
IF(TINT2.LT.0.033333) GO TO 100
FREQ=1.0/(2.0*TINT2)
FREQ=(FREQ+F2SET)/2.0
RADIUS=RADIUS2
A21,B21,B22,GAIN2=COEFF(FREQ,DELT,RADIUS)
F2SET=FREQ

* 100
FIRST NOTCH FILTER
F1OUT=FILTIN+A11*F111+F112-B11*F011-B12*F012

SECOND NOTCH FILTER
F2OUT=F1OUT+A21*F121+F122-B21*F021-B22*F022

ADJUST OUTPUT FOR DC GAIN = 1.0
F1LOUT=F2OUT*GAIN1*GAIN2
F112=F111
F111=FILTIN
F012=F011
F011=F1OUT
F122=F121
F121=F1OUT
F022=F021
F021=F2OUT

* 200
CONTINUE

* DERIVATIVE
MODEL OF THE THIRD ORDER PLANT

```

\*

```

PE=PC+PD
GAMA=PE+P8
FILTIIN=GAMA*KTHETA
P1=FILOUT
P2=DELTA*P1
P3=-P2-MA
MA=MALFA*ALFA
P4=ZDELTA*P1/VEL
P5=PR-P4-P6
P6=ZALFA*ALFA/VEL
P7=PR+P11
P8=KRTHET*P7
P9=INTGRL(0.0,PR)
PQ=P9+P10
P10=PSIRG*80
P11=PSIGA*BR
PR=INTGRL(0.0,P3)
ALFA=INTGRL(0.0,P5)

```

\*\*\*\*\*

MODEL OF LOW BAND BENDING MODE

```

BL1=GAINL/PSIGA*P1
BL2=ZETABL*BL1
BL3=BL2-ZETABL*BL4-BL5*WBL**2.0
BL4=INTGRL(0.0,BL3)
BL5=INTGRL(0.0,BL4)

```

\*\*\*\*\*

MODEL OF HIGH BAND BENDING MODE

```

BH1=GAINH/PSIGA*P1
BH2=ZETABH*BH1
BH3=BH2-ZETABH*BH4-BH5*WBH**2.0
BH4=INTGRL(0.0,BH3)
BH5=INTGRL(0.0,BH4)
BR=BH4+BL4
BQ=BH5+BL5

```

\*\*\*\*\*

MODEL OF THE PLANT WITHOUT BENDING MODES  
TO ESTABLISH NOMINAL PERFORMANCE .

P21=PC+P27

```

P22=P21+P31
P23=KTHETA*P22
P24=MDELTA*P23
P25=-P24-MALFA*P30
P26=INTGRL(0.0,P25)
P27=INTGRL(0.0,P26)
P28=ZDELTA/VEL*P23
P29=-P28-ZALFA/VEL*P30+P26
P30=INTGRL(0.0,P29)
P31=KRIHET*P26

```

# PROGRAM AND PLOTTER CONTROL

```

*
*
*
*
*

```

```

SAMPLE

```

```

CALL DRWG(1,1,TIME,P27)
CALL DRWG(1,2,TIME,P0)
CALL DRWG(2,1,TIME,F1SET)
CALL DRWG(2,2,TIME,F2SET)
CALL DRWG(2,3,TIME,LHZ)
CALL DRWG(2,4,TIME,HHZ)

```

```

TERMINAL

```

```

CALL ENDRW(NPLOT)
CONTRL FINTIM=2.0 , DELT=0.01, DELS=0.01
INTEG RKSF
PRINT 0.01,P0,BR,F1SET,F2SET
END
STOP

```

# FORTAN SUBROUTINE TO CALCULATE THE NOTCH FILTER COEFFICIENTS

```

FORTAN

```

```

SUBROUTINE COEFF(FREQ,DELT,RADIUS,A1,B1,B2,GAIN)

```

```

C
C
C
CALCULATE THE FILTER COEFFICIENTS

```

```

PI=3.14159
A1=-2.0*COS(FREQ*2.0*PI*DELT)
B1=-2.0*RADIUS*COS(FREQ*2.0*PI*DELT)
B2=RADIUS**2.0

```

```

C
C
C
ADJUST THE FILTER DC GAIN TO UNITY

```

```

GAIN=(1.0+B1+B2)/(2.0+A1)
RETURN

```

```

*
*
*//C.SYSPRINT DD DSN=,SYSDOUT=A
*//PLOT.STEPLIB DD DSN=C0044.Q,UNIT=3330,VOL=SER=DISK02,DISP=SHR
*//PLOT.PLOTARM DD *
*//PLOT.SCALE=0.45 &END
*//PLOT.SYSIN DD *
0.0 0.2 -0.08 0.01 10.0 10.0
0.0 0.2 5.0 1.0 10.0 10.0

```

5

5





\*\*

```
BL1OUT=0.15*BR-0.12354*BL11+0.030375*BL12+1.7228*BL21-0.88604*BL22
BL2OUT=0.1*BL1OUT-0.1*BL32+1.64725*BL41-0.81*BL42
BL12=BL11
BL11=BR
BL22=BL21
BL21=BL1OUT
BL32=BL31
BL31=BL1OUT
BL42=BL41
BL41=BL2OUT
```

\*\*\*\*\*

8 TO 15 HZ DIGITAL BANDPASS FILTER AND FREQUENCY DETECTOR

```
BH1OUT=0.465*BR-0.3761*BH11+0.1162*BH12+1.3753*BH21-0.7225*BH22
BH2OUT=0.1*BH1OUT-0.1*BH32+1.45625*BH41-0.81*BH42
BH12=BH11
BH11=BR
BH22=BH21
BH21=BH1OUT
BH32=BH31
BH31=BH1OUT
BH42=BH41
BH41=BH2OUT
```

\*\*\*\*\*

COMPUTE THE CENTER FREQUENCY FOR THE LOW FREQUENCY NOTCH.

```
TC1=CROSS(TIME,BL1OUT,0.0)
IF(TC1.EQ.0.0) GO TO 50
TINT1=TC1-LTINT1
LTINT1=TC1
IF(TINT1.GT.0.1) GO TO 50
IF(TINT1.LT.0.0625) GO TO 50
FREQ=1.0/(2.0*TINT1)
FREQ=(F1SET+FREQ)/2.0
RADIUS=RADIUS1
A11,B11,B12,GAIN1=COEFF(FREQ,DELT,RADIUS)
F1SET=FREQ
```

\*\*\*\*\*

COMPUTE THE CENTER FREQUENCY FOR THE HIGH FREQUENCY NOTCH

```

50      TC2=CROSS(TIME,BH2OUT,0.0)
      IF(TC2.EQ.0.0) GO TO 100
      TINT2=TC2-LTINT2
      LTINT2=TC2
      IF(TINT2.GT.0.0625) GO TO 100
      IF(TINT2.LT.0.033333) GO TO 100
      FREQ=1.0/(2.0*TINT2)
      FREQ=(FREQ+F2SET)/2.0
      RADIUS=RADIUS2
      A21,B21,B22,GAIN2=COEFF(FREQ,DELT,RADIUS)
      F2SET=FREQ

      FIRST NOTCH FILTER

      F1OUT=FILTIN+A11*F111+F112-B11*F011-B12*F012

      SECOND NOTCH FILTER

      F2OUT=F1OUT+A21*F121+F122-B21*F021-B22*F022

      ADJUST OUTPUT FOR DC GAIN = 1.0

      FILOUT=F2OUT*GAIN1*GAIN2
      F112=F111
      F111=FILTIN
      F012=F011
      F011=F1OUT
      F122=F121
      F121=F1OUT
      F022=F021
      F021=F2OUT

      200 CONTINUE

      DERIVATIVE

      MODEL OF THE THIRD ORDER PLANT

```



```

PE=PC+PQ
GAMA=PE+P8
FILTIN=GAMA*KTHETA
P1=FILOUT
P2=MDelta*P1
P3=-P2-MA
MA=MA*ALFA*ALFA
P4=ZDelta*P1/VEL
P5=PR-P4-P6
P6=ZALFA*ALFA/VEL
P7=PR+P11
P8=KRTHET*P7
P9=INTGRL(0.0,PR)
PQ=P9+P10
P10=PSIRG*BO
P11=PSIGA*BR
PR=INTGRL(0.0,P3)
ALFA=INTGRL(0.0,P5)

```

# MODEL OF LOW BAND BENDING MODE

```

BL1=GAINL/PSIGA*P1
BL2=ZETABL*BL1
BL3=BL2-ZETABL*BL4-BL5*WBL**2.0
BL4=INTGRL(0.0,BL3)
BL5=INTGRL(0.0,BL4)

```

# MODEL OF HIGH BAND BENDING MODE

```

BH1=GAINH/PSIGA*P1
BH2=ZETABH*BH1
BH3=BH2-ZETABH*BH4-BH5*WBH**2.0
BH4=INTGRL(0.0,BH3)
BH5=INTGRL(0.0,BH4)
BR=BH4+BL4
BO=BH5+BL5

```

# MODEL OF THE PLANT WITHOUT BENDING MODES TO ESTABLISH NOMINAL PERFORMANCE .

```

P21=PC+P27
P22=P21+P31

```

\*\*\*\*\*

\*\*\*\*\*

\*\*\*\*\*

```

P23=KTHETA*P22
P24=MDELTA*P23
P25=-P24-MALFA*P30
P26=INTGRL(0.0,P25)
P27=INTGRL(0.0,P26)
P28=ZDELTA/VEL*P23
P29=-P28-ZALFA/VEL*P30+P26
P30=INTGRL(0.0,P29)
P31=KRIHET*P26

```

# PROGRAM AND PLOTTER CONTROL

```

* * * * *

```

```

SAMPLE

```

```

CALL DRWG(1,1,TIME,P27)
CALL DRWG(1,2,TIME,P0)
CALL DRWG(2,1,TIME,F1SET)
CALL DRWG(2,2,TIME,F2SET)
CALL DRWG(2,3,TIME,LHZ)
CALL DRWG(2,4,TIME,HHZ)

```

```

TERMINAL

```

```

CALL ENDRW(NPLOT)
CONTRL FINTIM=2.0 , DELT=0.01, DELS=0.01
INTEG RKSFY
PRINT 0.01,P0,BR,F1SET,F2SET
END
STOP

```

```

* * * * *

```

## FORTRAN SUBROUTINE TO CALCULATE NOTCH FILTER COEFFICIENTS

```

FOKTRAN

```

```

SUBROUTINE COEFF(FREQ,DELT,RADIUS,A1,B1,B2,GAIN)

```

```

C
C
C

```

```

CALCULATE THE FILTER COEFFICIENTS

```

```

PI=3.14159
A1=-2.0*COS(FREQ*2.0*PI*DELT)
B1=-2.0*RADIUS*COS(FREQ*2.0*PI*DELT)
B2=RADIUS**2.0

```

```

C
C
C

```

```

ADJUST THE FILTER DC GAIN TO UNITY

```

```

GAIN=(1.0+B1+B2)/(2.0+A1)
RETURN
END

```

AD-A094 554

NAVAL POSTGRADUATE SCHOOL MONTEREY CA  
ADAPTIVE NOTCH FILTER SUPPRESSION OF BENDING MODES.(U)  
DEC 80 W L MARKS

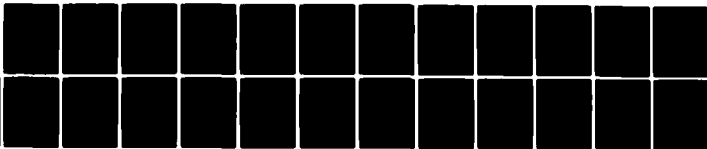
F/G 9/2

UNCLASSIFIED

NL

3 of 3

AD  
A094554



END  
DATE  
FILMED  
281  
DTIC

```

* * //C.SYSPRINT DD DSN=,SYSOUT=A
//PLOT.STEPLIB DD DSN=C0044.Q,UNIT=3330,VOL=SER=DISK02,DISP=SHR
//PLOT.PLOTPARM DD *
&PLOT.SCALE=0.45 &END
//PLOT.SYSIN DD *

```

5

5

0.0	0.2	-0.08	0.01	10.0	10.0
0.0	0.2	5.0	1.0	10.0	10.0

PROGRAM	4-6	4-6	4-7
ASSOCIATED FIGURES			

## PROGRAM CONTROL PARAMETERS

## SYSTEM PARAMETERS

PARAM	P SIGA=0.06
PARAM	P SIRG=0.06
PARAM	MALFA=28.625
PARAM	MDELTA=24.17
PARAM	ZALFA=180.0
PARAM	ZDELTA=113.75
PARAM	VEL=2500.0
PARAM	WBH=56.54
PARAM	ZETABH=1.19
PARAM	GAINH=20.0
PARAM	WBL=43.98
PARAM	ZETABL=0.1
PARAM	GAINL=240.0
PARAM	KTHETA=1.48



```

* * *
5 TO 8 HZ DIGITAL BANDPASS FILTER AND FREQUENCY DETECTOR

BL1OUT=0.15*BR-0.12354*BL11+0.030375*BL12+1.7228*BL21-0.88604*BL22
BL2OUT=0.1*BL1OUT-0.1*BL32+1.64725*BL41-0.81*BL42
BL12=BL11
BL11=BR
BL22=BL21
BL21=BL1OUT
BL32=BL31
BL31=BL1OUT
BL42=BL41
BL41=BL2OUT

* * * * *
8 TO 15 HZ DIGITAL BANDPASS FILTER AND FREQUENCY DETECTOR

BH1OUT=0.465*BR-0.3761*BH11+0.1162*BH12+1.3753*BH21-0.7225*BH22
BH2OUT=0.1*BH1OUT-0.1*BH32+1.45625*BH41-0.81*BH42
BH12=BH11
BH11=BR
BH22=BH21
BH21=BH1OUT
BH32=BH31
BH31=BH1OUT
BH42=BH41
BH41=BH2OUT

* * * * *
COMPUTE THE CENTER FREQUENCY FOR THE LOW FREQUENCY NOTCH.

TC1=CROSS(TIME,BL1OUT,0.0)
IF(TC1.EQ.0.0) GO TO 50
TINT1=TC1-LTINT1
LTINT1=TC1
IF(TINT1.GT.0.1) GO TO 50
IF(TINT1.LT.0.0625) GO TO 50
FREQ=1.0/(2.0*TINT1)
FREQ=(F1SET+FREQ)/2.0
RADIUS=RADIUS1
ALL,B11,B12,GAIN1=COEFF(FREQ,DELT,RADIUS)
F1SET=FREQ

* * * * *
COMPUTE THE CENTER FREQUENCY FOR THE HIGH FREQUENCY NOTCH

```

```

* 50
TC2=CROSS(TIME,BH2OUT,0.0)
IF(TC2.EQ.0.0) GO TO 100
TINT2=TC2-LTINT2
LTINT2=TC2
IF(TINT2.GT.0.0625) GO TO 100
IF(TINT2.LT.0.033333) GO TO 100
FREQ=1.0/(2.0*TINT2)
FREQ=(FREQ+F2SET)/2.0
RADIUS=RADIUS2
A21,B21,B22,GAIN2=COEFF(FREQ,DELT,RADIUS)
F2SET=FREQ

* 100
FIRST NOTCH FILTER
F1OUT=FLTIN+A11*F111+F112-B11*F011-B12*F012

SECOND NOTCH FILTER
F2OUT=F1OUT+A21*F121+F122-B21*F021-B22*F022

ADJUST OUTPUT FOR DC GAIN = 1.0
F11OUT=F2OUT*GAIN1*GAIN2
F112=F111
F111=FLTIN
F012=F011
F011=F1OUT
F122=F121
F121=F1OUT
F022=F021
F021=F2OUT

* 200
CONTINUE

*
DERIVATIVE
*
MODEL OF THE THIRD ORDER PLANT

```



PE=PC+PO  
 GAMA=PE+P8  
 FILTIN=GAMA\*KTHETA  
 P1=FILOUT  
 P2=MDELTA\*P1  
 P3=-P2-MA  
 MA=MALFA\*ALFA  
 P4=ZDELTA\*P1/VEL  
 P5=PR-P4-P6  
 P6=ZALFA\*ALFA/VEL  
 P7=PR+P11  
 P8=KRTHEI\*P7  
 P9=INTGRL(0.0,PR)  
 P10=PSIRG\*BO  
 P11=PSIGA\*BR  
 PR=INTGRL(0.0,P3)  
 ALFA=INTGRL(0.0,P5)

# MODEL OF LOW BAND BENDING MODE

BL1=GAINL/PSIGA\*P1  
 BL2=ZETABL\*BL1  
 BL3=BL2-ZETABL\*BL4-BL5\*WBL\*\*2.0  
 BL4=INTGRL(0.0,BL3)  
 BL5=INTGRL(0.0,BL4)

# MODEL OF HIGH BAND BENDING MODE

BH1=GAINH/PSIGA\*P1  
 BH2=ZETABH\*BH1  
 BH3=BH2-ZETABH\*BH4-BH5\*WBH\*\*2.0  
 BH4=INTGRL(0.0,BH3)  
 BH5=INTGRL(0.0,BH4)  
 BR=BH4+BL4  
 BO=BH5+BL5

MODEL OF THE PLANT WITHOUT BENDING MODES  
 TO ESTABLISH NOMINAL PERFORMANCE .

P21=PC+P27

\*\*\*  
PROGRAM AND PLOTTER CONTROL

```
CALL DRWG(1,1,TIME,P27)
CALL DRWG(1,2,TIME,PO)
CALL DRWG(2,1,TIME,F1SET)
CALL DRWG(2,2,TIME,F2SET)
CALL DRWG(2,3,TIME,LHZ)
CALL DRWG(2,4,TIME,HHZ)
```

5  
\*\* \*

FORTRAN

### CALCULATE THE FILTER COEFFICIENTS

```

C
C
C      ADJUST THE FILTER DC GAIN TO UNITY
      GAIN=(1.0+B1+B2)/(2.0+A1)
      RETURN

```

```

*
*
*//C.SYSPRINT DD DSN=,SYSOUT=A
*//PLOT.STEPLIB DD DSN=C0044.Q,UNIT=3330,VOL=SER=DISK02,DISP=SHR
*//PLOT.PLOTPARM DD *
*//PLOT.SCALE=0.45 &END
*//PLOT.SYSIN DD *
0.0 0.2 -0.08 0.01 10.0 10.0
0.0 0.2 5.0 1.0 10.0 10.0

```

5

5





```

* * *
5 TO 8 HZ DIGITAL BANDPASS FILTER AND FREQUENCY DETECTOR

BL1OUT=0.15*BR-0.12354*BL11+0.030375*BL12+1.7228*BL21-0.88604*BL22
BL2OUT=0.1*BL1OUT-0.1*BL32+1.64725*BL41-0.81*BL42
BL12=BL11
BL11=BR
BL22=BL21
BL21=BL1OUT
BL32=BL31
BL31=BL1OUT
BL42=BL41
BL41=BL2OUT

8 TO 15 HZ DIGITAL BANDPASS FILTER AND FREQUENCY DETECTOR

BH1OUT=0.465*BR-0.3761*BH11+0.1162*BH12+1.3753*BH21-0.7225*BH22
BH2OUT=0.1*BH1OUT-0.1*BH32+1.45625*BH41-0.81*BH42
BH12=BH11
BH11=BR
BH22=BH21
BH21=BH1OUT
BH32=BH31
BH31=BH1OUT
BH42=BH41
BH41=BH2OUT

COMPUTE THE CENTER FREQUENCY FOR THE LOW FREQUENCY NOTCH.

TC1=CROSS(TIME,BL1OUT,0.0)
IF(TC1-EQ.0.0) GO TO 50
TINT1=TC1-LTINT1
LTINT1=TC1
IF(TINT1-GT.0.1) GO TO 50
IF(TINT1-LT.0.0625) GO TO 50
FREQ=1.0/(2.0*TINT1)
FREQ=(F1SET+FREQ)/2.0
RADIUS=RADIUS1
ALL,B11,B12,GAIN1=COEFF(FREQ,DELT,RADIUS)
F1SET=FREQ

COMPUTE THE CENTER FREQUENCY FOR THE HIGH FREQUENCY NOTCH

```

```

* 50      TC2=CROSS(TIME,8H2OUT,0.0)
          IF(TC2.EQ.0.0) GO TO 100
          TINT2=TC2-LTINT2
          LTINT2=TC2
          IF(TINT2.GT.0.0625) GO TO 100
          IF(TINT2.LT.0.033333) GO TO 100
          FREQ=1.0/(2.0*TINT2)
          FREQ=(FREQ+F2SET)/2.0
          RADIUS=RADIUS2
          A21,B21,B22,GAIN2=COEFF(FREQ,DELT,RADIUS)
          F2SET=FREQ

* 100      FIRST NOTCH FILTER
          FIOUT=FILTIN+A11*FI11+FI12-B11*F011-B12*F012

          SECOND NOTCH FILTER
          F2OUT=FIOUT+A21*FI21+FI22-B21*F021-B22*F022

          ADJUST OUTPUT FOR DC GAIN = 1.0

          FILOUT=F2OUT*GAIN1*GAIN2
          FI12=FI11
          FI11=FILTIN
          F012=F011
          F011=FILOUT
          FI22=FI21
          FI21=FILOUT
          F022=F021
          F021=F2OUT

* 200      CONTINUE
          **
          ** DERIVATIVE
          **
          ** MODEL OF THE THIRD ORDER PLANT

```

\*

PE=PC+PO  
GAMA=PE+P8  
FILTIM=GAMA\*KTHETA  
P1=FILOUT  
P2=MDelta\*P1  
P3=-P2-MA  
MA=MALFA\*ALFA  
P4=ZDELTA\*P1/VEL  
P5=PR-P4-P6  
P6=ZALFA\*ALFA/VEL  
P7=PR+P11  
P8=KRTHET\*P7  
P9=INTGRL(0.0,PR)  
P0=P9+P10  
P10=PSIRG\*BQ  
P11=PSIGA\*BR  
PR=INTGRL(0.0,P3)  
ALFA=INTGRL(0.0,P5)

\*\*\*\*\*

MODEL OF LOW BAND BENDING MODE

BL1=GAINL/PSIGA\*P1  
BL2=ZETABL\*BL1  
BL3=BL2-ZETABL\*BL4-BL5\*WBL\*\*2.0  
BL4=INTGRL(0.0,BL3)  
BL5=INTGRL(0.0,BL4)

\*\*\*\*\*

MODEL OF HIGH BAND BENDING MODE

BH1=GAINH/PSIGA\*P1  
BH2=ZETABH\*BH1  
BH3=BH2-ZETABH\*BH4-BH5\*WBH\*\*2.0  
BH4=INTGRL(0.0,BH3)  
BH5=INTGRL(0.0,BH4)  
BR=BH4+BL4  
BO=BH5+BL5

\*\*\*\*\*

MODEL OF THE PLANT WITHOUT BENDING MODES  
TO ESTABLISH NOMINAL PERFORMANCE .

P21=PC+P27



PROGRAM AND PLOTTER CONTROL

```
CALL DRWG(1,1,TIME,P27)
CALL DRWG(1,2,TIME,PO)
CALL DRWG(2,1,TIME,F1SET)
CALL DRWG(2,2,TIME,F2SET)
CALL DRWG(2,3,TIME,LHZ)
CALL DRWG(2,4,TIME,HHZ)
```

### FORTRAN SUBROUTINE TO CALCULATE THE NOTCH FILTER COEFFICIENTS

CC  
SUBROUTINE COEFF (N,KQ,DELTA,PARADIOS  
CALCULATE THE FILTER COEFFICIENTS

```

C C C
      G2=RADIO3+2.0
      ADJUST THE FILTER DC GAIN TO UNITY
      GAIN=(1.0+B1+B2)/(2.0+A1)
      RETURN

```

```

*
*
*//C.SYSPRINT DD DSN=,SYSOUT=A
*//PLOT.STEPLIB DD DSN=C0044.Q,UNIT=3330,VOL=SER=DISK02,DISP=SHR
*//PLOT.PLOTPARM DD *
*//PLOT.SCALE=0.45 &END
*//PLOT.SYSIN DD *

```

0.0	0.2	-0.08	0.01	10.0	10.0	5
0.0	0.2	5.0	1.0	10.0	10.0	5

PROGRAM	4-10
ASSOCIATED FIGURES	4-10 4-11

## PROGRAM CONTROL PARAMETERS

## SYSTEM PARAMETERS

PARAM	PSIGA=0.06
PARAM	PSIRG=0.06
PARAM	MALFA=28.625
PARAM	DELTA=24.17
PARAM	ZALFA=180.0
PARAM	ZDELTA=113.75
PARAM	VEL=2500.0
PARAM	ZETABH=1.19
PARAM	GAINH=20.0
PARAM	ZETABL=0.1
PARAM	GAINL=240.0
PARAM	KHETA=1.48
PARAM	KRTHET=0.2



\*\*\*\*\*

# 5 TO 8 HZ DIGITAL BANDPASS FILTER AND FREQUENCY DETECTOR

```

BL1OUT=0.15*BR-0.12354*BL11+0.030375*BL12+1.7228*BL21-0.88604*BL22
BL2OUT=0.1*BL1OUT-0.1*BL32+1.64725*BL41-0.81*BL42
BL12=BL11
BL11=BR
BL22=BL21
BL21=BL1OUT
BL32=BL31
BL31=BL1OUT
BL42=BL41
BL41=BL2OUT

```

\*\*\*\*\*

# 8 TO 15 HZ DIGITAL BANDPASS FILTER AND FREQUENCY DETECTOR

```

BH1OUT=0.465*BR-0.3761*BH11+0.1162*BH12+1.3753*BH21-0.7225*BH22
BH2OUT=0.1*BH1OUT-0.1*BH32+1.45625*BH41-0.81*BH42
BH12=BH11
BH11=BR
BH22=BH21
BH21=BH1OUT
BH32=BH31
BH31=BH1OUT
BH42=BH41
BH41=BH2OUT

```

\*\*\*\*\*

# COMPUTE THE CENTER FREQUENCY FOR THE LOW FREQUENCY NOTCH.

```

TC1=CROSS(TIME,BL1OUT,0.0)
IF(TC1-EQ-0.0) GO TO 50
TINT1=TC1-LTINT1
LTINT1=TC1
IF(TINT1-LT-0.1) GO TO 50
IF(TINT1-LT-0.0625) GO TO 50
FREQ=1.0/(2.0*TINT1)
FREQ=(F1SET+FREQ)/2.0
RADIUS=RADIUS1
ALL,B11,B12,GAIN1=COEFF(FREQ,DELT,RADIUS)
F1SET=FREQ

```

\*\*\*\*\*

# COMPUTE THE CENTER FREQUENCY FOR THE HIGH FREQUENCY NOTCH

```

** 50
TC2=CROSS(TIME,BH2OUT,0.0)
IF(TC2.EQ.0.0) GO TO 100
TINT2=TC2-LTINT2
LTINT2=TC2
IF(TINT2.GT.0.0625) GO TO 100
IF(TINT2.LT.0.033333) GO TO 100
FREQ=1.0/(2.0*TINT2)
FREQ=(FREQ+F2SET)/2.0
RADIUS=RADIUS2
A21,B21,B22,GAIN2=COEFF(FREQ,DELT,RADIUS)
F2SET=FREQ

** 100
FIRST NOTCH FILTER
F1OUT=FILTIN+A11*F111+F112-B11*F011-B12*F012

SECOND NOTCH FILTER
F2OUT=F1OUT+A21*F121+F122-B21*F021-B22*F022

ADJUST OUTPUT FOR DC GAIN = 1.0
F1LOUT=F2OUT*GAIN1*GAIN2
F112=F111
F111=FILTIN
F012=F011
F011=F1OUT
F122=F121
F121=F1OUT
F022=F021
F021=F2OUT

** 200
CONTINUE

DERIVATIVE
MODEL OF THE THIRD ORDER PLANT

```

\* \*

PE=PC+PO  
GAMA=PE+P8  
FILTIIN=GAMA\*KTHETA  
P1=FILOUT  
P2=MDELTA\*P1  
P3=-P2-MA  
MA=MALFA\*ALFA  
P4=ZDELTA\*P1/VEL  
P5=PR-P4-P6  
P6=ZALFA\*ALFA/VEL  
P7=PR+P11  
P8=KRTHET\*P7  
P9=INTGRL(0.0,PR)  
P0=P9+P10  
P10=PSIRG\*80  
P11=PSIGA\*8R  
PR=INTGRL(0.0,P3)  
ALFA=INTGRL(0.0,P5)

\* \* \* \* \*

MODEL OF LOW BAND BENDING MODE

BL1=GAINL/PSIGA\*P1  
BL2=ZETABL\*BL1  
BL3=BL2-ZETABL\*BL4-BL5\*WBL\*\*2.0  
BL4=INTGRL(0.0,BL3)  
BL5=INTGRL(0.0,BL4)

\* \* \* \* \*

MODEL OF HIGH BAND BENDING MODE

BH1=GAINH/PSIGA\*P1  
BH2=ZETABH\*BH1  
BH3=BH2-ZETABH\*BH4-BH5\*WBH\*\*2.0  
BH4=INTGRL(0.0,BH3)  
BH5=INTGRL(0.0,BH4)  
BR=BH4+BL4  
BO=BH5+BL5

\* \* \* \* \*

MODEL OF THE PLANT WITHOUT BENDING MODES  
TO ESTABLISH NOMINAL PERFORMANCE .

```

P21=PG+P27
P22=P21+P31
P23=KTHETA*P22
P24=MDELTA*P23
P25=-P24-MALFA*P30
P26=INTGRL(0.0,P25)
P27=INTGRL(0.0,P26)
P28=ZDELTA/VEL*P23
P29=-P28-ZALFA/VEL*P30+P26
P30=INTGRL(0.0,P29)
P31=KRTHET*P26

```

```

PROGRAM AND PLOTTER CONTROL

```

```

* * * * *
SAMPLE

```

```

CALL DRWG(1,1,TIME,P27)
CALL DRWG(1,2,TIME,P0)
CALL DRWG(2,1,TIME,F1SET)
CALL DRWG(2,2,TIME,F2SET)
CALL DRWG(2,3,TIME,LHZ)
CALL DRWG(2,4,TIME,HHZ)

```

```

TERMINAL

```

```

CALL ENDRW(NPLOT)
CONTRL FINTIM=2.0 , DELT=0.01, DELS=0.01
INTEG RKSF
PRINT 0.01,P0,BR,LHZ,F1SET,HHZ,F2SET
END
STOP
* * * * *

```

```

FORTRAN SUBROUTINE TO CALCULATE THE NOTCH FILTER COEFFICIENTS

```

```

FORTRAN

```

```

SUBROUTINE COEFF(FREQ,DELT,RADIUS,A1,B1,B2,GAIN)

```

```

CALCULATE THE FILTER COEFFICIENTS

```

```

PI=3.14159
A1=-2.0*COS(FREQ*2.0*PI*DELT)
B1=-2.0*RADIUS*COS(FREQ*2.0*PI*DELT)
B2=RADIUS**2.0

```

```

ADJUST THE FILTER DC GAIN TO UNITY

```

```

GAIN=(1.0+B1+B2)/(2.0+A1)

```



```

*
*
**//C. SYSPRINT DD DSN=, SYSOUT=A
//PLOT. STEPLIB DD DSN=C0044.Q, UNIT=3330, VOL=SER=DISK02, DISP=SHR
//PLOT. PLOTARM DD *
//PLOT. SCALE=0.45 &END
//PLOT. SYSIN DD *
-
0.0 0.2 -0.08 0.01 10.0 10.0
-
0.0 0.2 5.0 1.0 10.0 10.0

```

5

5

PROGRAM	4-12	4-12	4-13
ASSOCIATED FIGURES	4-12	4-13	

## PROGRAM CONTROL PARAMETERS

## SYSTEM PARAMETERS

	PSIGA=	0.06
PARAM	PSIRG=	0.06
PARAM	MDELTA=	28.625
PARAM	WALFA=	24.17
PARAM	ZALFA=	180.0
PARAM	ZDELTA=	113.75
PARAM	VEL=	2500.0
PARAM	ZETABH=	1.19
PARAM	GAINH=	20.0
PARAM	ZETABL=	0.1
PARAM	GAINL=	240.0
PARAM	KHETA=	1.48
PARAM	KRTHE=	0.2



\* \* \* \*

# 5 TO 8 HZ DIGITAL BANDPASS FILTER AND FREQUENCY DETECTOR

```

BL1OUT=0.15*BR-0.12354*BL11+0.030375*BL12+1.7228*BL21-0.88604*BL22
BL2OUT=0.1*BL1OUT-0.1*BL32+1.64725*BL41-0.81*BL42
BL11=BR
BL22=BL21
BL21=BL1OUT
BL32=BL31
BL31=BL1OUT
BL42=BL41
BL41=BL2OUT

```

\* \* \* \* \*

# 8 TO 15 HZ DIGITAL BANDPASS FILTER AND FREQUENCY DETECTOR

```

BH1OUT=0.465*BR-0.3761*BH11+0.1162*BH12+1.3753*BH21-0.7225*BH22
BH2OUT=0.1*BH1OUT-0.1*BH32+1.45625*BH41-0.81*BH42
BH11=BR
BH22=BH21
BH21=BH1OUT
BH32=BH31
BH31=BH1OUT
BH42=BH41
BH41=BH2OUT

```

\* \* \* \* \*

# COMPUTE THE CENTER FREQUENCY FOR THE LOW FREQUENCY NOTCH.

```

TCI=CROSS(TIME,BL1OUT,0.0)
IF(TCI-EQ-0.0) GO TO 50
TINT1=TCI-LTINT1
LTINT1=TCI
IF(TINT1-GT-0.1) GO TO 50
IF(TINT1-LT-0.0625) GO TO 50
FREQ=1.0/(2.0*TINT1)
FREQ=(F1SET+FREQ)/2.0
RADIUS=RADIUS1
ALL,B11,B12,GAIN1=COEFF(FREQ,DELT,RADIUS)
F1SET=FREQ

```

\* \* \*

# COMPUTE THE CENTER FREQUENCY FOR THE HIGH FREQUENCY NOTCH

```

* * 50
TC2=CROSS(TIME,BH2OUT,0.0)
IF(TC2.EQ.0.0) GO TO 100
TINT2=TC2-LTINT2
LTINT2=TC2
IF(TINT2.GT.0.0625) GO TO 100
IF(TINT2.LT.0.033333) GO TO 100
FREQ=1.0/(2.0*TINT2)
FREQ=(FREQ+F2SET)/2.0
RADIUS=RADIUS2
A21,B21,B22,GAIN2=COEFF(FREQ,DELT,RADIUS)
F2SET=FREQ

* * * * *
* * 100
FIRST NOTCH FILTER
F1OUT=FILTIN+A11*F111+F112-B11*F011-B12*F012

SECOND NOTCH FILTER
F2OUT=F1OUT+A21*F121+F122-B21*F021-B22*F022

ADJUST OUTPUT FOR DC GAIN = 1.0

F1LOUT=F2OUT*GAIN1*GAIN2
F112=F111
F111=FILTIN
F012=F011
F011=F1OUT
F122=F121
F121=F1OUT
F022=F021
F021=F2OUT

* * 200
CONTINUE

* *
DERIVATIVE
* *
MODEL OF THE THIRD ORDER PLANT

```

\*\*

PE=PC+PO  
GAMA=PE+P8  
FILTN=GAMA\*KTHETA  
P1=FILEOUT\*P1  
P2=MDelta\*P1  
P3=-P2-MA  
MA=MALFA\*ALFA  
P4=ZDELTA\*P1/VEL  
P5=PR-P4-P6  
P6=ZALFA\*ALFA/VEL  
P7=PR+P1  
P8=KRTHT\*P7  
P9=INTGRL(0.0,PR)  
PQ=P9+P10  
P10=PSIRG\*BO  
P11=PSIGA\*BR  
PR=INTGRL(0.0,P3)  
ALFA=INTGRL(0.0,P5)

\*\*\*\*\*

MODEL OF LOW BAND BENDING MODE

BL1=GAINL/PSIGA\*P1  
BL2=ZETABL\*BL1  
BL3=BL2-ZETABL\*BL4-BL5\*WBL\*\*2.0  
BL4=INTGRL(0.0,BL3)  
BL5=INTGRL(0.0,BL4)

\*\*\*\*\*

MODEL OF HIGH BAND BENDING MODE

BH1=GAINH/PSIGA\*P1  
BH2=ZETABH\*BH1  
BH3=BH2-ZETABH\*BH4-BH5\*WBH\*\*2.0  
BH4=INTGRL(0.0,BH3)  
BH5=INTGRL(0.0,BH4)  
BR=BH4+BL4  
BO=BH5+BL5

\*\*\*\*\*

MODEL OF THE PLANT WITHOUT BENDING MODES  
TO ESTABLISH NOMINAL PERFORMANCE.

```

P21=PC+P27
P22=P21+P31
P23=KTHETA*P22
P24=MDELTA*P23
P25=-P24-MALFA*P30
P26=INTGRL(0.0,P25)
P27=INTGRL(0.0,P26)
P28=ZDELTA/VEL*P23
P29=-P28-ZALFA/VEL*P30+P26
P30=INTGRL(0.0,P29)
P31=KRTHEI*P26

```

```

PROGRAM AND PLOTTER CONTROL

```

```

**
**
**
**
**
SAMPLE

```

```

CALL DRWG(1,1,TIME,P27)
CALL DRWG(1,2,TIME,P0)
CALL DRWG(2,1,TIME,F1SET)
CALL DRWG(2,2,TIME,F2SET)
CALL DRWG(2,3,TIME,LHZ)
CALL DRWG(2,4,TIME,HHZ)

```

```

TERMINAL
CALL ENDRW(NPLOT)
CONTRL FINTIM=2.0 , DELT=0.01, DELS=0.01
INTEG RKSF
PRINT 0.01,P0,BR,LHZ,F1SET,HHZ,F2SET
END
STOP
**

```

```

FORTHAN SUBROUTINE TO CALCULATE THE NOTCH FILTER COEFFICIENTS

```

```

FORTHAN SUBROUTINE COEFF(FREQ,DELT,RADIUS,A1,B1,B2,GAIN)

```

```

C CALCULATE THE FILTER COEFFICIENTS
C
C

```

```

PI=3.14159
A1=-2.0*COS(FREQ*2.0*PI*DELT)
B1=-2.0*RADIUS*COS(FREQ*2.0*PI*DELT)
B2=RADIUS**2.0

```

```

C ADJUST THE FILTER DC GAIN TO UNITY
C
C GAIN=(1.0+B1+B2)/(2.0+A1)

```

RETURN  
END

```
*
* //C.SYSPRINT DD DSN=,SYSOUT=A
//PLOT.STEPLIB DD DSN=C0044.Q,UNIT=3330,VOL=SER=DISK02,DISP=SHR
//PLOT.PLOTPARM DD *
  &PLOT.SCALE=0.45 &END
//PLOT.SYSIN DD *
```

0.0	0.2	-0.08	0.01	10.0	10.0	5
0.0	0.2	5.0	1.0	10.0	10.0	5



## LIST OF REFERENCES

1. General Dynamics/Astronautics, San Diego, California, Report 80P, Study of Coupling of Natural Bending Modes with the Autopilot for the XSM-65 Series Missile, by S. Loucks, July 1958.
2. Haeussermann, W., Guidance and Control of Saturn Launch Vehicles, Paper Presented at the Second Annual Meeting of the American Institute of Aeronautics and Astronautics, San Francisco, California, 26 July 1965.
3. Lockheed Missiles and Space Company, Sunnyvale, California, Technical Report 1200, Body Bending Alleviation Concepts Annual Report, G. D. Swart and M. H. Fong, 22 December 1977.
4. Thaler, G. J., Design of Feedback Systems, P. 25-26, Dowden, Hutchinson and Ross, 1973.
5. Chen, Chi-Tsong, Analysis and Synthesis of Linear Control Systems, P. 109-112, Pond Woods Press, 1978.
6. Lockheed Missile and Space Company, Sunnyvale, California, Technical Report 1306, Technical Notes on the Simplified Fleet Ballistic Missile Models, by W. W. Szeto, 21 May 1980.
7. Desjardins, B., A User's Manual for Linear Control Programs on the IBM/360, M.S.E.E. Thesis, Naval Postgraduate School, Monterey, California, December 1979.
8. Lam, H. Y-F, Analog and Digital Filters, Design and Realization, Prentice-Hall, 1979.
9. Syn, W.M., Turner, N.N., and Wyman, D.G., DSL/360 Digital Simulation Language User's Manual, IBM Corporation, San Jose, California, November 1968.

# INITIAL DISTRIBUTION LIST

	No. Copies
1. Defense Technical Information Center Cameron Station Alexandria, Virginia 22314	2
2. Library, Code 0142 Naval Postgraduate School Monterey, California 93940	2
3. Department Chariman, Code 62 Department of Electrical Engineering Naval Postgraduate School Monterey, California 93940	2
4. Associate Professor R. D. Strum, Code 62St Department of Electrical Engineering Naval Postgraduate School Monterey, California 93940	10
5. Commander William L. Marks, USN 13668 Freeport Road San Diego, California 92129	1

DATE  
FILMED  
— 8